

LABORATORY EXPERIMENTS ON IMPROVEMENT OF BURIED FLEXIBLE
PIPES BY USING GEOFOAM

A THESIS SUBMITTED TO
THE GRADUATE SCHOOL OF NATURAL AND APPLIED SCIENCES
OF
MIDDLE EAST TECHNICAL UNIVERSITY

BY

BERKAN SÖYLEMEZ

IN PARTIAL FULFILLMENT OF THE REQUIREMENTS
FOR
THE DEGREE OF MASTER OF SCIENCE
IN
CIVIL ENGINEERING

SEPTEMBER 2017

Approval of the thesis:

**LABORATORY EXPERIMENTS ON IMPROVEMENT OF BURIED
FLEXIBLE PIPES BY USING GEOFOAM**

submitted by **BERKAN SÖYLEMEZ** in partial fulfillment of the requirements for
the degree of **Master of Science in Civil Engineering Department, Middle East
Technical University** by,

Prof. Dr. Gülbin DURAL ÜNVER
Dean, Graduate School of **Natural and Applied Sciences**

Prof. Dr. İsmail Özgür YAMAN
Head of Department, **Civil Engineering**

Asst. Prof. Dr. Nejan Huvaj SARIHAN
Supervisor, **Civil Engineering Dept., METU**

Examining Committee Members:

Prof. Dr. Erdal ÇOKÇA
Civil Engineering Dept., METU

Asst. Prof Dr. Nejan Huvaj SARIHAN
Civil Engineering Dept., METU

Asst. Prof. Dr. N. Kartal TOKER
Civil Engineering Dept., METU

Prof. Dr. Bahadır Sadık BAKIR
Civil Engineering Dept., METU

Assoc. Prof. Dr. Berna UNUTMAZ
Civil Engineering Dept., Hacettepe University

Date: 08.09.2017

I hereby declare that all information in this document has been obtained and presented in accordance with academic rules and ethical conduct. I also declare that, as required by these rules and conduct, I have fully cited and referenced all material and results that are not original to this work.

Name, Last Name: Berkan SÖYLEMEZ

Signature:

ABSTRACT

LABORATORY EXPERIMENTS ON IMPROVEMENT OF BURIED FLEXIBLE PIPES BY USING GEOFOAM

SÖYLEMEZ, Berkan

M.Sc., Department of Civil Engineering

Supervisor: Asst. Prof. Dr. Nejan HUVAJ SARIHAN

September 2017, 85 pages

Buried pipelines have become one of the most common, economical and safe means of conveying fluids (water, gas, petroleum, etc..) from a region to another ranging from very small (hundreds of meters) to large distances (thousands of kilometers). These pipes may be damaged and deform due to the application of different kinds of loading such as traffic loads, heavy static loads, sloping ground, etc. Such unwanted scenarios can be avoided by using geofoams in the flexible buried pipeline projects.

In this study, the effect of geofoam for the improvement of a buried flexible pipe is investigated in laboratory physical model tests. The laboratory experiments are conducted in a box having 1 m x 1 m area and 0.6 m height, where a clean sand is used as the bedding and surrounding material. A 20-cm-diameter PVC pipe is positioned on the bedding soil layer, over which EPS geofoam having different densities and dimensions are placed. Incremental static loading is applied to the ground surface via a circular steel plate (such as in a plate load test) and deformations of the pipe, as well as that of the ground surface, are measured. Introduction of geofoam above the pipe creates a compressible layer, which results in soil arching. This action reduces the loads by transferring some portion of the weight of the soil prism above the pipe to the

side soil and leads to smaller deformations of the pipe cross-section. By applying different geofoams, the improvement effect –if any- was compared in terms of thickness, width and density of the geofoam panels. Moreover, the location of the geofoam relative to the pipe crown was also part of the study and related experiments were conducted. For two-layer geofoam applications, the effect of geofoam layer spacing on the pipe deformation behavior is also studied. In all of the experiments, the change in the compressible zone above the pipe and arching effect is investigated.

The benefit of using geofoam is demonstrated by comparing subgrade modulus values for the cases of pipe with or without geofoam. It is found that, in nearly all experiments where geofoam was used, until the geofoam yields, it improved the pipe deformation under static loading. However, it is also seen that once the geofoam fails at large vertical deformations, they worsen the system significantly, when compared with the experiments in which geofoam was not used. It can be concluded that the benefit of using geofoam over pipes depends on the magnitude of the applied vertical stresses, in relation to the geofoam compression failure stress.

This study aims to contribute to a greater understanding of the benefit and efficiency of geofoam usage and the importance of geofoam characteristics for the flexible PVC buried pipeline projects under static loads, ultimately to aid the efficient design of such systems.

Keywords: Buried pipeline, geofoam, PVC pipe, ground deformation, ground improvement, model tests.

ÖZ

GÖMÜLÜ ESNEK BORULARIN KÖPÜK KULLANIMIYLA İYİLEŞTİRMESİNE YÖNELİK LABORATUVAR DENEYLERİ

SÖYLEMEZ, BERKAN

Yüksek Lisans, İnşaat Mühendisliği Bölümü

Tez Yöneticisi: Yrd. Doç. Dr. Nejan HUVAJ SARIHAN

Eylül 2017, 85 sayfa

Gömülü boru hatları, bir bölgeden diğerine, kısa mesafelerden (yüzlerce metre) uzun mesafelere (binlerce kilometre) kadar akışkan (su, gaz, petrol vb.) taşınmasının en yaygın, ekonomik ve güvenli yöntemlerinden biridir. Bu borular, trafik yükleri, ağır statik yükler, eğimli zemin yükleri vb. gibi farklı yüklemeler altında hasar görebilir veya deforme olabilir. Bu tür istenmeyen senaryolar, gömülü esnek boru hatları projelerinde köpüklerin (geofoam) kullanılması ile engellenebilir.

Bu çalışmada, gömülmüş esnek bir borunun iyileştirilmesi için üzerine geofoam köpük yerleştirilmesinin etkisi laboratuvarda 1-g fiziksel model deneylerle incelenmiştir. Deneyler 1 m x 1 m x 1m kutuda, yatak malzemesi olarak temiz kum kullanılarak yapılmıştır. 20-cm çapında PVC boru yatak tabakası üzerine yerleştirilmiş, ve üzerine farklı yoğunluklarda ve boyutlarda geofoam köpük malzemesi konulmuştur. Yüzeyde dairesel bir plaka ile uygulanan, kademeli artan statik yükler altında borunun ve zemin yüzeyinin düşey deformasyonları ölçülmüştür (bir statik plaka yükleme deneyinde olduğu gibi). Borunun üzerine geofoam köpük yerleştirilmesi, sıkıştırılabilir bir tabaka oluşturur ve bu da toprağın kemerlenmesine neden olur. Bu da, borunun üzerindeki toprak prizmasının ağırlığının bir kısmını yanlardaki zemine aktararak, boru

üzerindeki yüklerin azalmasını ve boru yüzey alanının daha az deformasyon göstermesini sağlar. Bu çalışmada, farklı köpükler uygulanarak – varsa- boru üzerindeki iyileştirme etkisi, köpük panellerinin kalınlığı, genişliği ve yoğunluğu açısından karşılaştırılmıştır. Ayrıca, boru tacına göre köpüklerin konumu da çalışmanın bir parçası olarak ele alınmış ve ilgili deneyler yapılmıştır. İki katlı geofom köpük uygulaması için, iki geofom tabakası arasındaki mesafesinin etkisi ve boru deformasyon davranışı üzerindeki verimliliği de araştırılmıştır. Tüm bu deneylerde borunun üstündeki sıkışabilir bölgedeki değişim ve bunun kemerlenme oluşumu üzerindeki etkisi incelenmiştir.

Geofom köpük kullanımının etkileri, yatak katsayısı (modülü) değerlerini kıyasladığımızda, köpük kullanımının, köpüksüz sadece boru kullanılan deneylere kıyasla borunun üzerinde bir sıkıştırılabilir katman oluşturduğunu göstermektedir. Köpükler büyük düşey deformasyonlar altında yenilene kadarki süreçte, neredeyse tüm köpük deneyleri statik yükleme altında boru deformasyonunu azaltmıştır. Bununla birlikte köpükler yenildiklerinde, yalnızca boruların kullanıldığı deneylerle karşılaştırıldığında sistemi daha da kötüleştirdikleri görülmektedir. Borular üzerinde geofom kullanmanın yararı, geofom basınç yenilme gerilimiyle ilişkili olarak uygulanan düşey yüklemelerin büyüklüğüne bağlı olduğu sonucu çıkarılabilir.

Bu çalışma, statik yükler altında gömülü esnek PVC boru hattı projeleri için köpük kullanımının verimliliği ve geofom özelliklerinin önemi hakkında daha fazla bilgi sahibi olmaya, nihai olarak da böyle sistemlerin daha etkili dizayn edilmesine katkıda bulunmayı amaçlamaktadır.

Anahtar kelimeler: Gömülü boru hattı, köpük, PVC boru, zemin deformasyonu, zemin iyileştirmesi, model testleri

To my Family,

ACKNOWLEDGEMENTS

Foremost, I would like to express my special thanks to my supervisor Prof. Dr. Nejan Huvaj Sarihan for her guidance, technical support, encouragement and patience throughout all process of this thesis.

I would like to express my deepest gratitude to Asst. Prof. Dr. Nabi Kartal Toker for his advices and solutions with our test setup preparation. It was a great chance for me to benefit from his knowledge and experience.

I would like to thank to the members of my thesis examining committee; Dr. Erdal Çokça, Dr. Bahadır Sadık Bakır and Dr. Berna Unutmaz for their interests on my thesis topic and valuable contributions to this study.

It was my pleasure and honor to work with my thesis mate Can Şimşek. We both became desperate and hopeful about the progress from time to time. I am very grateful for his endless support, guidance and all the funny moments that we lived during experiments.

I am grateful for my colleagues for their support and suggestions about the thesis progress. I specifically want to express my gratitude to my office mate Emir Ahmet Oğuz for his help in the experiments, Melih Kenanoğlu for his invaluable help about the testing equipment and Hilmi Bayraktaroğlu for his creative solutions.

I would like to thank to the laboratory technicians Kamber Bilgen, Ali Bal, Ulaş Nacar, Cuma Yıldırım and especially Mustafa Yalçın (mechanical engineering) for their solutions to problems and support during experiments.

I would like to state my deepest gratitude to my beloved family, my mother Songül Söylemez for her endless love and care, my father Cafer Söylemez for his mentoring and contribution to my education life, my brother Serkan Söylemez for his help and accompany. I would also appreciate the motivation and patience of Catyushka. Her sweet voice and kotky smile gave me the biggest motivation. Shortly, I would not be able to succeed in this thesis without their support.

TABLE OF CONTENTS

ABSTRACT	v
ÖZ.....	vii
ACKNOWLEDGEMENTS	x
TABLE OF CONTENTS	xii
LIST OF TABLES	xiv
LIST OF FIGURES.....	xv
CHAPTERS	
1. INTRODUCTION.....	1
1.1. Problem Statement.....	3
1.2. Research Objectives	4
1.3. Scope	5
2. LITERATURE REVIEW.....	7
3. TEST MATERIALS AND SET UP.....	25
3.1. Çine Sand.....	25
3.2. Flexible Pipe	27
3.3. EPS Geofoam	30
3.4. Test set-up.....	34
3.5. Linear Potentiometers, Load Cell and Dial Gages	35
3.6. Data Acquisition System	37
4. TEST PREPARATION.....	39
4.1. Flexible Pipe Preparation.....	39
4.2. Test tank preparation	42
4.3. Load plate and dial gages	46
5. EXPERIMENTS AND FINDINGS	53
5.1. Introduction	53
5.2. No-geofoam experiments	55
5.3. Effect of width.....	57
5.4. Effect of density.....	61
5.5. Effect of thickness	65
5.6. Location criteria.....	68
5.7. Effect of spacing between multiple geofoams.....	70
5.8. Effects on surface settlement and subgrade reaction modulus	72

6. CONCLUSION AND FUTURE STUDIES	77
6.1. Conclusion.....	77
6.2. Future Studies.....	80
REFERENCES.....	81

LIST OF TABLES

Table 2.1. Summary of the field observations (Vaslestad et al. 2010)	15
Table 2.2. Effect of geofom width and material modulus on pipe load reduction (Kim and Yoo, 2005)	16
Table 3.1. Çine sand index properties	26
Table 3.2. Direct shear test results for Çine Sand	26
Table 3.3. Material properties of PVC (* is taken from http://www.dielectriccorp.com)	30
Table 3.4. Geofom compression test results.....	31
Table 3.5. %10 compressive stress for EPS16, loading rate=5.0 mm/min (by TİPOR)	32
Table 3.6. %10 compressive stress for EPS26 loading rate=4.9 mm/min (by TİPOR)	32
Table 3.7. Linear trend coefficients of the potentiometers	35
Table 5.1. Experiment program and geofom properties.....	54
Table 5.2. Summary of the results of the experiments (Subgrade modulus, geofom stress and strain, surface settlements)	75

LIST OF FIGURES

Figure 1.1. Examples of buried pipes (a) failure of a rigid pipe (b) a utility pipe (c) failure of a rigid pipe, (d) flexible pipes from (www.cbpengeering.com).....	2
Figure 1.2. Deformation and load transfer behavior of rigid and flexible buried pipes (http://www.blogplastics.com/en/rigid-pipes-or-flexible-pipes-buried/).....	3
Figure 2.1. Movement of columns above pipe (a) Rigid pipe, (b) Flexible Pipe (Moser, 1990)	7
Figure 2.2. Various types of conduit installations (a) Trench installation, (b) Embankment installation (positive projecting), (c) Embankment installation (negative projecting), (d) Imperfect trench installation (Kang, 2007)	8
Figure 2.3. Mobilization of shear forces in imperfect trench method.....	9
Figure 2.4. Summary of conduit installation types	10
Figure 2.5. Behavior of (a) rigid pipe and (b) flexible pipe under embankment installation, (Moser, 1990)	11
Figure 2.6. Comparison of compressibility test results with other materials. (McAfee and Valsangkar, 2004)	13
Figure 2.7. Locations of pressure cells and EPS geofom above the pipe-Eidanger (Vaslestad et al. 2010).....	14
Figure 2.8. Numerical modeling geometry for the box culvert.....	15
Figure 2.9. Effect of geofom height (thickness) on pipe load reduction.....	16
Figure 2.10. Model-Scale lab results for double space geofom layer	17
Figure 2.11. Centrifuge test set up for box culvert	18
Figure 2.12. Double culvert test setup	19
Figure 2.13. Pipe deformation for varying geofom applications	20
Figure 2.14. FLAC results for geofom applications on culvert ... (Sun et al., 2005).....	21
Figure 2.15. Effect of double layer and spacing on pipe, FLAC results.....	22
Figure 2.16. Geofom effect for geofom uplift field tests (Lingwall, 2009)	23
Figure 2.17. Geofom application for earthquake-induced excess pipe displacement	24
Figure 3.1. Grain size distribution of Çine sand (3 experiments)	25
Figure 3.2. Comparison of Çine sand test results from FHWA (Schmertman, 1978).....	27
Figure 3.3. Parallel Plate Test Set-up.....	28
Figure 3.4. Parallel plate test results for the 15 cm long PVC pipe with 20 cm diameter	28
Figure 3.5. Elongation Test results for PVC material	29
Figure 3.6. Compression test results for varying geofom geometry and densities ..	31
Figure 3.7. Load vs. Elongation Graph for EPS16 (by TIPOR)	32
Figure 3.8. Load vs. Elongation Graph for EPS26 (by TIPOR)	33
Figure 3.9. Geofom Loading Experiments in Material Lab	33
Figure 3.10. Test Setup Components	34
Figure 3.11. Tire/Road contact area and force component directions	36
Figure 3.12. TDG Test box 1001 Data Acquisition System	37

Figure 4.1. A 2-meter long pipe (a) & pipe cutting (b).....	40
Figure 4.2. Special tools for the potentiometer measurement.....	40
Figure 4.3. Potentiometer Installation (a) & steel member with groove (b)	41
Figure 4.4. Potentiometers in 90 cm long pipe (a), pipe covered by tape at the ends (b)	42
Figure 4.5. Laminar box interfaces are taped inside and outside (a) & Vibratory hammer (b).....	42
Figure 4.6. Compaction order of the soil layer	43
Figure 4.7. Installation of density boxes (a) & compaction order in pipe layer (b) ...	44
Figure 4.8. Placing of the geofoam & leveler to smoothen the surface	45
Figure 4.9. Last two compressed soil layers after geofoam placement.....	46
Figure 4.10. 26-cm steel plate and load cell (a), spacers added to ensure full contact with load cell (b)	47
Figure 4.11. Reference bars to place dial gages on the steel plate	47
Figure 4.12. Dial gage installation with bubble gage (a) & final form (b)	48
Figure 4.13. A general view of active devices during an experiment	49
Figure 4.14. Regulator valve to increase pressure (a) & a reading example (b).....	49
Figure 4.15. During experiment (a) & after experiment (b).....	50
Figure 4.16. A closer photo of the deformed geofoam closer (a) & test tank with deformed geofoam (b).....	51
Figure 4.17. Surface plate and geofoam geometry after failure.....	51
Figure 4.18. Geofoam over the pipe (a) and density boxes (b).....	52
Figure 5.1. Pipe deformation vs. stress curves	55
Figure 5.2. Side and front view of the heavily distorted pipe (with red tape) and collapsed pipe.....	57
Figure 5.3. Geofoam widths for 2 cm thickness	58
Figure 5.4. EPS15 thickness 4 cm, width comparison up to (a) 5.0% & (b) 1.8% pipe vertical deformation	59
Figure 5.5. EPS15 thickness 2 cm, width comparison up to (a) 6.0% & (b) 1.6% pipe vertical deformation	60
Figure 5.6. Four tests conducted to investigate the effect of geofoam density	61
Figure 5.7. Width 30 cm & thickness 4 cm, EPS density comparison up to (a) 5.0% & (b) 2.0% of the pipe vertical deformation	63
Figure 5.8. Width 20 cm & thickness 2 cm, EPS density comparison up to (a) 5.0% & (b) 3.0% pipe vertical deformation	64
Figure 5.9. Three different geofoam thicknesses used in experiments	65
Figure 5.10. Width 20 cm, thickness comparison up to (a) 6.0% & (b) 2.0% pipe vertical deformation	66
Figure 5.11. Width 40 cm, thickness comparison up to (a) 7.0% & (b) 2.5% pipe vertical deformation	67
Figure 5.12. Experiments with varying vertical distance between geofoam and pipe crown.....	68

Figure 5.13. Comparison according to geofoam distance related to the pipe crown up to (a) 6.0% & (b) 2.5% pipe vertical deformation	69
Figure 5.14. Location of two geofoams in the experiments.....	70
Figure 5.15. Spacing of double layers comparison up to (a) 6.0% & (b) 2.0% pipe vertical deformation	71
Figure 5.16. Surface settlements observed till the end of the experiments.....	73
Figure 5.17. 5% vertical pipe deformations observed in the experiments	73
Figure 5.18. Surface settlements observed till 15 mm	74
Figure 5.19. 2% vertical pipe deformations observed in the experiments	74
Figure 6.1. Geofoams are cut to measure final strain %	79

CHAPTER 1

INTRODUCTION

In today's industrial world, buried pipelines have become one of the most common, economical and safe means of conveying fluids (water, gas, petroleum, etc.) from a region to another ranging from very small (a few meters) to large distances (thousands of kilometers).

Pipes may confront different loads such as embankment, traffic, earthquake, uplift, etc. Numerous factors affect the behavior of the pipe such as bedding condition, backfill material, trench width, buried depth and pipe material properties. Some of the loads considered in buried pipe design are: internal pressure, vertical earth loads, surface live loads, surface impact loads, buoyancy, thermal expansion, relative pipe-soil displacement, movement of pipe bends, subsidence, earthquake, etc. (American Lifetime Alliance guidelines). Important points to consider when designing buried pipes are:

- Applied static and live loads
- Deflection and stress due to soil weight
- Pipe wall bending
- Maximum surface impact load
- Differential movement of pipes
- Effect of soil spring (axial and lateral) etc.

The pipes could be damaged during their service life under the applied load conditions (Figure 1.1.)



(a)



(b)



(c)



(d)

Figure 1.1. Examples of buried pipes (a) failure of a rigid pipe (b) a utility pipe (c) failure of a rigid pipe, (d) flexible pipes from (www.cbpengeering.com)

Rigid pipes are typically made of steel or concrete, and they are relatively more rigid as compared to the ground surrounding them. Their design considers no deformation in the rigid pipe and therefore the pipe has to carry significant loads without deforming/breaking throughout its service life. This influences the selection of wall thickness of the pipe. Flexible pipes are typically made from polymers such as PVC, HDPE, etc. and they deflect under applied vertical loads and transfer the loads to the surrounding soil (Figure 1.2). The maximum allowable deformation in the flexible pipes has been established as 5% of its diameter in 50-year service life, according to American Lifetime Alliance.

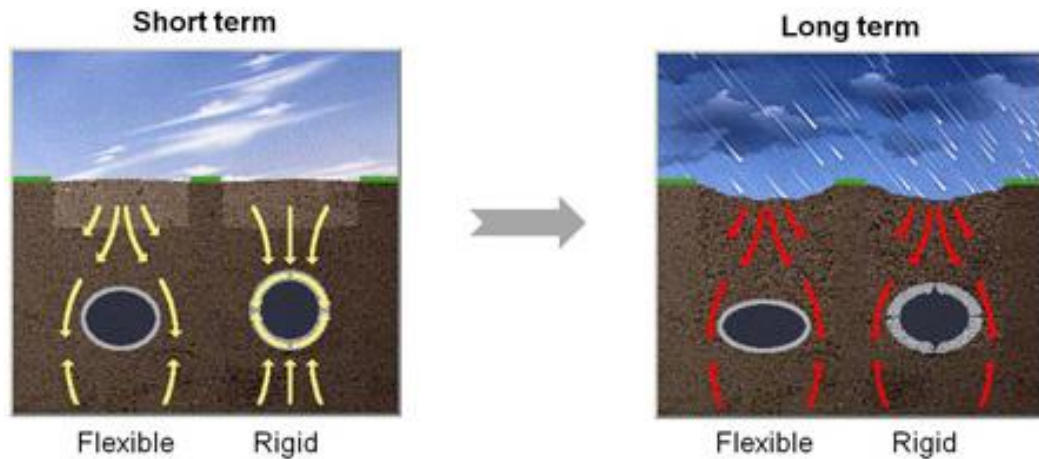


Figure 1.2. Deformation and load transfer behavior of rigid and flexible buried pipes (<http://www.blogplastics.com/en/rigid-pipes-or-flexible-pipes-buried/>)

Engineers have started to use different geosynthetics to improve the behavior of buried pipes against failures. Geofoams are one of those materials which can be used as a compressible inclusion above the pipe and reduce the load on the pipe.

1.1.Problem Statement

Compressible inclusions have been used in geotechnical applications, typically between a below-ground structure and surrounding soil layer (Horvath, 1997). Hay bales or cardboards were used to benefit from vertical arching over pipes (Spangler & Handy, 1982). In France, the tire-soil mixture was used in several projects to create a compressible fill material for induced trench applications (Jean, P.& Long, N. 1990). However, these materials have a stress-strain behavior which is hard to predict or control. Some of them may also decompose when they are wet. On the other hand, EPS geofoam is an excellent material as a compressible inclusion, because it has predictable and controllable stress-strain behavior and maintains predictable behavior when wet. Some studies are showing the improvement effect of the geofoam applications for buried pipelines. Application of geofoam blocks under high embankment loads for concrete and steel pipes was studied in Norway (Vaslestad et al., 1994). The effects of double geofoam layers on flexible steel pipes were studied

by Kim et al. (2010). Akinay et al. (2016) investigated the effect of geofoam location on a corrugated buried pipe. After an extensive literature search, it is seen that PVC pipes with and without geofoam under a static loading, and the effect of geofoam density or thickness of the geofoam in lab scale experiments were not studied. Also, shallowly buried pipes are not studied with geofoam applications; literature search showed that pipes were buried very deep in terms of depth to diameter ratio. After these factors described above, it is seen necessary to compare the effects of geofoam factors on a flexible PVC pipe in lab scale tests.

1.2. Research Objectives

The main purpose of this thesis study is to investigate the improvement effect of geofoam applications for a buried flexible PVC pipe under a static load by doing lab-scale experiments. Other objectives are:

1. If there is an improvement, to determine the upper load limit that can be applied to the system and to observe what will be the consequences if the limit is passed.
2. To compare the surface settlement values (coefficient of subgrade reaction) in terms of varying geofoam applications
3. To determine a pattern against the varying parameters and to figure out which parameter affects the results most.

This study may be a reference for future pipeline projects considering the geometric and configurational variety of the geofoams and their effects on vertical pipe deformation and surface settlement, and also will make the designer cautious about the results of failed geofoams.

1.3. Scope

In this study, laboratory-scale experiments are conducted to see the effect of varying geofoam properties such as the width, thickness, density and configuration of geofoam over a buried flexible pipe subjected to static loading. Vertical deformation of the pipe, load carrying capacity of the geofoams and settlement of the soil surface are compared among these experiment results. A summary of pipe characteristics and behavior, pipe installation methods are presented in Chapter 2. Previous studies about pipe behavior and improvement of pipes are also briefly explained in that chapter. Materials and test devices used in lab experiments are explained in Chapter 3. The steps to prepare an experiment are explained briefly in chapter 4. In Chapter 5 all experiment results are shown. Effects of the parameters explained briefly. In chapter 6, the overall study and findings are summarized in conclusion part and possible future studies are recommended.

CHAPTER 2

LITERATURE REVIEW

It goes back to the beginning of the 20th century when the story of the formal study of buried pipe structures begins. Dr. Anson Marston was the first person to analyze soil pressure on buried culverts in Iowa, America. Earliest systematic approaches about the structural mechanics of buried pipes were published by him (Marston & Anderson, 1913; Marston, 1930). This is how Marston Theory of Loads on buried conduits emerged. Marston Load Theory states that the load on a buried pipe, which is the weight of the column of soil, or central prism, directly above the pipe, is modified by the response of the pipe and the relative movement of the side columns of soil, or external prisms (adjacent to the pipe, between the pipe and the trench walls on either side), to the central prism. Shortly, the relative movement of the central prism and the side prisms result in shearing stresses or frictional forces (Rahman, 2010).

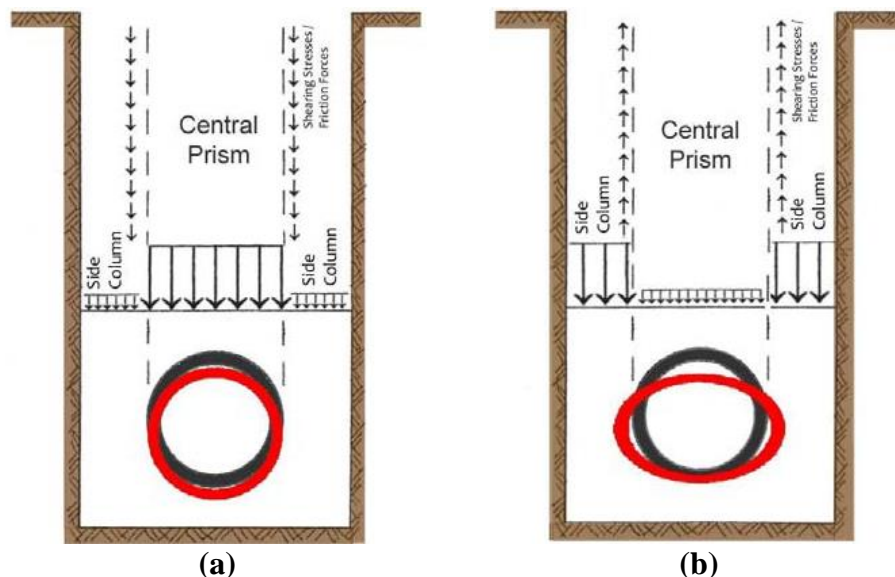


Figure 2.1. Movement of columns above pipe (a) Rigid pipe, (b) Flexible Pipe (Moser, 1990)

In the external load analysis, Marston (1930) defined two major types of loading conditions on the buried pipes, a ditch conduit (mainly stated as trench load condition), and a projecting conduit (mainly stated as an embankment condition). A trench (ditch) conduit as defined by Marston was a relatively narrow ditch dug in undisturbed soil. In trench condition, conduit/pipe is placed between vertical or sloping walls of undisturbed soil extending to the surface (ACPA 1994). Frictional forces between the backfill material and the sides of the trench help to support the central prism soil overlaying the conduit.

In embankment installation conditions, the pipe is placed on natural ground and soil is placed in layers above the existing ground. Embankment installations are further subdivided based on their location relative to the original ground level. Conduits founded partially or totally above the original ground level are classified as positive projecting conduits (Figure 2.2). Conduits founded in a trench excavated below the original ground level beneath the embankment are classified as negative projecting conduits.

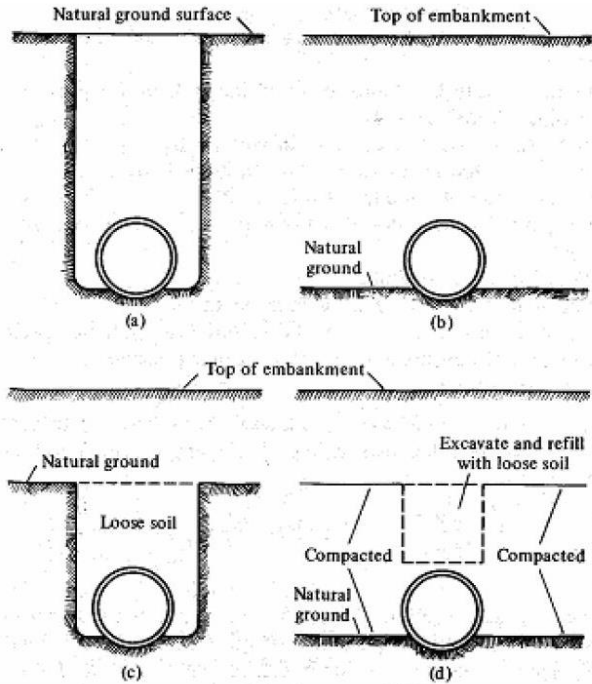


Figure 2.2. Various types of conduit installations (a) Trench installation, (b) Embankment installation (positive projecting), (c) Embankment installation (negative projecting), (d) Imperfect trench installation (Kang, 2007)

Negative projection conduit is a very favorable method of installing a railway or highway conduit since the load produced by a given height of fill is generally less than it would be in the case of a positive projecting conduit (Kang, 2007).

Imperfect trench installation method was developed to achieve the trench advantages in an embankment condition (Marston 1922). In imperfect trench application, backfill is placed on the pipe and thoroughly compacted on both sides up to a level above the projecting embankment conduit. Then a section of the compacted soil above the pipe is excavated to form a trench and replaced by a very loose lightweight material, such as leaves, baled hay or straw, EPS having the same width of the formed trench (Figure 2.2 d). When this trench with the light material is subjected to higher settlement comparing with the adjacent soil prisms, the upward frictional forces similar to those in the trench installations will be developed (Figure 2.3).

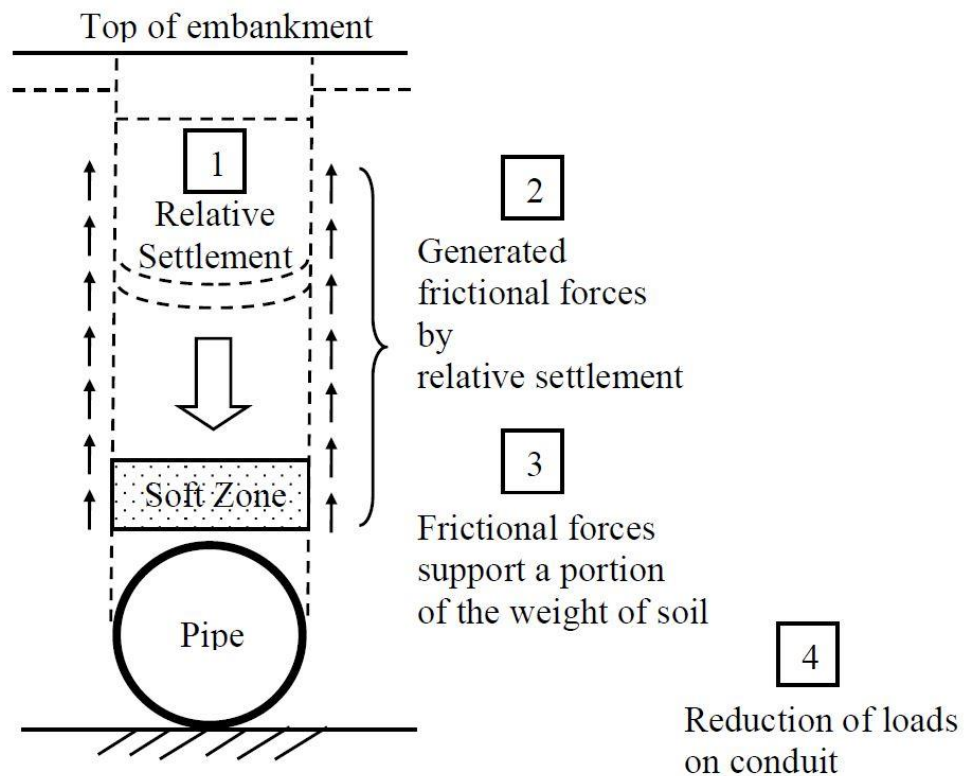


Figure 2.3. Mobilization of shear forces in imperfect trench method
(Kang, 2007)

The imperfect trench conduit is a special case that is kind of akin to the negative projecting conduit but is even more favorable regarding load reduction on the pipe. A summary of these various conduits and their description can be seen in Figure 2.4 (Rahman, 2010).




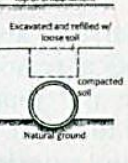
Marston's Conduit Installation Type	Present Day Nomenclature	Description	Diagram
Ditch Conduit / Trench Load Condition			
Ditch Conduit	Trench Load Condition	Pipe is installed in a narrow trench (generally, trench width $\leq 2 \times$ pipe diameter) in undisturbed soil, then backfilled to natural ground surface level	
Projecting Conduit / Embankment Condition			
Positive Projecting Conduit	Positive Embankment Condition / Positive Projecting Embankment	Pipe is installed underneath an embankment, in shallow bedding, w/ its top projecting above the surface of the natural ground	
Negative Projecting Conduit	Negative Embankment Condition / Negative Projecting Embankment	Pipe is installed underneath an embankment, in narrow and shallow trench, with its top at an elevation below natural ground surface	
Imperfect Ditch Conduit	Induced Trench Condition	Special case, similar to Negative Embankment Condition, but more favorable from standpoint of load reduction on pipe, used in very deep installations. Difficult to achieve for large-diameter pipes.	

Figure 2.4. Summary of conduit installation types (Rahman, 2010)

Terzaghi (1943) defines the mechanism of the positive arching in two phases: a reduction of the earth pressure on a yielding part of the structure and an increase in the earth pressure on the adjacent non-yielding areas. Bjerrum et al. (1972) mentioned that increase in pressure on the adjacent stationary areas is equal to or larger than the pressure reduction in the yielded zone.

The loading on deeply buried conduits is mainly affected by soil arching. Conduit stiffness and installation method also have the paramount effect on soil arching as importantly as installation methods. Soil arching is mobilized differently in rigid and flexible pipe cases (Figure 2.5).

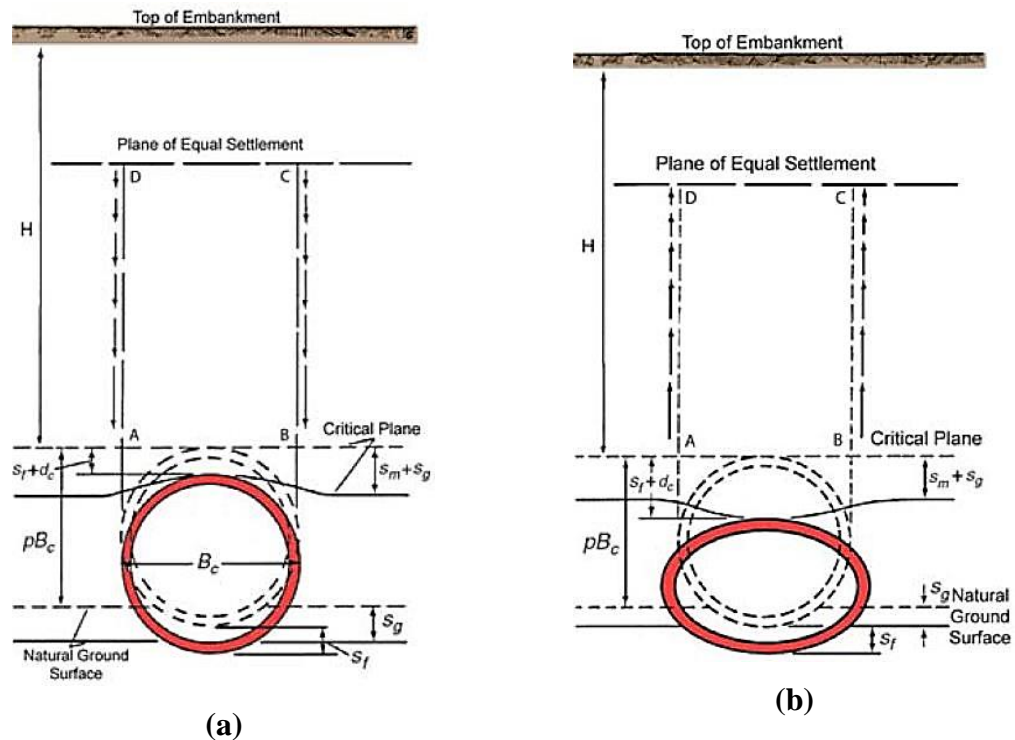


Figure 2.5. Behavior of (a) rigid pipe and (b) flexible pipe under embankment installation, (Moser, 1990)

A rigid pipe is stiffer compared to the soil around the pipe. Therefore, under loading, the rigid pipe will deform less compared to soil blocks around the pipe. This deformation difference will cause friction forces between the blocks, load on the pipe will be increased due to negative soil arching. On the other hand, for a flexible pipe, the pipe is likely to deform more compared to the soil around. Therefore, the soil block above the pipe will move downward more compared to around soil block, which will create a positive soil arching above the pipe. Some of the soil block load is transferred to side soil layers and load on the pipe is reduced.

Marston (1930) recognized that in a trench (generally, trench width $\leq 2 \times$ pipe diameter) when the side columns of soil are more compressible than the pipe due to its

inherent rigidity, this causes the pipe to take higher load than the load generated across the width of the pipe. The shearing stresses developed due to the differential settlement of the external prisms and the central prism are additive to the load of the central prism alone. Pipes that behave in this manner are referred to as rigid pipes. Generally, rigid pipes start showing signs of structural distress before being vertically deformed by 2 percent of their diameter (Rahman, 2010).

Moser (1990) states that performance of flexible pipelines is related by deformation. Vertical deformation is expressed as the change in the pipe diameter in the vertical direction divided by the original pipe diameter, usually in percentile form. Deformations may happen during transportation, installation or under service loads. Excess deformation may reduce the flow capacity due to cracks or due to geometry change in pipe cross-section. In buried pipeline applications, vertical deformation limits the design load. In a soil box, Spangler observed excessive steel pipe ring deflection up to 20%, so he recommended a maximum allowable ring deflection of 5%, which provides a factor of safety of 4. (Suleiman, 2002)

Corrugated PVC and steel pipes are relatively flexible. Therefore a small amount of reverse soil arching is induced. Maybe because of that, research regarding the effects of imperfect trench installation on flexible pipes is limited (Yoo & Kang, 2007). However, changing the zone subjected to arching may result in a higher percent of load transfer to side soil. Therefore, applying imperfect trench construction in flexible pipe projects will very possibly decrease the pipe deformation.

Several types of compressible material over buried pipelines were used in the construction of the imperfect trench throughout the 20th century. Leaves (Spangler 1958), baled straw (Larson 1962), tire-soil mixtures (Jean & Long, 1990), cardboards (Edgar et al., 1991), sawdust (Hastey, 2000; McAfee and Valsangkar 2004), woodchips (McQueen, 2000; McAfee and Valsangkar 2004) and hay (McQueen, 2000) have been used as compressible materials. Compressible inclusions are achieved with these materials, however, in general, it is hard to predict and control their stress-strain behavior (especially for cardboard) when they become wet. Moreover, some of these materials are biodegradable and decomposition of these materials will create a large void and it will lead to surface depression (Horvath, 1997). Recently, geof foam

has been preferred for compressible inclusions because it does not suffer from these drawbacks.

McAfee and Valsangkar (2004) compared the behavior of sawdust, wood chips and hay with other compressible materials. Large-scale direct shear and consolidometer tests were made to find out their properties to use in numerical modeling of imperfect trench applications. Their experiment results show that these three materials are more compressible compared to granular compressible materials. Moreover, to achieve their peak shear strength parameters, these materials needed large shear displacements. The compressibility of materials is compared in Figure 2.6.

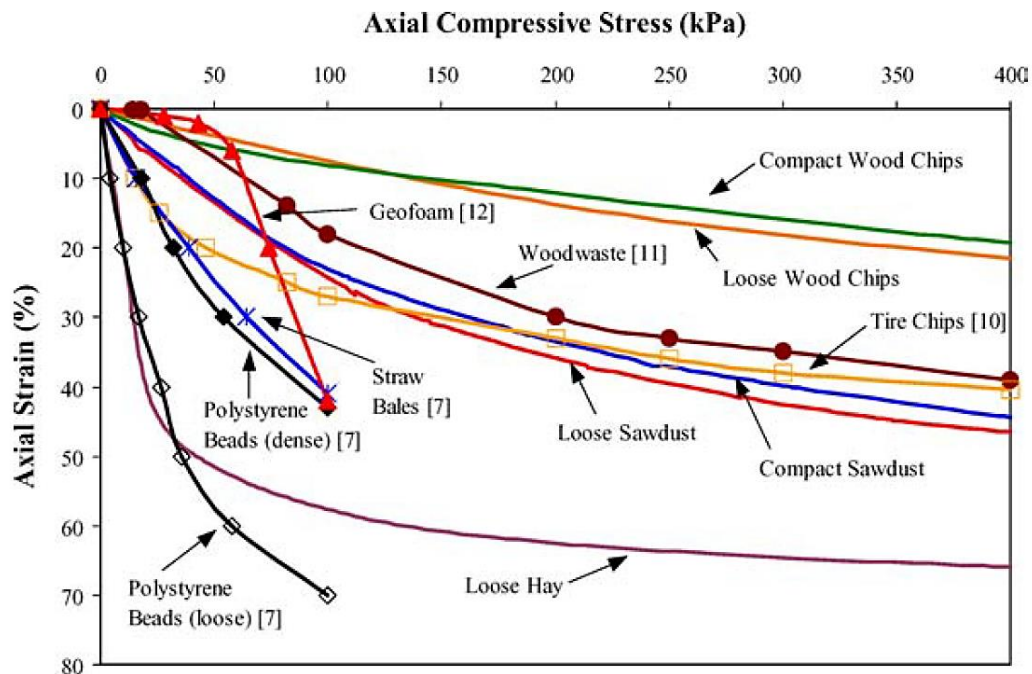


Figure 2.6. Comparison of compressibility test results with other materials. (McAfee and Valsangkar, 2004)

EPS geofoam blocks are a good alternative in terms of vertical load reduction on buried pipes and culverts under highway fills. Vaslestad et al. (2011) showed the effect of geofoam placement in buried pipes and culverts for varying backfill soil. Four different projects that were constructed in Norway have been monitored nearly 21 years. They inserted earth pressure cell and settlement tubes in the construction (Figure 2.7). Field observations are shown in Table 2.1. According to the observations, the type of soil

used in the embankment construction significantly affects the performance of induced arching. 20 year long observations reveal that cohesionless backfill is more effective in arching inducement comparing with cohesive backfills. Consequently, EPS in cohesive soils is prone to deform more compared to cohesionless soil case. It was also seen that without geofoam application, the box culvert is subject to 1.24 times the calculated overburden load in silty clay backfill case (Vaslestad et al., 1993).

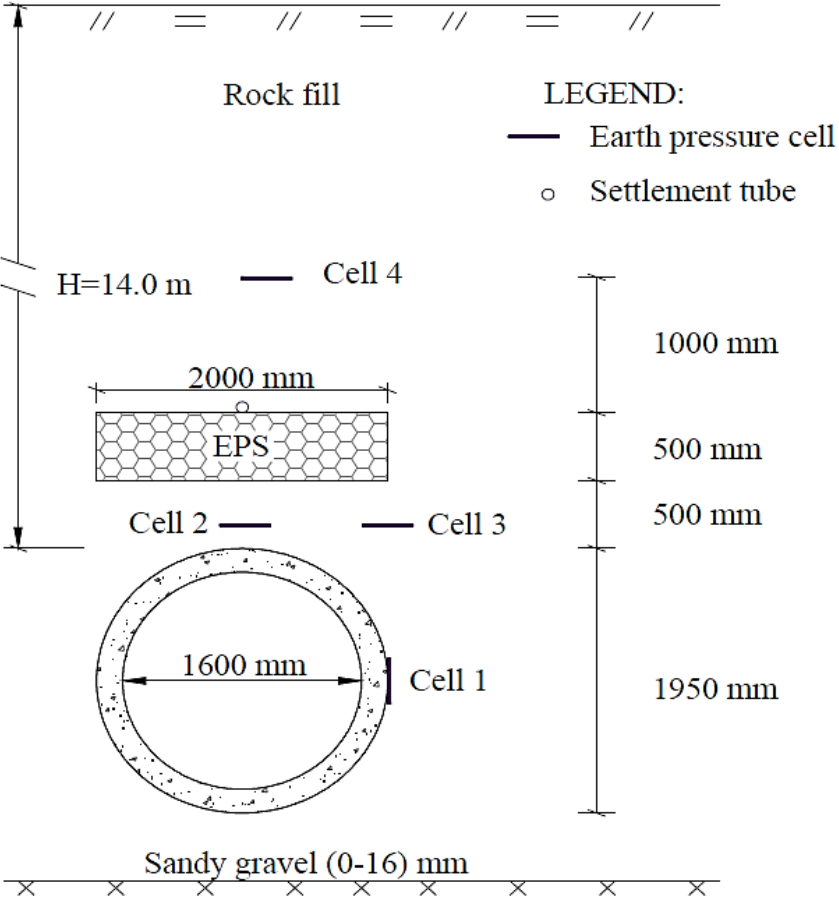


Figure 2.7. Locations of pressure cells and EPS geofoam above the pipe-Eidanger (Vaslestad et al. 2010)

Table 2.1. Summary of the field observations (Vaslestad et al. 2010)

Location	Pipe/ culvert properties	Geofoam geometry	Embankment height, m	Backfill	Observation	Geofoam deform. after embankment	Measured geofoam deformation, final
Eidanger, (1988)	concrete pipe, 1.95 m outer diameter & 1.6 m	w =2 m t=50 cm	14	rock fill	earth pressure on top of pipe = %25 of calculated	%28 of initial thickness	%28 of initial thickness, no increase
Sveio, 1989	concrete pipe, 1.71 m outer diameter & 1.4 m	w =3 m t=50 cm	15	rock fill	earth pressure on top of pipe = %25 of calculated	%30 of initial thickness	%38 of initial thickness
Hallumsdalen, 1989	concrete box, width 2 m, length 2.55 m	w =2 m t=50 cm	10.8	silty clay	earth pressure on top of pipe = %45 of calculated	%50 of initial thickness	%54 of initial thickness
Hallumsdalen, 1989	concrete box, width 2 m, length 2.55 m	no geofoam	9.8	silty clay	earth pressure on top of pipe = %124 of calculated	no geofoam	no geofoam
Tømtebekken, 1991	concrete pipe, 1.73 m outer diameter & 1.4 m	w =2.75 m t=50 cm	22	no info	earth pressure on top of pipe = %23 of calculated	%32 of initial thickness	%38 of initial thickness

Kim and Yoo (2005) performed an analytical study, comparing the importance of imperfect trench parameters in terms of load reduction on a buried concrete box (Figure 2.8). They showed that in the correct combination of loose material modulus and width of the loose material, load reduction could be up to 85% of the overburden load (Table 2.2). They also showed that no significant load reduction was achieved if the width of the compressible inclusion was greater than 1.5 times of the pipe diameter or if the height of the compressible layer is greater than 1.5 times of pipe height.

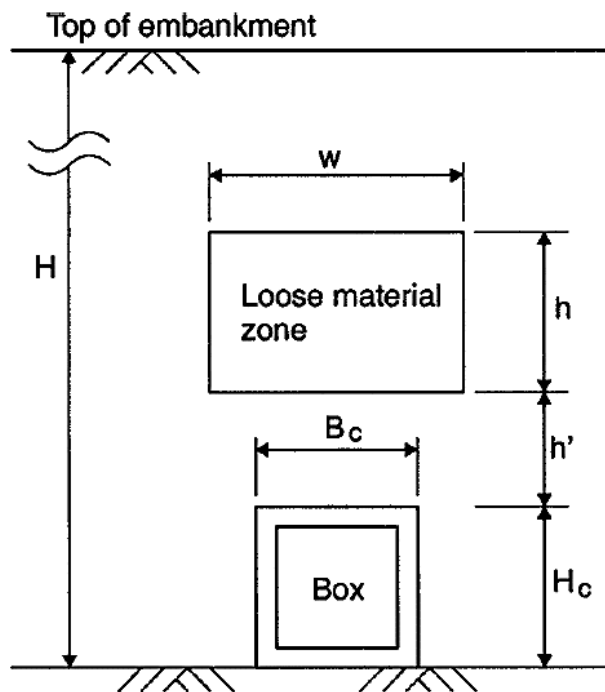


Figure 2.8. Numerical modeling geometry for the box culvert

(Kim and Yoo, 2005)

Table 2.2. Effect of geofoam width and material modulus on pipe load reduction (Kim and Yoo, 2005)

Modulus of lightweight material	Width of back fill layer, w/B_c			
	1.0	1.5	2.0	2.5
47.9 kPa (100 ksf)	32.8	41.1	39.1	36.7
23.9 kPa (50 ksf)	43.6	58.6	57.0	54.3
4.79 kPa (10 ksf)	56.9	83.7	85.3	84.8

Their study also revealed that if the height of the compressible layer is greater than 1.5 times of pipe height, no more significant load reduction is observed (Figure 2.9).

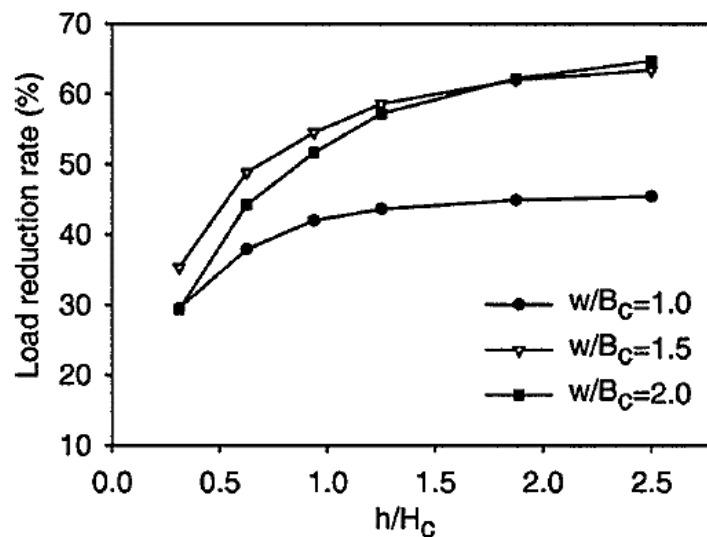
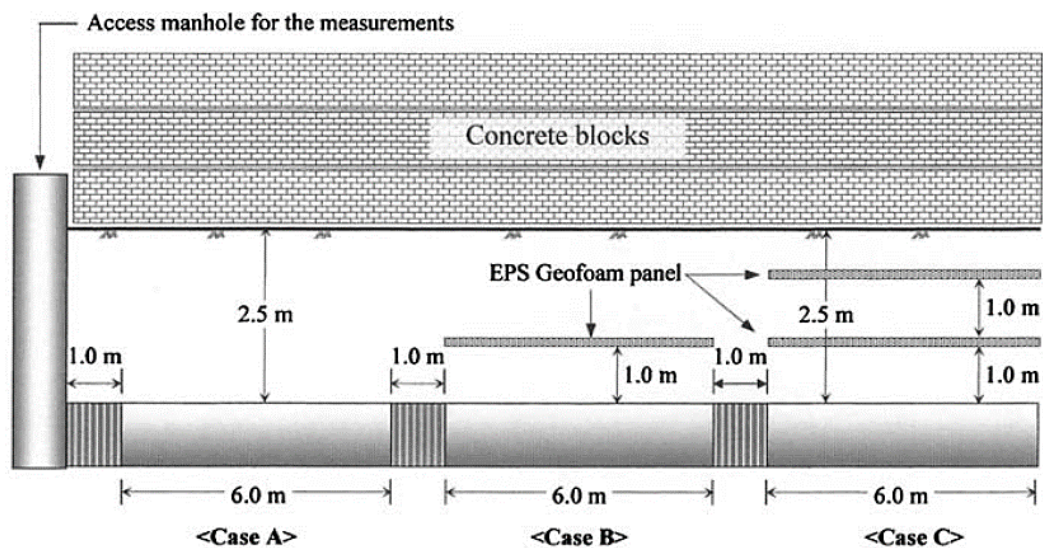


Figure 2.9. Effect of geofoam height (thickness) on pipe load reduction (Kim and Yoo, 2005)

McAfee (2005) used centrifuge tests to simulate different H/B_c (embankment height/box width) ratios of field prototype structures installed using the imperfect trench method, both for single and twin box culverts, and compared the results to results of positive projection method. Results from the study confirmed a significant reduction in vertical pressure for each condition but increased lateral pressures on the

sidewalls for induced trench method. McAfee observed that the compressibility, width, and height of the compressible layer are important factors to the load reduction.

Kim et al. (2010) studied to find the optimum configuration of EPS compressible inclusions for the induced trench application in both model-scale and full-scale tests. It is seen that double layer geofoam application does not reduce the vertical load on pipe significantly comparing to one geofoam layer; for model-scale tests 73% vs. 71% and full-scale test 37% vs. 36%, respectively. However, the lateral stress acting on the pipe spring line differs greatly such as one layer of geofoam (case B) reduced the horizontal pressure by 5% whereas two layer geofoam application (case C) reduced the horizontal stress by %37 compared to the pipe without EPS case (case A) (Figure 2.10).

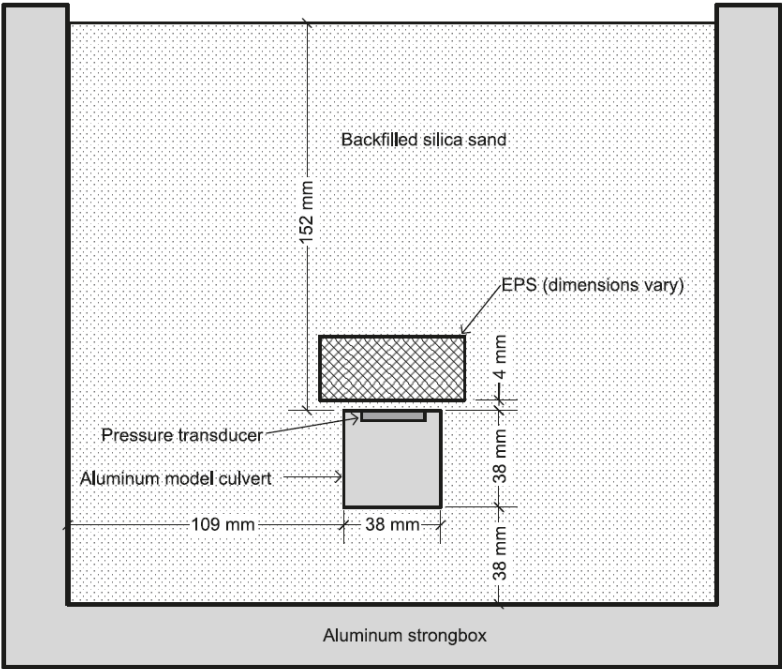


**Figure 2.10. Model-Scale lab results for double space geofoam layer
(Kim, Choi & Kim, 2010)**

Okobayashi et al. (1994) is the pioneer study in centrifuge testing for box culverts. A total of 14 experiments were made to compare the effects of culvert location, flexible material application (geofoam material), geofoam geometry and location. Tests were made with 52% relative density Toyoura Sand for a 60 mm x 60 mm hard aluminum box culvert. Centrifugal acceleration was increased to 80g by a stepwise 10g. Their study shows that the flexible material makes a great contribution to reducing the

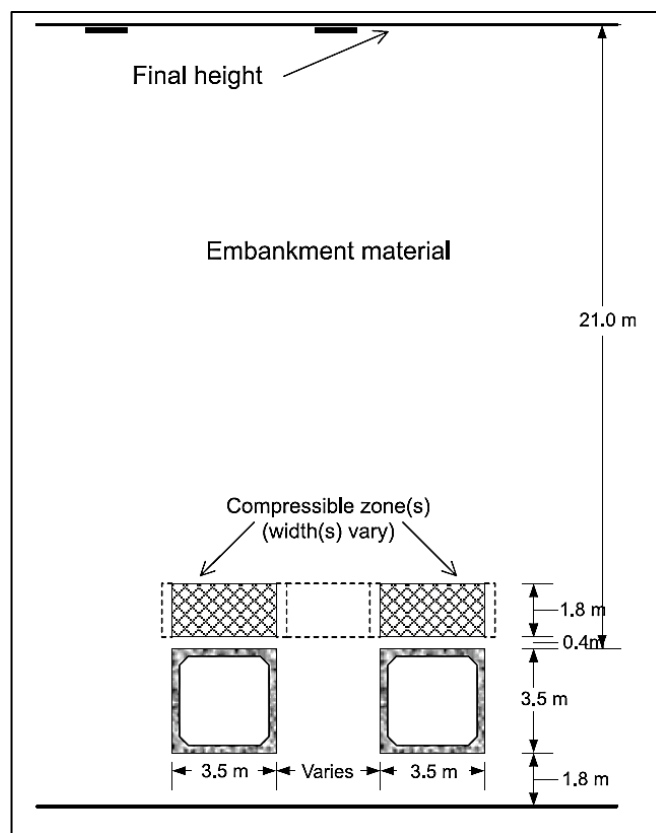
vertical earth pressure to values less than the overburden pressure. The setting of the flexible material is equal to altering the projection into ditch type. The mechanism of arching effect was also visualized by photoelastic experimental methods.

McGuigan and Valsangkar (2010) made centrifuge testing for 38 mm x 38 mm aluminum box culvert (Figure 2.11). Centrifuge test results showed that for the positive projecting case, the average earth pressure on the top of the culvert is 1.33 times calculated overburden pressure, while for the induced trench condition the earth pressure on the top was reduced to 24% of the expected overburden pressure. FLAC program was used to compare the test results and a good agreement was found with numerical model analysis. The effect of foundation rigidity (yielding vs. non-yielding) and stiffness of compressible zone material were the points of interest in the numerical studies. Yielding foundation (bedding) resulted in lower overburden pressure and higher lateral earth pressure on culvert compared to non-yielding foundation. Moreover, higher stiffness compressible zone appeared to cause higher vertical loads on the culvert.



**Figure 2.11. Centrifuge test set up for box culvert
(McGuigan and Valsangkar, 2010)**

Centrifuge tests were made to see the effects of construction methods, the spacing of box culverts and compressible zone geometry on double trench box culverts (Bourque, 2002; McAffe, 2005, McGuigan and Valsangkar, 2010). McGuigan and Valsangkar, (2011) showed in their study that base contact pressures are significantly lower in induced trench method compared with positive projection method. However, they also stated that in trench method box culverts, contact pressure values were greater than the top pressure plus dead load due to mobilized shear stresses along the sidewalls. Their study involves the effect of the distance between two box culverts (Figure 2.12). For the positive projection construction, lowest vertical stress is observed when distance was $0.5B$. As the distance increased from $0.5B$ to $1.5B$, vertical stress values approached to those calculated for single box culvert. Their study also investigated the compressible zone geometry. It is seen that if the spacing between culverts is more than $0.5B$, instead of using one wide geofoam that covers both of the culverts, it is better to use individual geofoams over each culvert.



**Figure 2.12. Double culvert test setup
(McGuigan and Valsangkar, 2011)**

Akınay et al. (2016) made 1:1 scale model tests by using geofoams for buried HDPE pipe to reduce soil stress on it. HDPE pipe, a flexible pipe with 30 cm outer diameter and 8.8 kN/m² ring stiffness was tested in 1.5 m x 1.5 m x 1.5 m test tank. For backfill material, a poorly graded sand with relative density %25 was used. Vertical and horizontal deformations of the pipe were measured. A total of 4 experiments were done. A reference experiment without any geofoam and three experiments with EPS10 geofoam panels. Geofoam panels have dimensions as 34 cm width and 5 cm thickness. Geofoams are placed in three different manners: a) just above the pipe crown, b) just below the pipe invert and c) both in pipe crown and invert. Test results showed that compared to the reference test, the vertical stress acting on pipe crown reduced 76% when geofoam placed on pipe crown; vertical stress acting on pipe invert reduced 49% when geofoam is placed under the pipe. Applying two geofoams both in pipe crown and invert did not contribute anything significant on load reduce. It is observed that lateral stresses on the pipe reduced 56% to 72% on geofoam used experiments. Compared to reference experiment, geofoam applications resulted in the pipe to elongate in the vertical axis and shorten in the horizontal axis (Figure 2.13).

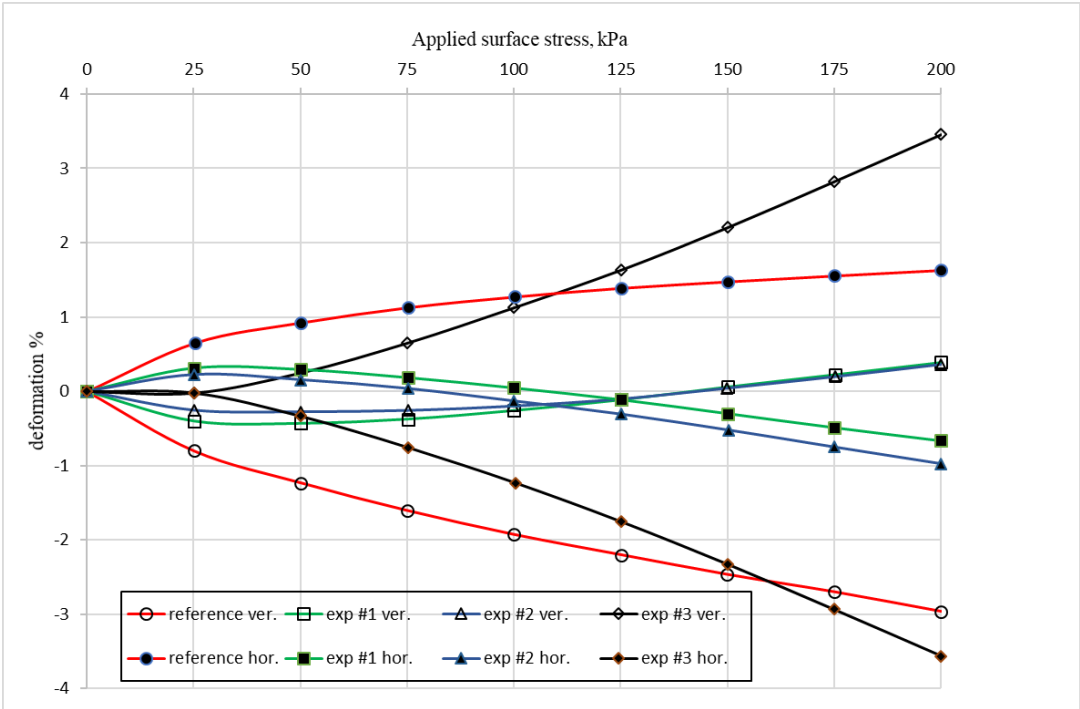


Figure 2.13. Pipe deformation for varying geofoam applications
(Akınay et al., 2016)

Oshati et al. (2012) compared the earth pressures on a double-cell rectangular box culvert constructed by induced trench method under a 25 m embankment. Measure vertical load on the top of the culvert was only 42% of the calculated overburden pressure. Moreover, they observed that the vertical load at the bottom of the culvert was %25 more than the anticipated value of overburden pressure plus dead load of the culvert, showing the downward drag force development along the box culvert sidewalls. Centrifuge tests were done on a model culvert and good agreement was achieved between prototype structure data and model test data.

EPS application to reduce the load on culverts were studied in terms of numerical analysis, by (Sun, Hopkins and Beckham, (2005). FLAC 4.00 was used to investigate the effect of EPS width. Numerical results showed that EPS application reduced the load on the top and bottom of the culvert very significantly (Figure 2.14). It was also seen that whether EPS was applied or not, maximum moments acting on the sides did not change much. As it is seen in the Figure 2.14, the load on the culvert was nearly the same even though EPS width was increased by 50%.

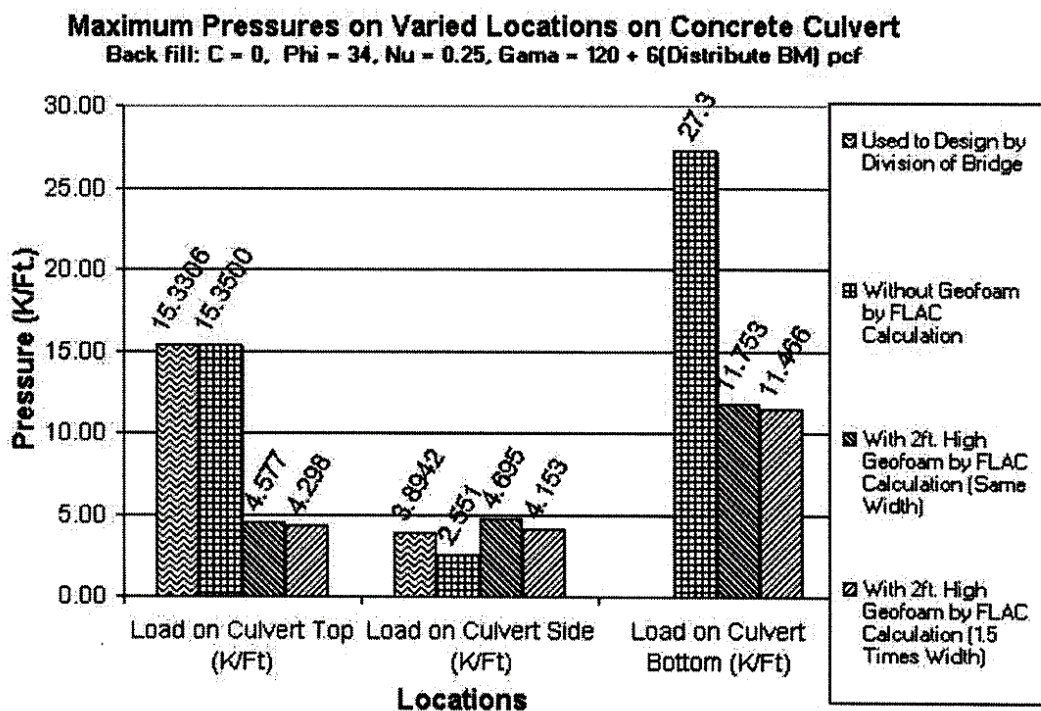


Figure 2.14. FLAC results for geofoam applications on culvert(Sun et al., 2005)

Withoef and Kim (2016) made numerical analysis to obtain the optimum geometry of the geofoam. Based on lab model tests by Kim (2010), a numerical model is established and calibrated. Boundary conditions were based on two conditions: the magnitude of vertical stress at the crown of the pipe should be as small as possible while the uniformity of stresses around the pipe should be achieved (the difference between horizontal stress at pipe spring line and vertical stress at pipe crown should not be more than 10%). According to these criteria, for their case in which a steel pipe with 10 cm diameter used, it was seen that width of geofoam should not be more than 1.5 times pipe diameter and geofoam thickness should not be more than 5 cm. Next, they modeled the application of two-layer geofoam with the above-defined geometry by only changing the spacing between them (Figure 2.15). The results showed that two-layer geofoam has no improvement effect regarding earth stress on the pipe. The reason behind this result is that second geofoam was placed under the equal settlement region, which did not change arching region. Equal settlement layer is the region above which no soil arching is observed. Neither does load transfer (Figure 2.5). The second geofoam should have been placed above the equal settlement layer. (Withoef and Kim, 2016).

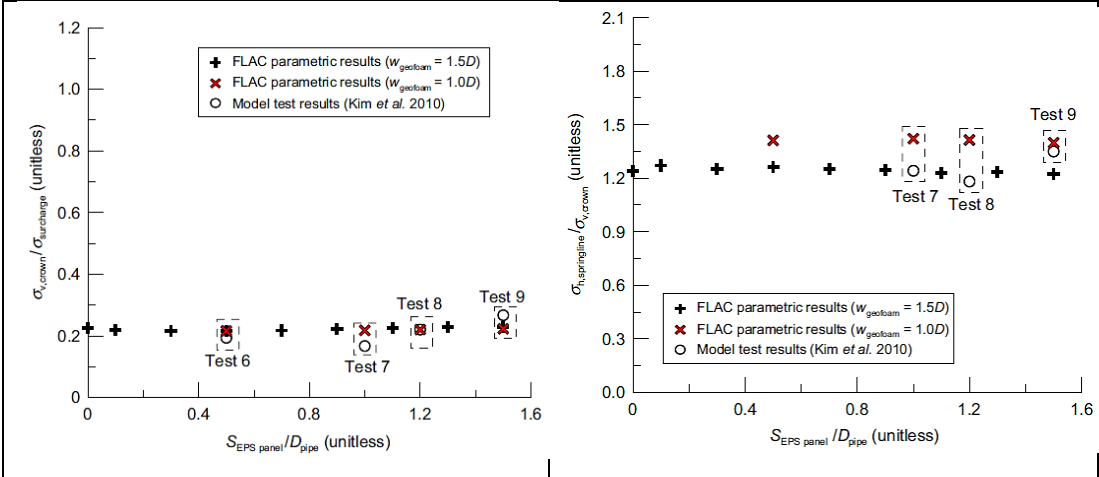


Figure 2.15. Effect of double layer and spacing on pipe, FLAC results (Withoef and Kim, 2016)

Its light-weight and relatively compressible nature makes geofoam favorable to be used as backfill and cover material to protect pipelines from the deleterious effects of

permanent ground displacement (Yoshizaki and Sakanoue, 2003; Choo et al. 2007; and Lingwall, 2009). Yoshizaki and Sakanoue (2003) observed that compared to typical sand cover, geofoam placement above the 100-mm steel pipe reduced the peak horizontal force on the pipe up to 40-60% when the pipe displaced 150 mm horizontally. Choo et al. (2007) applied geofoams both on the cover of pipe and sidewalls of the trench. According to centrifuge testing of scaled model results, depending on the geofoam block placement manner, peak transverse lateral force can be reduced to 80-90% of the no-geofoam case. This resulted in 45-60% reduction in pipe bending strain compared to without EPS geofoam design. Lingwall (2009) made two full-scale tests to see the effect of EPS geofoam on the buried steel pipeline for a potential vertical offset situation. In the first test, EPS29 was used as a cover material on the pipe whereas the second test is made by the typical sand cover. 6.1 m length, 32.4 cm outer diameter steel X42 pipe buried in the trench is slowly pushed up by using a crane to simulate vertical offset.

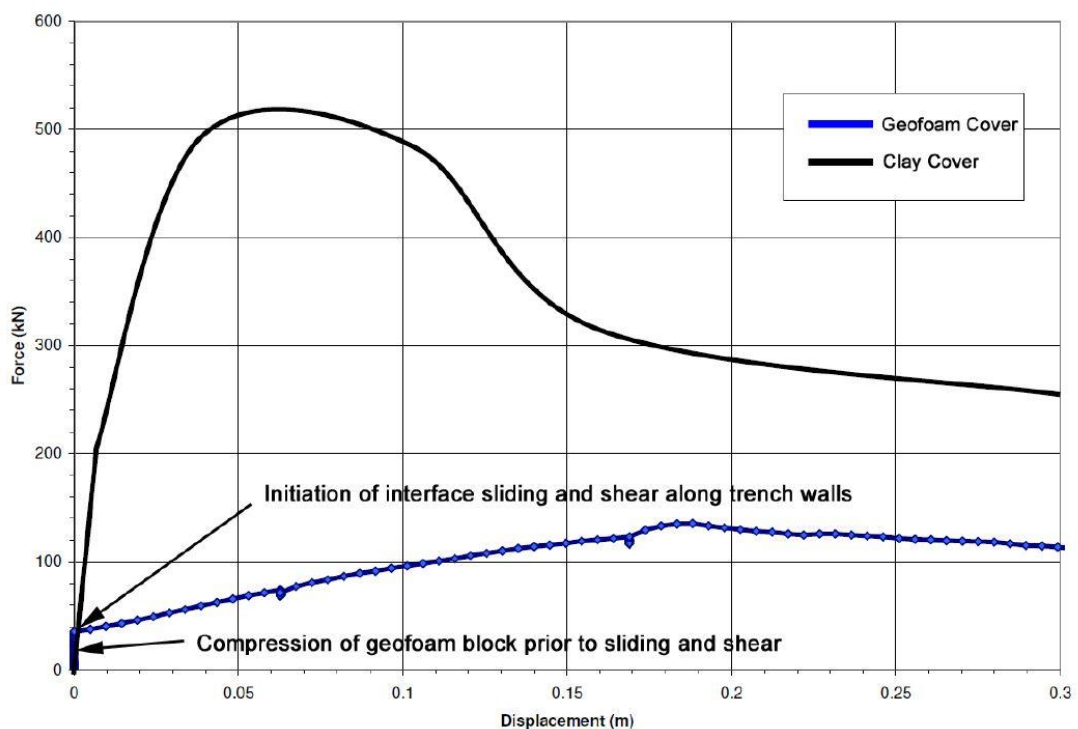


Figure 2.16. Geofoam effect for geofoam uplift field tests (Lingwall, 2009)



Figure 2.17. Geofabric application for earthquake-induced excess pipe displacement

(Bartlett et al. 2011)

Test results showed that the former experiment reduced the peak force on the pipe to 136 kN, compared to the sand covered experiment with a peak uplift force as 520 Kn (Figure 2.16). Moreover, the force-displacement behavior of the geofabric system was more desirable; it showed that about 2.75 times more displacement was required to mobilize the peak uplift resistance (Lingwall 2009). Numerous other studies about the improvement of the pipe against excessive displacement were done experimentally and numerically (Figure 2.17). (Bartlett et al. 2011; Lingwall and Bartlett, 2014; Bartlett et al. 2015)

Geofabric layers were also used to improve the impact behavior of buried pipelines. (Anil et al., 2015; Anil et al., 2017). Anil et al. (2015) made lab experiments by dropping a 5.25 kg hammer from 50 cm distance to buried steel and composite pipelines. Three different protective layers were used for these two different pipes: an extra 13 cm sand cover, a 50 mm thick EPS30 panel and a 30 mm thick EPS30 panel. Regardless of the tested pipe material, placement of the EPS panel with 5 cm thickness improved the pipe impact behavior most by reducing acceleration and displacements and increasing energy absorption. ABAQUS program is also used to compare the test results and it was seen to be very consistent with lab results in terms of acceleration and displacement.

CHAPTER 3

TEST MATERIALS AND SET UP

3.1. Çine Sand

In the laboratory tests, a granular soil is preferred to represent the fill used in buried pipeline installations. Çine sand was used as bedding material and backfill soil in the laboratory model experiments. Laboratory tests were done to determine the soil characteristics of the sand. According to the corresponding test results, Çine sand can be classified as a poorly-graded sand, SP referring to the Unified Soil Classification System. Grain size distribution test results of three samples taken from Çine sand can be seen in Figure 3.1.

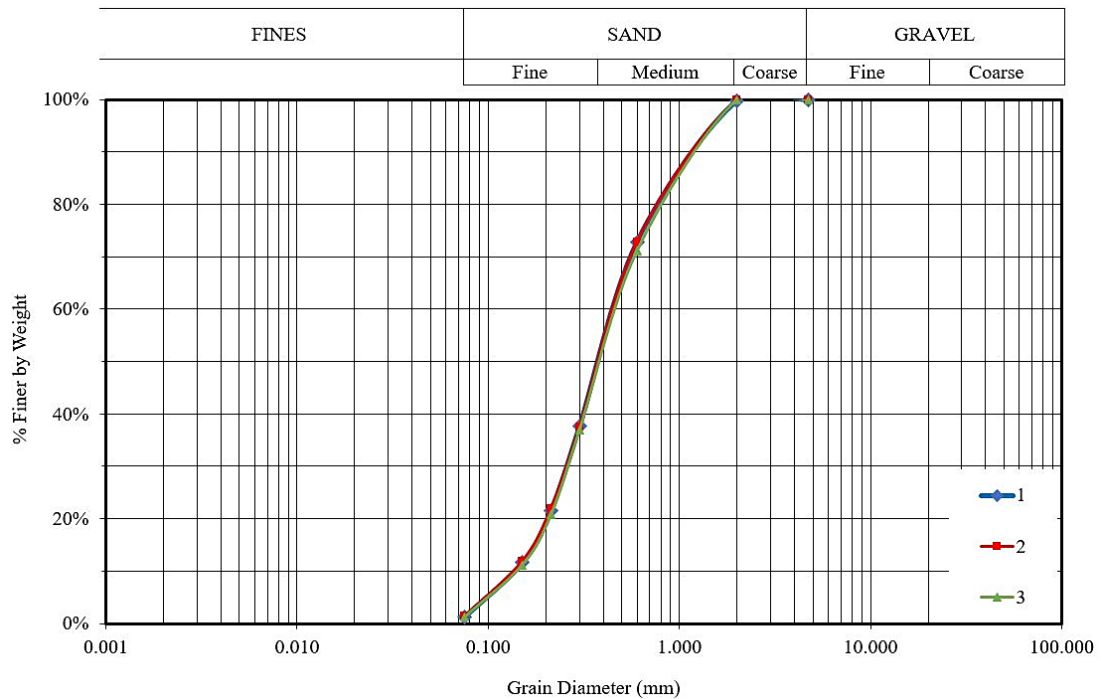


Figure 3.1. Grain size distribution of Çine sand (3 experiments)

The maximum void ratio of the sand was determined by pouring the sand through a funnel from the least height above the container. Conversely, to obtain the minimum void ratio, the sand sample was compacted by using a vibratory hammer. These studies resulted in the maximum void ratio as 0.805 and minimum void ratio as 0.505. Index properties of the Çine sand can be seen in Table 3.1. In the model tests, a void ratio of the sand was always less than or equal to 0.540 to achieve a relative density of %90 or more.

Table 3.1. Çine sand index properties

D ₁₀ (mm)	0.135
D ₃₀ (mm)	0.255
D ₆₀ (mm)	0.47
C _c (coefficient of curvature)	1.02
C _u (coefficient of uniformity)	3.76
Fines content % (% finer than #200 sieve size)	1.35
Maximum Void Ratio (e _{max})	0.825
Minimum Void Ratio (e _{min})	0.505
Void ratio achieved in model tests (e)	≤ 0.540
Specific Gravity	2.66

The specific gravity of the sand was determined as 2.66. Then, a series of direct shear tests were done on Çine sand at different relative densities (34%, 50% and 70%) under varying normal stress values (50, 100, 200, 400 and 700 kPa) with a shearing rate of 0.61 mm/min. It is a well-known fact for the sand that as the relative density increases, peak friction angle increases, too. Results are shown in Table 3.2 and Figure 3.2. Comparing with Schmertman (1978) chart (Figure 3.2), Çine sand shows the behavior of uniform fine sand and confirms it by having nearly %60 of passing material as seen in Figure 3.1

Table 3.2. Direct shear test results for Çine Sand

relative density, %	φ', °
34	32.6
50	34.5
70	37.9

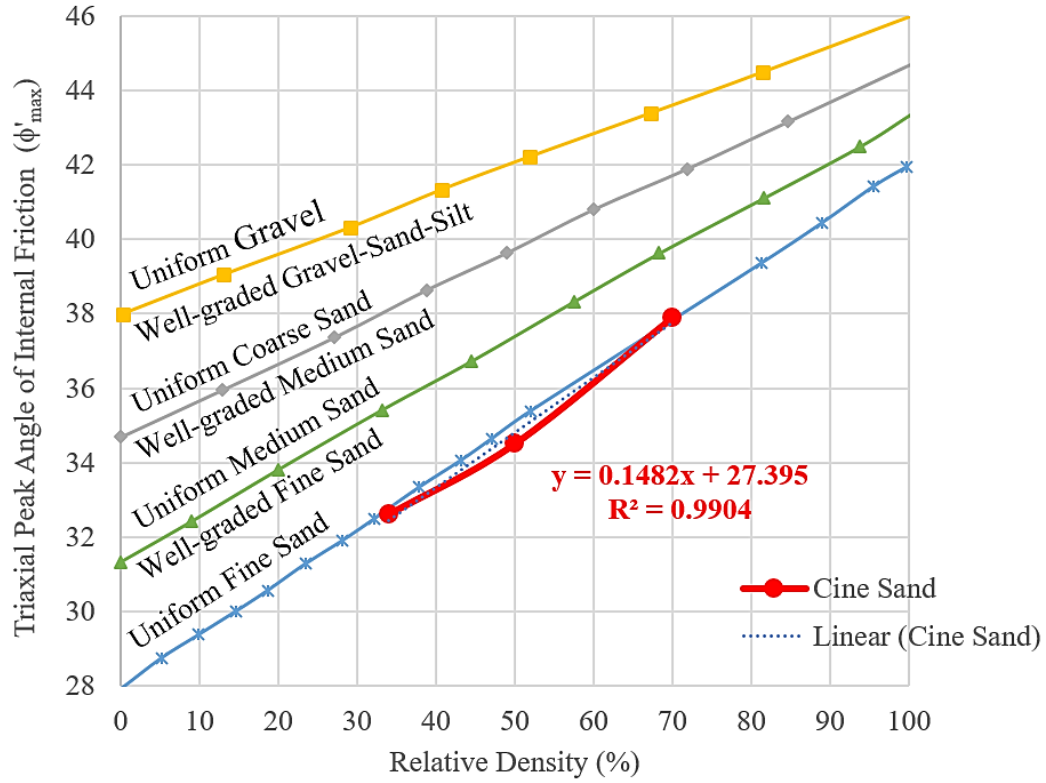


Figure 3.2. Comparison of Çine sand test results from FHWA (Schmertman, 1978)

3.2. Flexible Pipe

In the experiments, GEDIZ PVC pipe having 200 mm diameter was used. This pipe is mainly used for underground drinking water and wastewater networks. These pipes have a nominal outer diameter as 200 mm with 3.9 mm thickness along the section. Mechanical properties of the pipe could not be gathered from the manufacturer. Hence some tests were done in Construction Material Laboratory and General Directorate of State Hydraulic Works laboratory. In the material lab, pipe stiffness of the 15 cm long pipe was aimed to find (Figure 3.3). Parallel plate load test was conducted as explained in ASTM D-2412 and the corresponding graph shown below is obtained (Figure 3.4). The specimen is compressed at a constant rate of 12.5 ± 0.5 mm/min.



Figure 3.3. Parallel Plate Test Setup

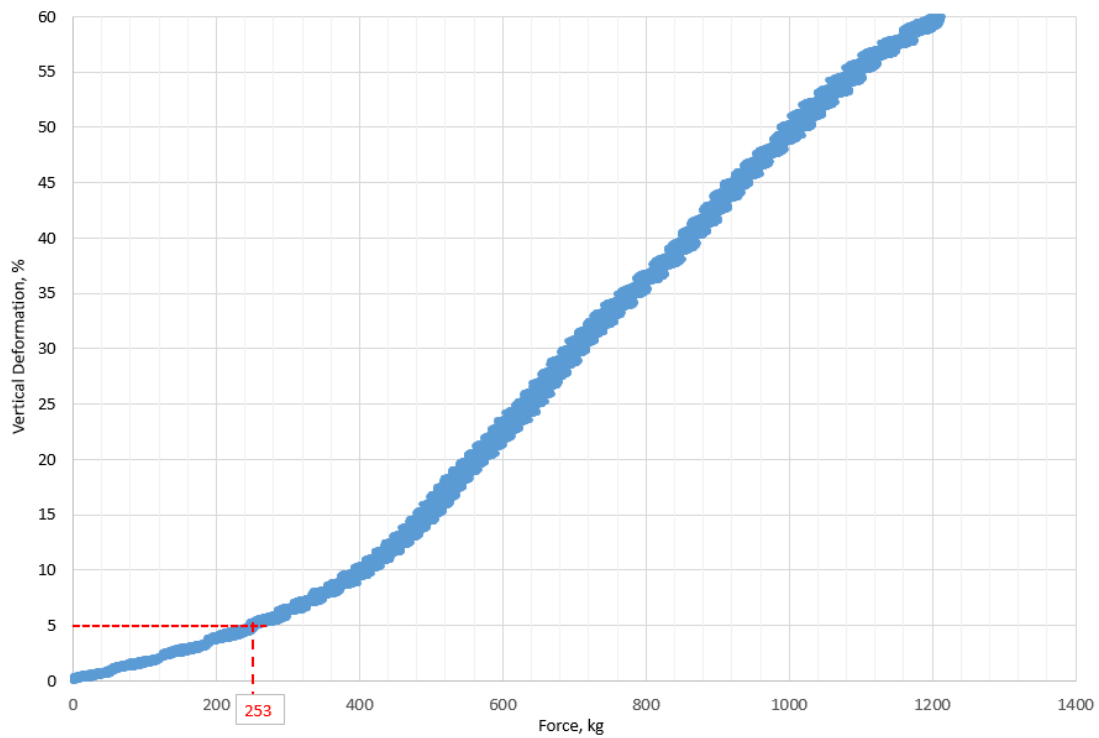


Figure 3.4. Parallel plate test results for the 15 cm long PVC pipe with 20 cm diameter

$$\text{Pipe stiffness} = \frac{F}{L \cdot \Delta y} \quad (3.1)$$

where F= load applied at the crown of the pipe

L= pipe length

Δy = the vertical deflection of the pipe.

According to ASTM D-2412, pipe stiffness is calculated as 1.68 MPa.

In the laboratory of the General Directorate of State Hydraulic Works, elongation tests were done for the pipe material. The pipe was cut in defined geometry for elongation tests, and five tests were applied (Figure 3.5). The elastic modulus of the pipe material was determined and compared with Dielectric Corporation data. Corresponding charts and tables are shown below (Table 3.3).

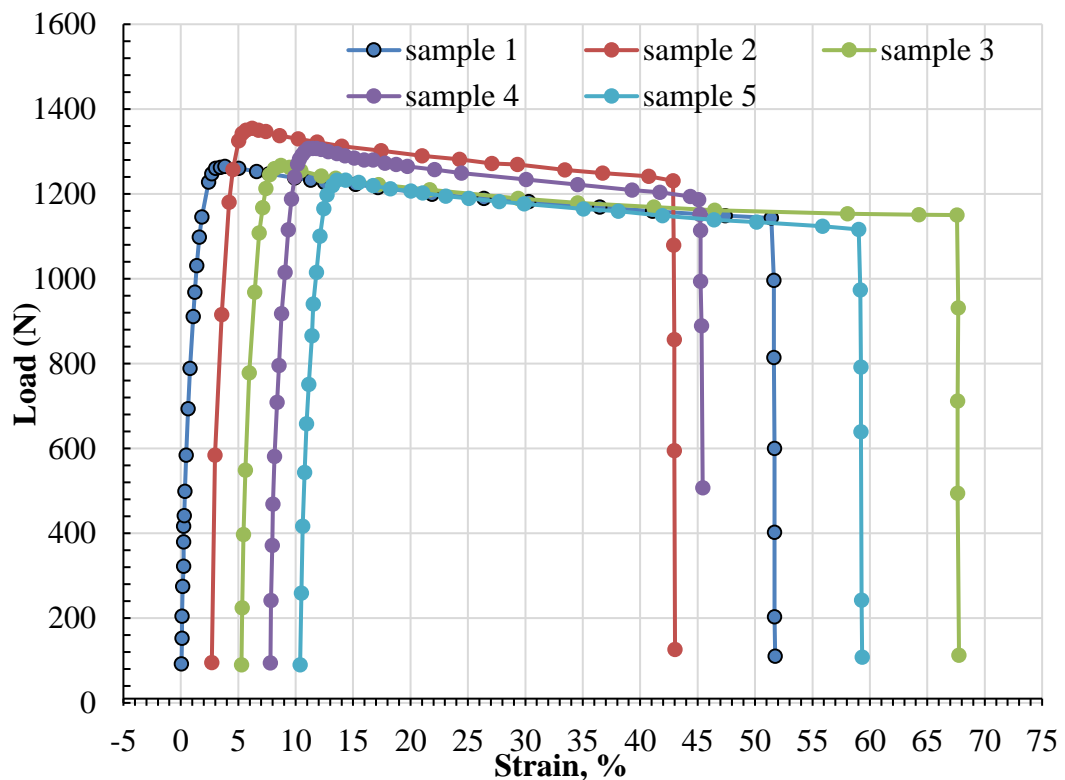


Figure 3.5. Elongation Test results for PVC material

Table 3.3. Material properties of PVC (* is taken from <http://www.dielectriccorp.com>)

Sample #	1	2	3	4	5	Average	Dielectric Corp. *
Yield strength, Mpa	32.93	31.1	32.25	34.01	32.45	32.55	41.4 - 52.7
Tensile strength, Mpa	32.93	31.1	32.25	34.01	32.45	32.55	41.4 - 52.7
Elongation, %	51.32	40.17	62.26	37.47	48.65	47.97	40 - 80
Young's modulus, Gpa	2.50	3.63	2.82	3.50	2.45	2.98	2.48 - 3.30
Poisson Ratio	-	-	-	-	-	-	0.40

3.3. EPS Geofom

The American Society of Testing and Materials (ASTM) defines geofom as a block or planar rigid cellular foam polymeric material used in geotechnical engineering applications. It also defines expanded polystyrene (EPS) as a type of foamed plastic formed by the expansion of polystyrene resin beads in a molding process (American Society for Testing and Materials 2007).

In the experiments, geofoms with varying geometries (thickness, width) and densities were tested (EPS 15, 22 and 30). Also for the same geometrical properties and same density, the effect of the configuration of the geofom (comparing to the location of pipe) and the distance between two identical geofoms (spacing) were studied.

Geofoms used in the tests were obtained from the company Tipor Strafor. The manufacturer provided mechanical properties of the EPS16 (Table 3.5 & Figure 3.7) and EPS26 (Table 3.6 & Figure 3.8). It is known that strength of the EPS depends on dimensions and density of the material, therefore in the Materials of Construction Lab, six more specimens were tested to figure out the corresponding stress values at 1, 5 and 10% strain values (Figure 3.6). Each specimen was loaded at %10 strain/per minute as described in ASTM- D6817. 2 cube samples with 10 cm dimensions and densities as 21.7 and 21 kg/m³ were loaded with normal plates whereas four other specimens (length 100 cm, width 50 cm) whose thickness values are 3 cm and 5 cm

and density values are 10, 16 or 20 kg/m³ were loaded through 26 cm-steel plate (Figure 3.9). Tabular results can be seen in Table 3.4.

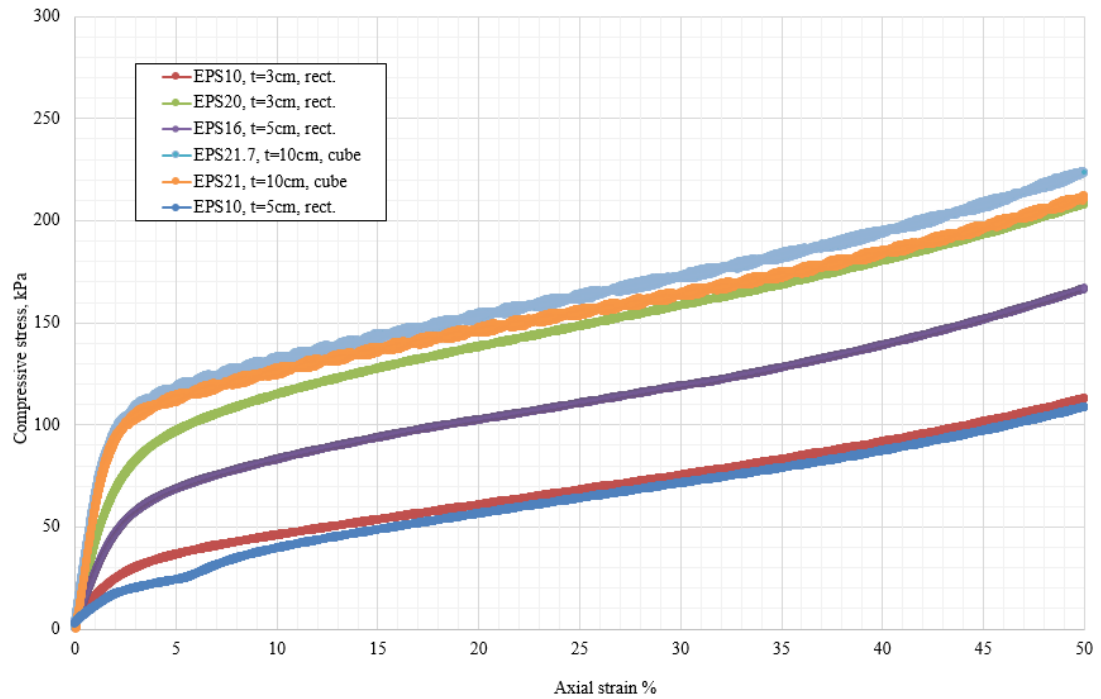


Figure 3.6. Compression test results for varying geofoam geometry and densities

Table 3.4. Geofoam compression test results

EPS 21.7, cube		EPS 21, cube		EPS 20, t=3 cm	
Strain,%	Stress, kPa	Strain,%	Stress, kPa	Strain,%	Stress, kPa
1	64.79	1	58.43	1	41.65
5	117.80	5	112.44	5	96.82
10	131.67	10	125.73	10	114.79
EPS 16, t=5 cm		EPS 10, t=3 cm		EPS 10, t=5 cm	
Strain,%	Stress, kPa	Strain,%	Stress, kPa	Strain,%	Stress, kPa
1	27.34	1	15.75	1	11.09
5	68.42	5	36.43	5	24.12
10	83.05	10	45.98	10	39.53

Table 3.5. %10 compressive stress for EPS16, loading rate=5.0 mm/min (by TIPOR)

sample #	Width, mm	Length, mm	Height, mm	% 10 compressive load, N	% 10 comps. Strength, kPa
1	49.58	49.04	50.3	298.4	122.7
2	49.28	49.11	50.65	296.4	122.5
3	49.07	48.89	50.49	290	120.9
AVERAGE				294.93	122.03

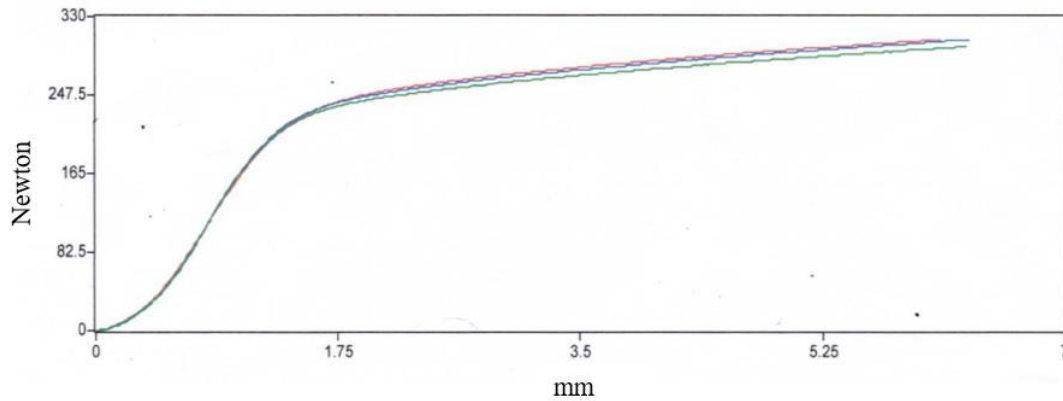


Figure 3.7. Load vs. Elongation Graph for EPS16 (by TIPOR)

Table 3.6. %10 compressive stress for EPS26 loading rate=4.9 mm/min (by TIPOR)

sample #	Width, mm	Length, mm	Height, mm	% 10 compressive load, N	% 10 comps. Strength, kPa
1	51.04	50.13	49.26	557.7	218
2	51.11	49.92	49.47	560.5	219.7
3	51.09	50.92	49.11	535.9	206
AVERAGE				551.37	214.57

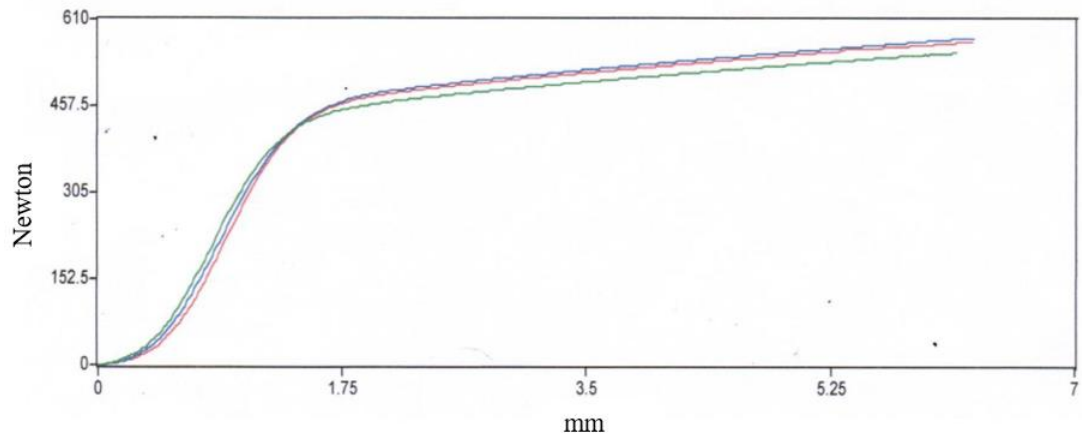


Figure 3.8. Load vs. Elongation Graph for EPS26 (by TIPOR)



Figure 3.9. Geoforce Loading Experiments in Material Lab

3.4. Test set-up

The test setup mainly composed of two parts, a testing tank and hydraulic loading part. The testing tank is composed of aluminum segments which have a geometry as 100 cm x 100 cm square cross-section, with a 10 cm height. The front part of the aluminum segments is partly plexiglass (Figure 3.9). In this thesis study, total experiment height was constant and 60 cm, i.e., a total number of 6 segments are required during the tests. The lowest segment is fixed on the roller surface; the remaining frames put sequentially above the lowest one. To prevent leakage of sand during the experiments through the frames, frame interfaces were taped inside and outside.

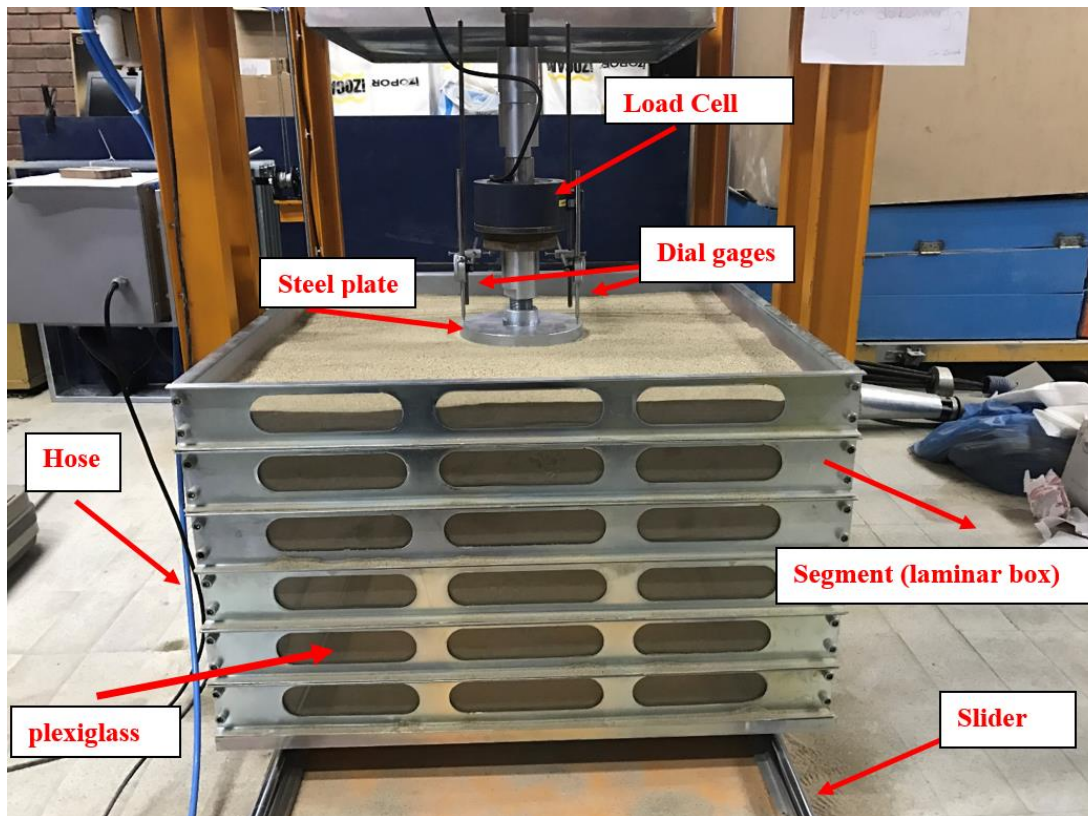


Figure 3.10. Test Setup Components

The test setup enables the user to move the testing tank easily on the slider. At the end of the slider, there are rubber materials to prevent strong collision to the edges during movement. Once the testing tank is ready, it is moved along the rollers to pneumatic loading section. The set-up also has a sand pluviation section, in which a huge box is perforated by 2 mm holes, a pulley system adjusts the box elevation and it is subjected

to vibration by a vibratory motor connected to the setup to rain the sand to create a required soil density as homogeneously as possible. However, this section was never used for this thesis experiments because required density for the experiments was higher than what could be achieved by using pluviation system.

The pneumatic loading device is designed in such a way that 6 bar of air pressure could come close to simulating the truck tire pressure of 720 kPa (Figure 3.10). In the experiments, once the test setup is prepared, i.e., inserting the pipe and geofoam(s) in defined locations and filling the tank with sand, testing tank slides over the rollers to the loading piston location. Pneumatic jack is connected to the compressor by a hose, and presses on the 26 cm diameter steel plate, to apply the load incrementally to the sand in the tank. The steel plate geometry is taken from AASHTO specifications. The pneumatic piston has a stroke of 10 cm, i.e., it can extend its tip 10 cm lower from the initial position. In order to eliminate this height constraint, custom produced segments are used to arrange the location inside the tank by plugging to end of the pneumatic load shaft.

3.5. Linear Potentiometers, Load Cell and Dial Gages

Two linear potentiometers -resistive linear position transducers- were used for the experiments to determine the horizontal and vertical deformations inside the pipe. Their model is OPKON SLPS 25-5K, which has 25 mm stroke and 5 K resistance. Resolution of the potentiometers is 0.01 mm. Their calibrations were done using a micrometer. According to calibration cycles results for 10 V input, potentiometer 1, PT1 and potentiometer 2, PT2 calibration coefficients for linear trend are shown in Table 3.7.

Table 3.7. Linear trend coefficients of the potentiometers

	Coefficient, mm/V	R ²
PT1	2.4819	0.9988
PT2	2.5004	0.9945

Even though they were operating very well, in some experiments the horizontal one - regardless PT1 or PT2- stopped measuring deformation because of either leaving its socket inside the pipe or rotating excessively or simply getting stuck inside the pipe socket. Therefore, horizontal deformations were not successfully obtained in every experiment. However, there was not any problem in vertical deformation measuring potentiometers.

Pneumatic jack was connected to an annular load cell to enable the user to observe the applied load at any time. Available load cell that could be used in the experiments has a 20000 kg capacity. As input values of the load cell, only the capacity of the load cell and fractional output values of the volt is required. Fractional value of the volt is stated as 2.0006 mv/V on the product.

During the experiments, settlement of the steel plate on the surface was also measured by using two 100 mm range dial gages with 0.01 mm accuracy located on the opposite sides of the 26-cm diameter steel plate. Two dial gages were used to check that no differential settlement happened. In pavement design, it is assumed that tire pressure is distributed uniformly over a circular area (Kawa et al., 1998). 26 cm diameter steel plate was manufactured based on ASSHTO LRFD 1998 specification (Figure 3.11).

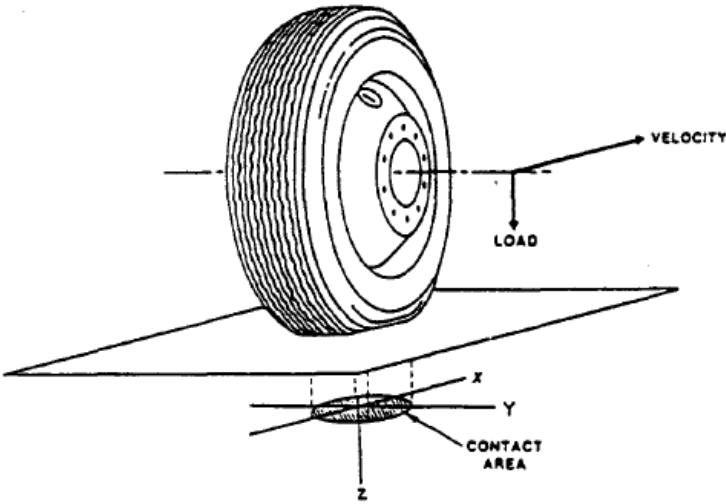


Figure 3.11. Tire/Road contact area and force component directions (Yap, 1989)

3.6. Data Acquisition System

TDG TESTBOX 1001 Data Acquisition System was used in these experiments. This is an 8-channel 16-bit integrating A/D converter that connects to a PC via the serial port. Three channels were used for the studies: one for load cell and other two were for potentiometers (Figure 3.12). In order to read a more accurate data for load, the channel gain of the load cell was increased to 890. Excitation value of the load cell data was 5 Volt. On the other hand, no channel gain applied for the potentiometer channels except for the corresponding excitation value was arranged as 10 Volts.

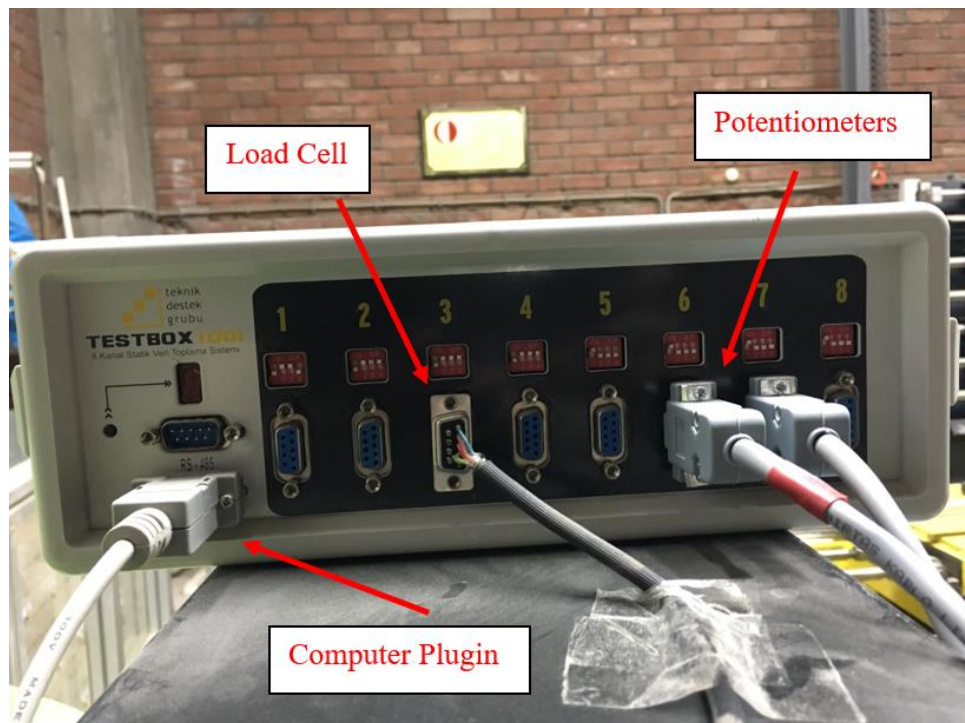


Figure 3.12. TDG Test box 1001 Data Acquisition System

The software is composed of two parts: experiment preparation part and data recording part. In the first part, calibration parameters and calibration validity duration of the devices, the format of the output data are defined. Active channels are appointed and after these steps, the corresponding document is saved as an experiment with a defined name. In the second part of the software, the program calls the defined experiment and once data recording is initiated, active channels show their corresponding readings, i.e., load in kg and horizontal and vertical deformations in mm.

CHAPTER 4

TEST PREPARATION

These studies are done to show the improvement effects of geofoms – if any - for a buried flexible pipeline under a static loading. The main concern about the experiments is to observe the deformation of axial pipe geometry, especially vertical deformation, settlement of the loading plate on the surface and the load which is responsible for this changes in the system. It was needed to ensure that sand has the required relative density at least 85% which is stated in General Technical Specification for HDPE Pipelines by State Water Works (Devlet Su İşleri) hence the relative density of the sand layers are also checked.

4.1. Flexible Pipe Preparation

As stated previously, GEDİZ flexible pipes with 200 mm diameters are used for this study. Commercially these pipes are sold in 2-meter lengths. Therefore firstly these pipes are cut into two segments by using electrical saw whose lengths are 90 cm (Figure 4.1). Pipe lengths are chosen 90 cm because of few reasons:

1. Test tank has 100 cm * 100 cm geometry. Therefore a 90 cm long pipe would subject to no frictional resistance on the edges of the test tank.
2. Loading above the pipe would be acting totally on the pipe geometry, i.e., the pipe would be long enough to eliminate boundary conditions for the loading area.



(a)



(b)

Figure 4.1. A 2-meter long pipe (a) & pipe cutting (b)

Potentiometers were used to measure the deformation of the pipe on its axes. The total length of the potentiometers is nearly 16 cm and for a 20 cm pipe, contact to pipe surface was not likely to be achieved. Some tools were made to arrange the height of the potentiometers inside the pipe and fix the potentiometer (Figure 4.2).

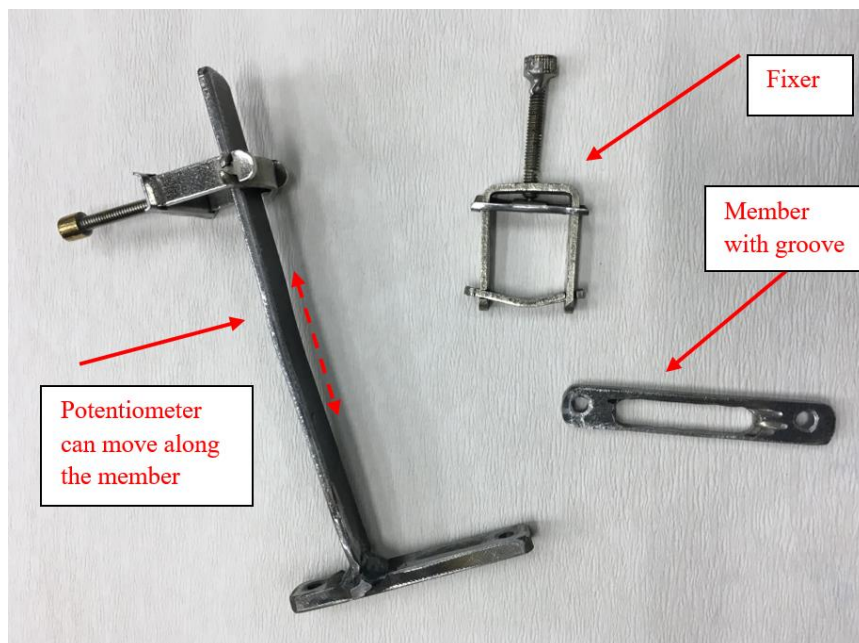


Figure 4.2. Special tools for the potentiometer measurement

Potentiometer could slide above this tool and it can be fixed with two apparatuses once the desired configuration is achieved. Also, to ensure that potentiometers will not move or rotate inside the pipe, during the experiments, a steel member with a groove in the middle portion was attached to the pipe for the tip side of the potentiometer (Figure 4.3). Total 8 holes with 4 mm diameters are drilled on the pipe to attach these members inside the pipe. 4 mm screws were used to fix the members.



(a)



(b)

Figure 4.3. Potentiometer Installation (a) & steel member with groove (b)

Vertical deformation of the pipe is measured at the midpoint of the pipe, whereas horizontal deformation of the pipe was measured 3 centimeters away from the vertical deformation measurement location to prevent the contact of the potentiometers inside the pipe. To check if the potentiometers are working well inside the pipe, after they were implanted inside the pipe, they are connected to the data logger; a little load is applied and released on the pipe in few cycles to ensure potentiometer tip is not stuck after some deformation. Once the system is proven to work, the ends of the pipe are covered with package tapes to prevent soil entrance (Figure 4.4).



(a)



(b)

Figure 4.4. Potentiometers in 90 cm long pipe (a), pipe covered by tape at the ends (b)

4.2. Test tank preparation

All experiments are done in a total of 60 cm height test tank. Six aluminum frames compose this height, the lowest one is fixed to the slider but can move freely. The frames are covered from inside and outside with tapes to prevent soil leakage while filling the tank, vibrating the soil or applying a load to the plate (Figure 4.5).



(a)



(b)

Figure 4.5. Laminar box interfaces are taped inside and outside (a) & Vibratory hammer (b)

Test tank is moved to the end, closer to the sand tanks. Sufficient amount of sand to create an 11-12 centimeters height of layer is put into the test tank by shovels; then its surface is leveled. By using a 30 cm x 30 cm wooden plate in between soil layer and vibratory hammer, sand is compacted as homogeneously as possible. Each compaction activity is done with nine steps, except for the layers which have a pipe inside it. Starting from the one edge of the tank, corners are compacted successively first, and then the mid part of the edge (Figure 4.6). Once one side is done, then the other side is compacted in the same way. In the end, the middle part of the tank is compacted, starting from the edges and finishing with the center of the tank. If there is a pipe, i.e., 2nd and 3rd frames from the bottom, these layers are compacted in 6 steps; same procedure described for nine steps above except for the last three vibration stages. Vibration is continued in a layer until the plate is completely penetrated into the loose sand - generally takes less than 20 seconds.

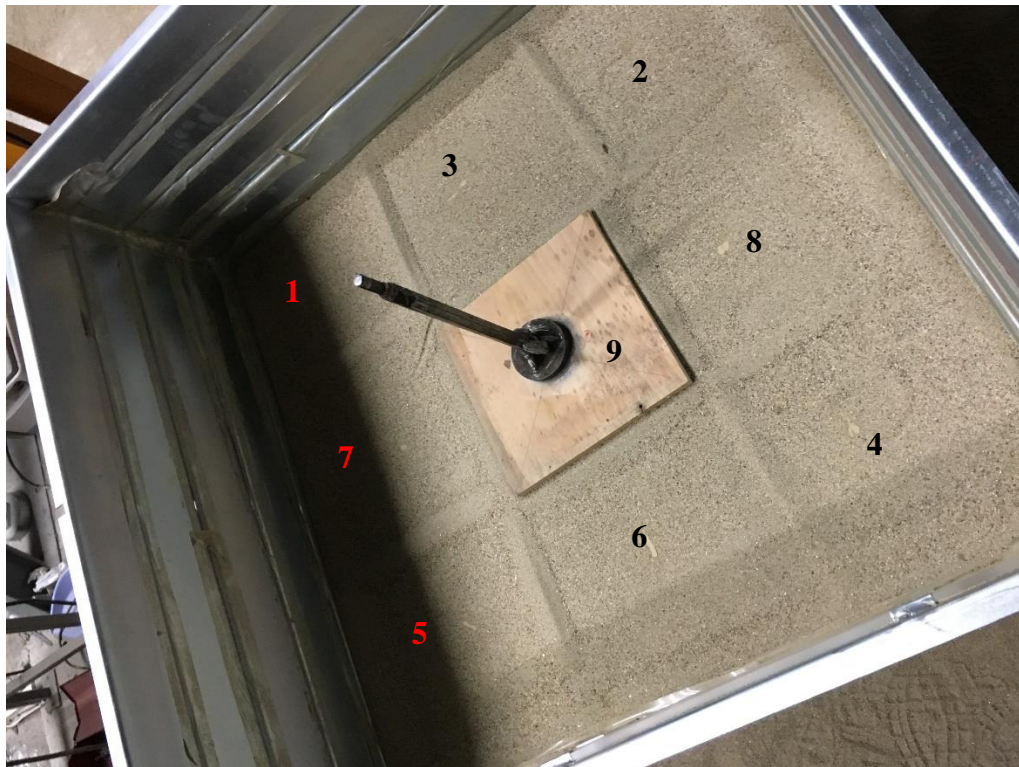


Figure 4.6. Compaction order of the soil layer

Once the first layer, i.e., bedding layer is compacted, leveling is done. Then the pipe is laid on the sand. Attention is paid to ensure that pipe stays exactly in the middle of

the tank, in perfect shape, so that horizontal and vertical deformations are real values, without any distortion. Before filling the second level, all readings of horizontal and vertical potentiometers are set to zero. Also for the layers with a pipe, soil density boxes are put on the pipe sides, 3 per each side, to calculate the relative density of the compacted sand at the end of the experiments (Figure 4.7). Then the second layer is started to be filled with sand, again a total of nearly 11 cm soil layer height is created by throwing sand using a shovel. Leveling is done once the required height is achieved, then sand is compacted in 6 steps. The process is repeated for the 3rd level (6 more density boxes, 11 cm soil compacted at 6 locations), burying the pipe into the sand. Again the pipe's vicinity is not compacted. To summarize, once the lower 30 cm of the tank is filled, the test tank has a pipe in the compacted soil with 12 density boxes.



Figure 4.7. Installation of density boxes (a) & compaction order in pipe layer (b)

In the experiments, except for the ones in which aim is to see the effect of the location of the geofoam for buried pipeline improvement, all geofoams are placed 5 centimeters above the pipe crown. Therefore, an extra of nearly 6 centimeters of sand is created in the test tank, and compaction is done in 9 stages. Leveling of the soil surface is done and geofoam is located in the middle part of the test tank (Figure 4.8). Also, four density boxes are put on the geofoam layer, two to be on each side. Up to now, 35 centimeters of compacted sand, a pipe totally buried inside it beneath nearly 5 centimeters below the surface, 12 density boxes buried in the sand, a geofoam laying on the surface of the compacted soil with four density boxes around it. It is important

to state, during the filling part of the experiments, firstly the horizontal deformation was more significant and the pipe was compressed along the horizontal axis and extended in the vertical direction. This is very understandable since, in the layers containing pipe, only sides of the pipe are compacted, which caused an increase in lateral pressure acting on the pipe. However, after the 35-centimeter layer, soil above the pipe is also started to be compacted, so the pipe is compressed in the vertical direction and elongated in the horizontal direction. Once all the tank is filled with compacted sand, just before starting the experiment, deformation in the pipe in any axes was either zero or insignificantly small (0.1 to 0.3 mm). Therefore, all the deformations measured in the pipe were referenced to the placement of the pipe.

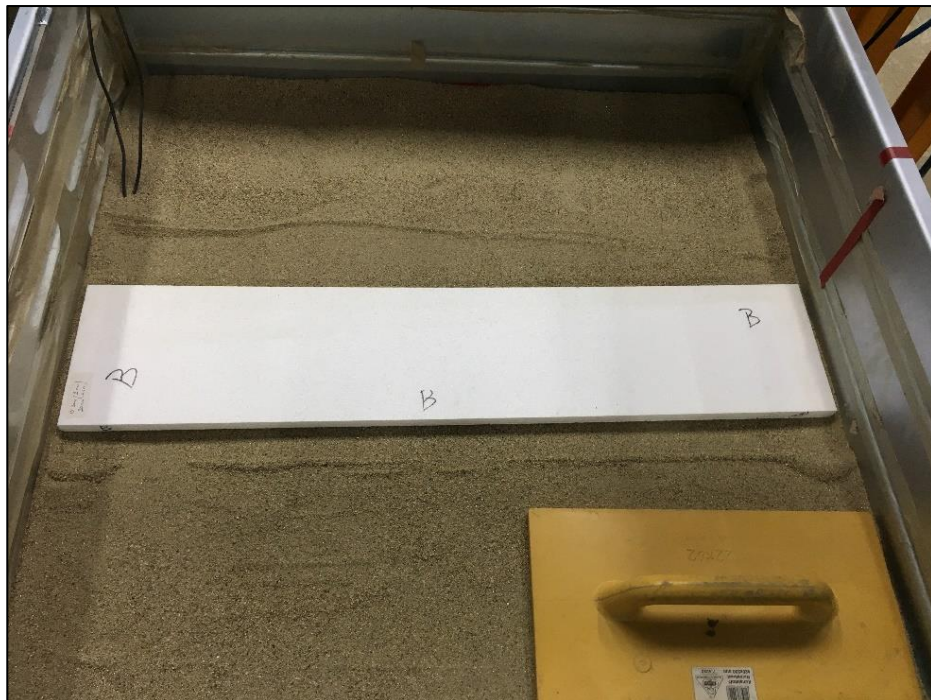


Figure 4.8. Placing of the geofabric & leveler to smoothen the surface

After this step, if no other geofabric is going to be placed (double layer geofabric), the 5th level of the tank, filled with the sand and compacted at 9 locations. Then compaction by the vibratory hammer is done. After the compaction, another four density boxes are put on the leveled surface. And to finish the test tank preparation part, it is totally filled with sand and the 6th level is compacted (Figure 4.9). The surface

is leveled for the loading plate. The result is a tank full of compacted sand, nearly 59-60 cm sand height, and inside, there is a flexible pipe with two potentiometers located in its axes to measure the horizontal and vertical deformation, 20 density boxes to check the relative density of the compacted sand, and one or two geofoams. Test tank is ready to experiment.



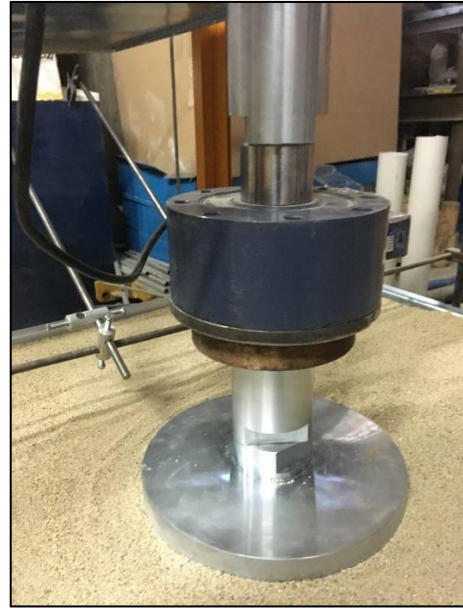
Figure 4.9. Last two compressed soil layers after geofoam placement

4.3. Load plate and dial gages

After the top surface of the compacted sand is leveled, the 26-cm-diameter steel plate is located at the midpoint of the test tank. To make sure that it is exactly under the loading piston, test tank is moved to pneumatic loading part while the plate is resting on the soil surface, and comparing with the male part of the steel plate concerning female part of the load cell; exact alignment is achieved. The load cell is attached to the pneumatic loading device. Once it is ensured that steel plate is placed correctly, spacers are put onto the steel plate to cover the jut and also to ensure that load cell surface will be totally covered by a plate which is as close as possible in order not to waste stroke of the piston (Figure 4.10). After this arrangement, reference bars are arranged to place dial gages on the steel plate. These bars are not attached to the test setup, an independent system that stays outside of the test setup (Figure 4.11). Bar connections can move horizontally or vertically to place the dial gages correctly.



(a)



(b)

Figure 4.10. 26-cm steel plate and load cell (a), spacers added to ensure full contact with load cell (b)



Figure 4.11. Reference bars to place dial gages on the steel plate

After that, 10 cm stroke dial gages are placed on the steel plate on opposite sides. Attention should be paid that dial gages and reference bars will never contact with the

rest of the setup throughout the test and also dial gages are vertical (Figure 4.12). During the placement of the gages, a bubble level is used.

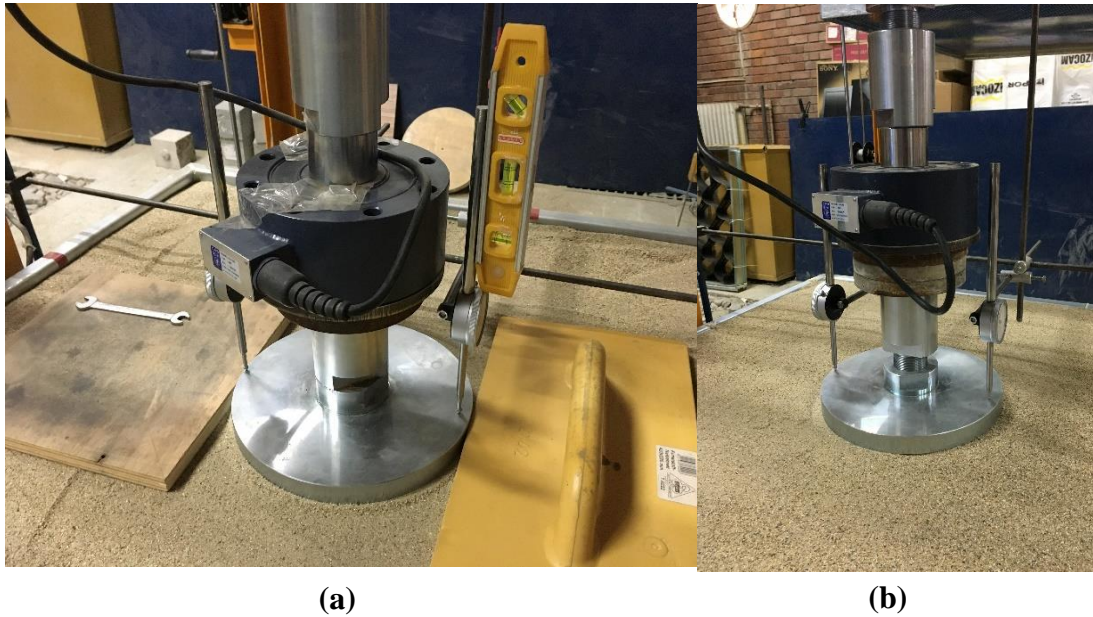


Figure 4.12. Dial gage installation with bubble gage (a) & final form (b)

In each experiment, there are five sets of data to record: applied load in kg by the load cell, horizontal and vertical deformations of the pipe in mm by potentiometers, and settlement of the steel plate in mm by two dial gages. Once the dial gages are put in place, these 5 data are recorded for the first time, without the loading plates touching the soil (zero). Then the air in the piston is softly released so that loading components will start to go down with their own weight. After full contact is achieved and air pressure is decreased to zero, these five readings are recorded once again (Seating). The difference between zero and seating steps are nearly a 15 kg increase in kg, up to 1 mm settlement in steel plate. No difference or very negligible difference is observed in pipe dimensions between these steps (Figure 4.13).

The hose from the compressor is directly plugged to the pneumatic piston. From now on, the pressure in the cylinder is progressively increased by increments of 0.25 bars, which corresponds to approximately 200-kilogram-force per each reading (Figure 4.14). After each increment, we wait until stabilization in potentiometric rulers and dial gages. It takes 2-3 minutes for the first readings and increases to 6-8 minutes once the geofoam fails. The procedure is continued until a total of 1.1 cm vertical

deformation (more than 5% pipe diameter vertical deformation) value is observed in pipe geometry. Once this value is reached, compressor valve is closed, the experiment is finished.

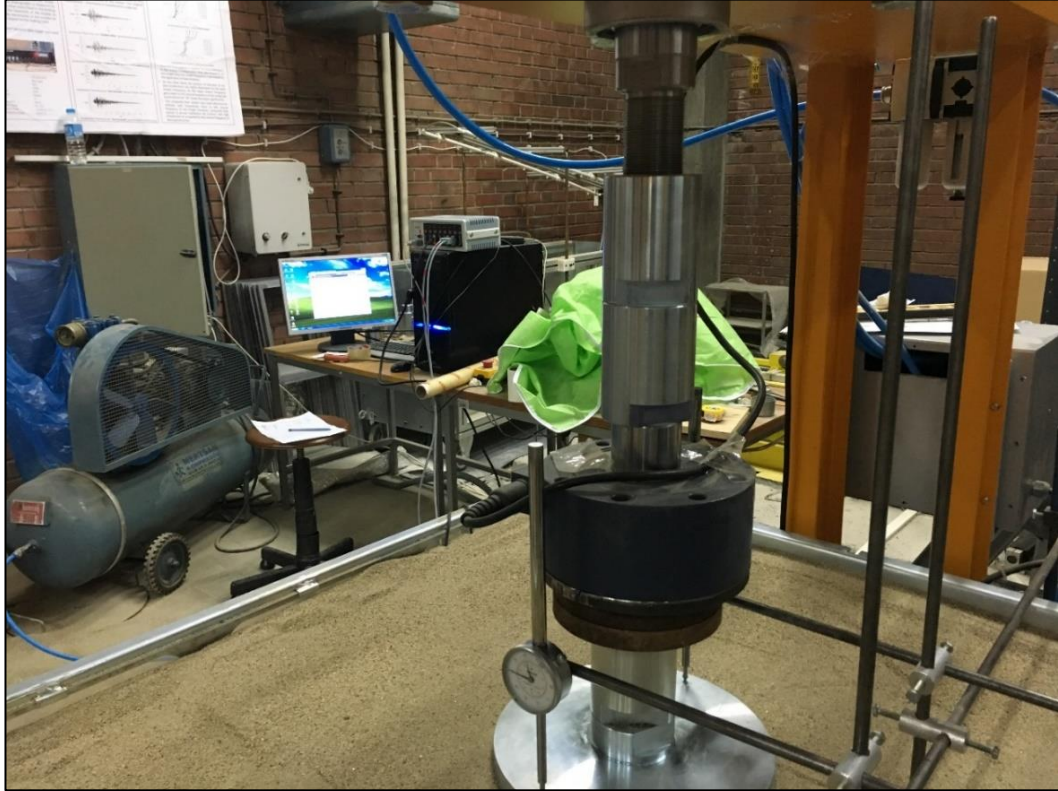
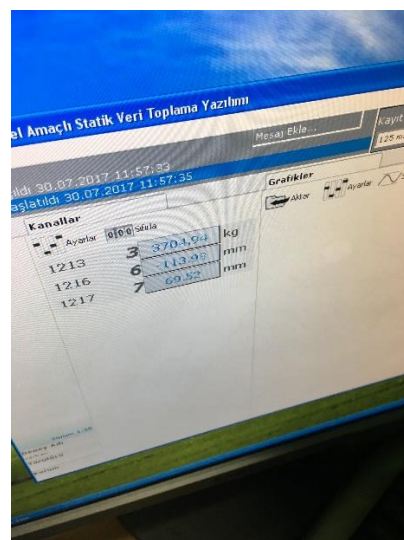


Figure 4.13. A general view of active devices during an experiment



(a)



(b)

Figure 4.14. Regulator valve to increase pressure (a) & a reading example (b)

Firstly, the dial gages are removed from the system (Figure 4.15). Then all air pressure inside the hydraulic cylinder is released. Once total pressure is zero, bypass hose is removed from the system and replaced with machine hose to activate dynamic loading system. Next, the pressure is increased to 2 bars for the machine to uplift the pneumatic loading. Load cell unit is elevated from the steel plate by the vacuum of the machine.



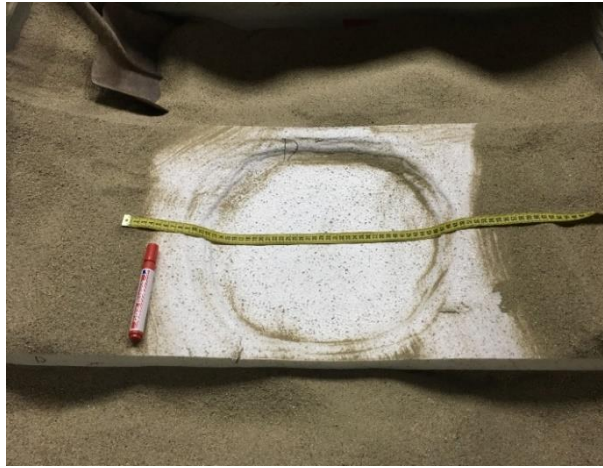
(a)



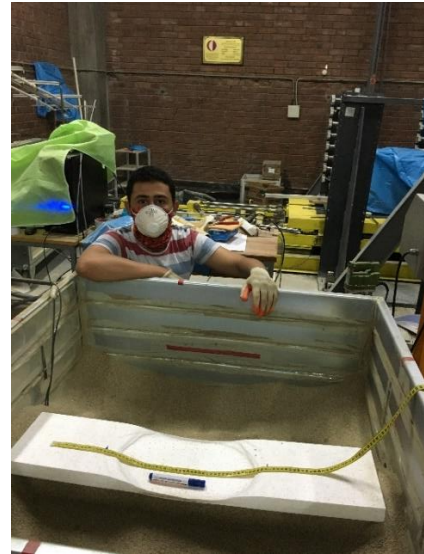
(b)

Figure 4.15. During experiment (a) & after experiment (b)

Next, test tank is moved to the edge of the slider, close to the soil tanks and excavation procedure starts. Density boxes locations are known, therefore around these points, sensitive excavations are done- with a little shovel, without hitting the box and causing the density to change- geofoam is removed from the system once required measurements and photos are taken (Figure 4.16 and Figure 4.18). Pipe section was also excavated gently starting from the edges of the tank and progressing to the pipe location. Once the pipe can move, it is removed from the buried place without damaging its cables plugged to the data logger.



(a)



(b)

Figure 4.16. A closer photo of the deformed geofabric closer (a) & test tank with deformed geofabric (b)

It is seen for all experiments that failed geofabric surface has an area larger than steel plate surface (Figure 4.17). It is an expected observation since the load on the surface is distributed over a larger area which is composed by 2V:1H geometric pattern based on the steel plate geometry and depth in soil layer.

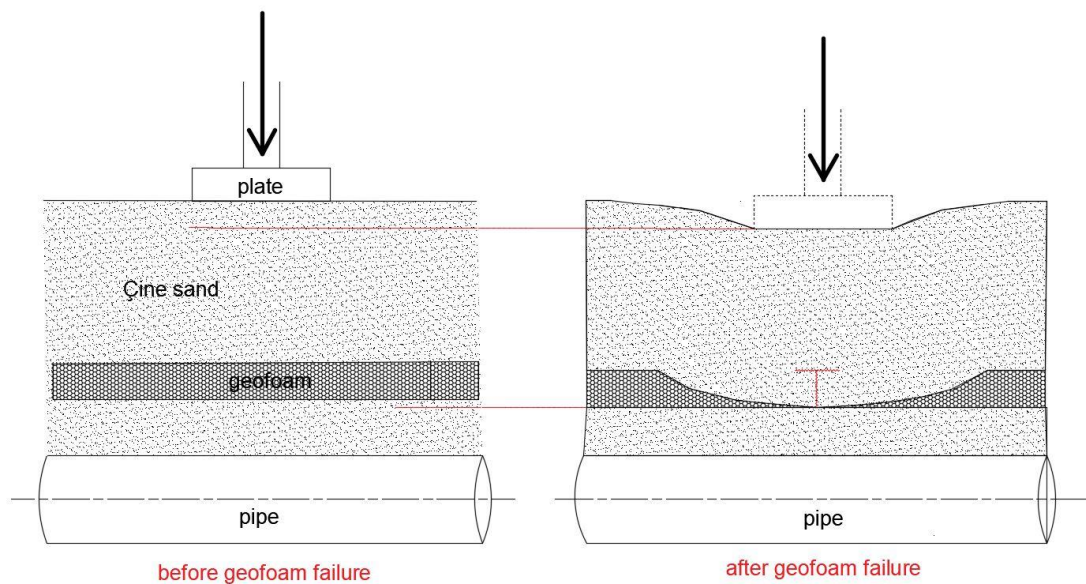


Figure 4.17. Surface plate and geofabric geometry after failure



(a)



(b)

Figure 4.18. Geofoam over the pipe (a) and density boxes (b)

In all experiments, it is seen that plastic vertical deformation in the pipe diameter was very small, varying between 0 to 0.3 millimeters. We can say that pipe had elastic deformation during the experiments. Therefore, the same pipe is used for 6-7 experiments.

CHAPTER 5

EXPERIMENTS AND FINDINGS

5.1. Introduction

Inserting geofoam above the buried structure creates a more compressible layer, compared with the dense sand. This compressible layer is more likely to move/deform once a load applied, compared to the dense sand without geofoam on the sides. As described in the previous chapters, arching will be generated and some percent of the load will be transferred to the stiffer sides (stationary blocks). Amount of reduced load depends on the geometry and material behavior of the geofoam.

Under the light of the explanation above, a total of 16 experiments were conducted to observe the effect of:

1. Geofoam panel width
2. Geofoam panel thickness
3. Geofoam density
4. Geofoam location
5. Geofoam number and spacing between them.

Effects of abovementioned parameters are compared with the no-geofoam case, i.e., the situation with the only pipe. In all experiments, failure criterion was determined as 10 mm vertical change in pipe diameter which corresponds to a %5 change in vertical pipe dimension. The 5% limit is based on a factor of safety of four applied to the historically accepted limit of 20% deformation to avoid snap-through buckling and damage to the pipe (Rogers et al., 1995). In geofoam case, unless it is stated, geofoams are put 5 cm above the pipe crown. To observe the effect of location of geofoam, this height was changed to 0 and 10 cm.

All the geofoams used in test tank are supplied by TIPOR Strafor Company and for that reason, it is believed that the geofoams with same geometry and density have very similar properties.

In this study, all the geofoams are applied above the pipe. In Table 5.1, Crown-5cm means the geofoam is placed 5 cm above the pipe crown. Experiments 15 and 16 are done to see the effect of spacing in double layer geofoam application. Therefore, crown-5 & space 5 means that the first geofoam is placed 5 cm above the pipe and the second geofoam is placed 5 cm above the first placed geofoam (i.e., 10 cm above the crown).

Table 5.1. Experiment program and geofoam properties

experiment number	Location above pipe & configuration	EPS			
		Density, kg/m ³	Length, cm	Width, cm	Thickness, cm
1	Crown-5cm	15.4	97	20	4
2	Crown-5cm	28	97	20	2
3	Crown-5cm	13.4	97	40	4
4	Crown-5cm	16.3	96.5	20	2
5	Crown-5cm	15.5	97	40	2
6	no geofoam				
7	Crown-5cm	21.5	90	30	2
8	Crown-5cm	28.2	90	30	4
9	Crown-5cm	14.3	90	30	4
10	Crown-5cm	14.4	90	20	4
11	Crown-5cm	18	90	19.5	5
12	Crown-0cm	14.3	90	20	4
13	Crown-10cm	14.4	90	20	4
14	no geofoam 2				
15	Crown-5 & space 5	16.2	90	30	2
16	Crown-5 & space 10	16.2	90	30	2

The following sections have graphs demonstrating the results of the geofoam applied cases. In the results, there is a term as EPS AA XX-Y-Z, in which AA symbolizes the density of the geofoam in kg/m^3 , XX denotes the geofoam panel length in cm; Y and Z indicate the width and the thickness of the geofoam panel in cm, respectively.

5.2. No-geofoam experiments

In order to observe the behavior of pipe under static loading applied through a 26-cm diameter steel plate in a dense sand layer, two experiments were done for two different pipes, 95 cm and 90 cm long respectively. Vertical and horizontal deformation of the pipes under static loads is shown in Figure 5.1.

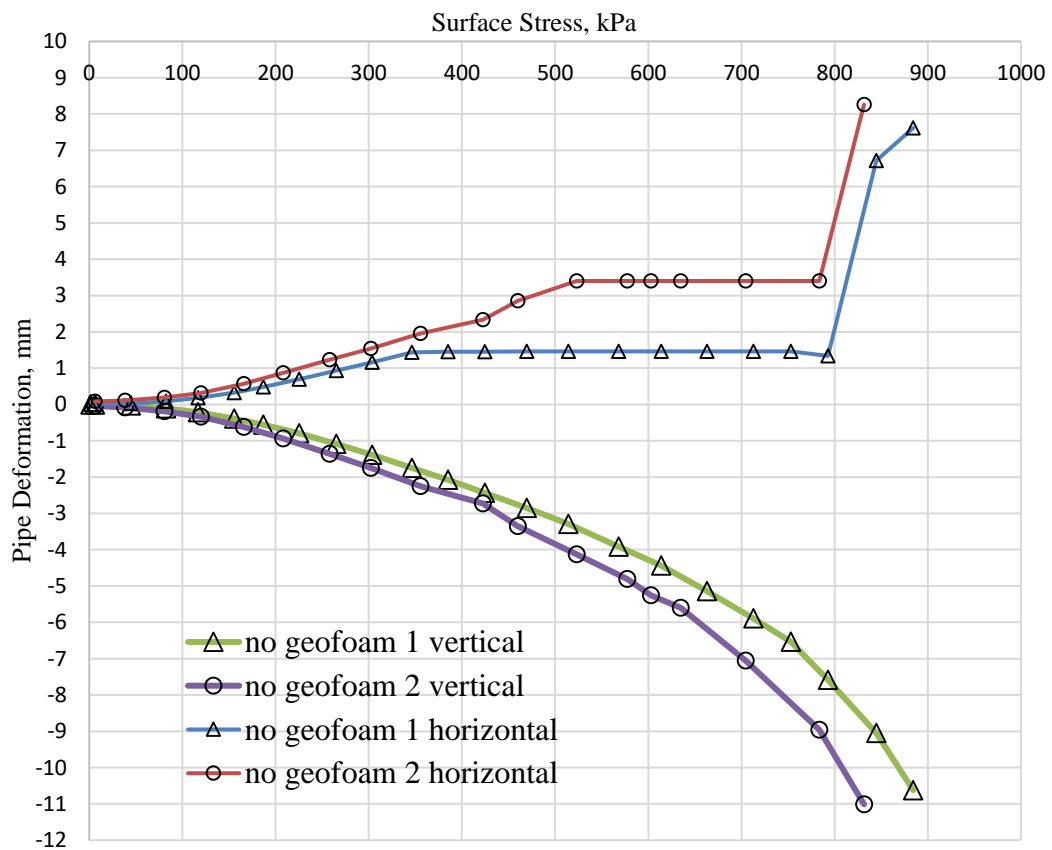


Figure 5.1. Pipe deformation vs. stress curves

In many experiments, the horizontal dial gage inside the pipe did not measure the deformation correctly. As seen in Figure 5.1., horizontal deformation seems to stop for some loading range, and then suddenly increases dramatically without significant change in vertical deformation. This behavior is only due to the equipment problem inside the pipe, which could be caused by the, possibly temporary, loss of contact between the horizontal dial gage and pipe inner surface, or dial gage being stuck in a position for some time. Therefore, horizontal deformation measurements are not deemed reliable, only the vertical deformation of the pipe is considered for different geof foam applications.

It is seen that during the experiments pipes showed elastic behavior in the stress range up to 800 kPa (pressure applied to the circular plate at ground surface). There was no or very little residual (plastic) deformation left in the pipe after the experiment was finished and the pipe was taken out from the test tank. The residual deformation values ranged from 0.1 to 0.3 mm, and that is why the same pipes were used in other experiments unless an accident occurred causing damage to the pipe. In two cases, the pipe failed. The first one was due to the extra perforated holes on the pipe circumference, and the pipe collapsed under compressive loading. The second failure of pipe (the one with the red tape in Figure 5.2) was due to overload under nearly 5.5 tons of vertical force. Pipe showed excessive permanent deformation on its cross section area such that one of the potentiometers was broken.



Figure 5.2. Side and front view of the heavily distorted pipe (with red tape) and collapsed pipe

5.3. Effect of width

In all experiments, the aim was to create a more compressible zone above the pipe. By doing so an immediate settlement above the pipe would initiate and it would result in arching. For that reason, factors that may affect this compressible zone were studied in the experiments. The width of the geofoam changed the behavior of pipe under loading according to the lab test results shown below. Three different widths of geofoams (20, 30 and 40 cm) are used in experiments (Figure 5.3). In these three tests, (test numbers: 4, 5 and 7, in Table 5.1.) the thickness of the geofoams was 2 cm and the geofoams were placed 5 cm above the crown of the pipe.

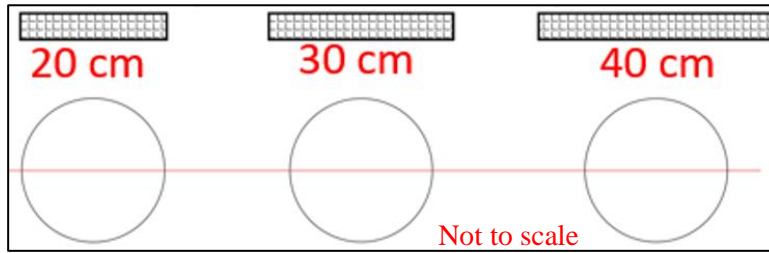


Figure 5.3. Geofoam widths for 2 cm thickness

For the geofoam blocks whose densities are approximately 15 kg/m^3 , as the width of the panel increased, higher surface stresses are required to cause the same amount of vertical pipe deformation. Up to approximately 300 kPa, the addition of geofoam decreases the vertical deformation of the pipe by a factor of 2.5 to 3 compared to the no-geofoam case. These improvements can be seen until the geofoam blocks fail under compression (at about 2 to 4% axial strain in geofoam, see Figure 3.5 for compression behavior of geofoams), after which a significant settlement occurs under the circular plate. In Figure 5.4 (b), at 260 to 330 kPa surface stress, there is a sharp increase in vertical pipe deformation due to the failure of geofoam; and the pressure is applied to the pipe from a closer vertical distance compared to the initial case. Under the same pressure applied at a closer level, pipe deforms more than the no-geofoam case. In summary, once the geofoam fails, the overall performance of the system is worse compared to the no-geofoam case.

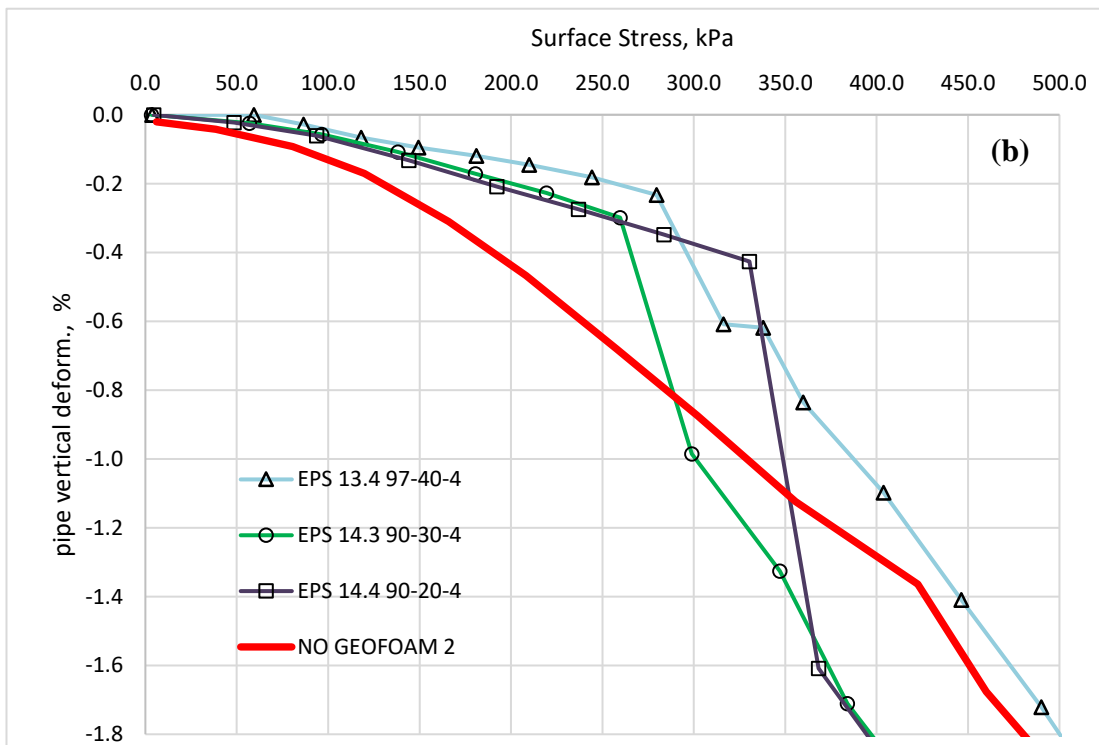
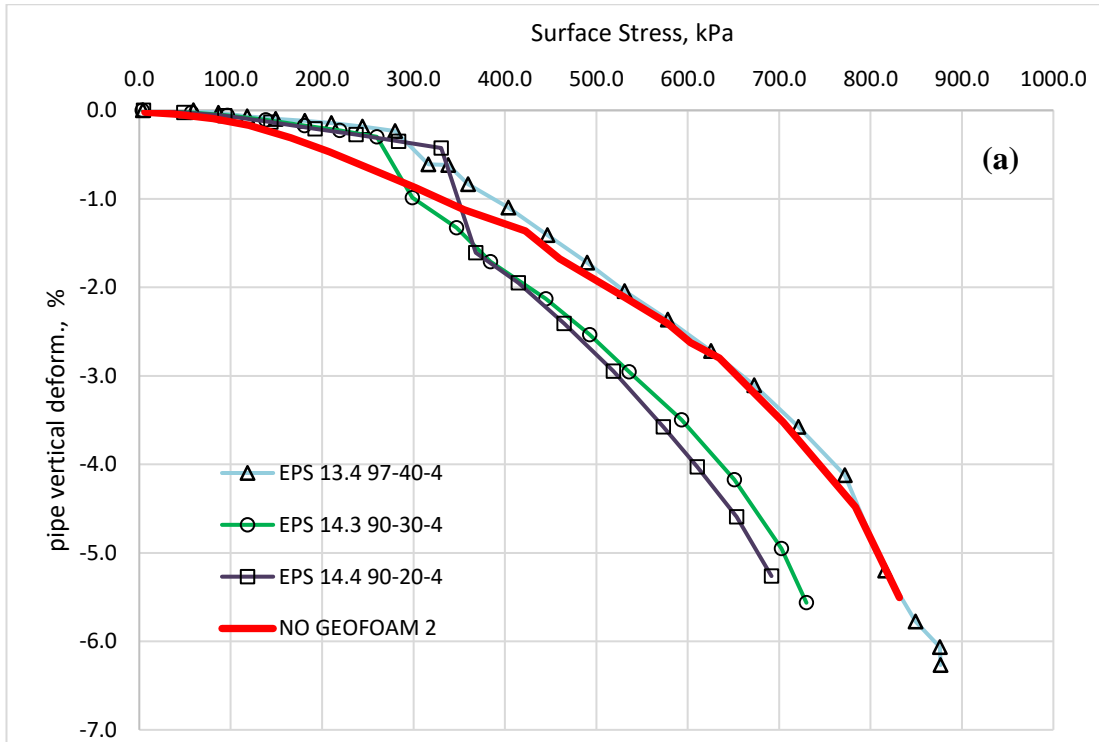


Figure 5.4. EPS15 thickness 4 cm, width comparison up to (a) 5.0% & (b) 1.8% pipe vertical deformation

Same trend and conclusions are valid when the geofoam thickness is reduced to 2 cm. (Figure 5.5 (a) and (b)).

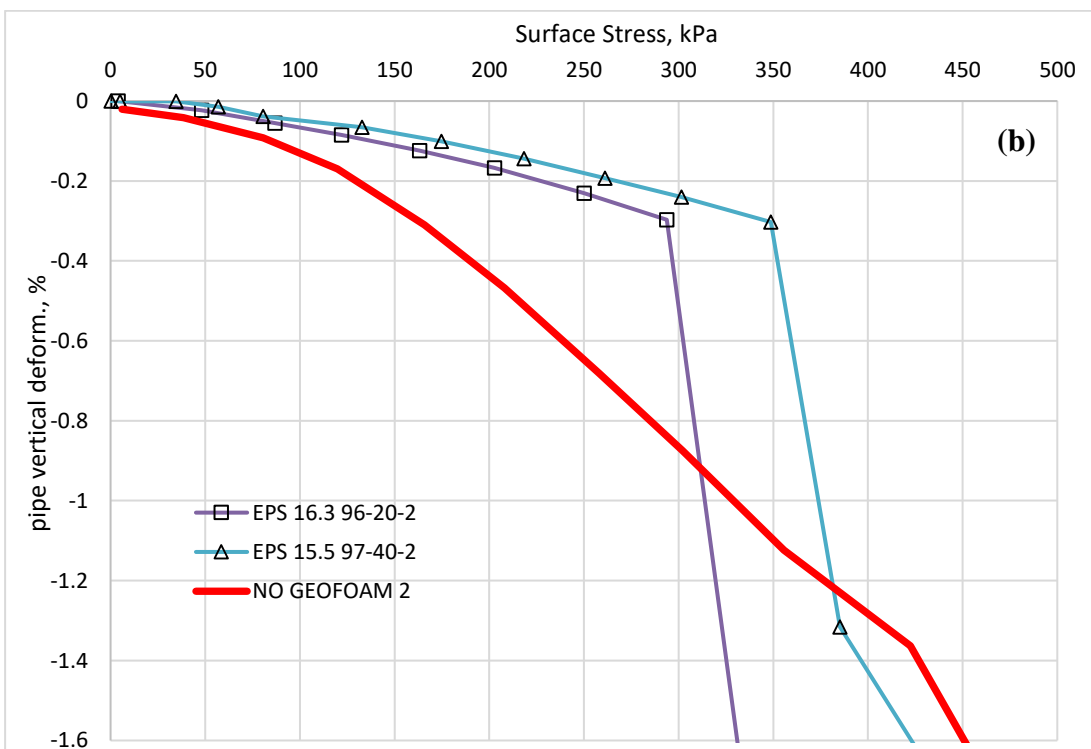
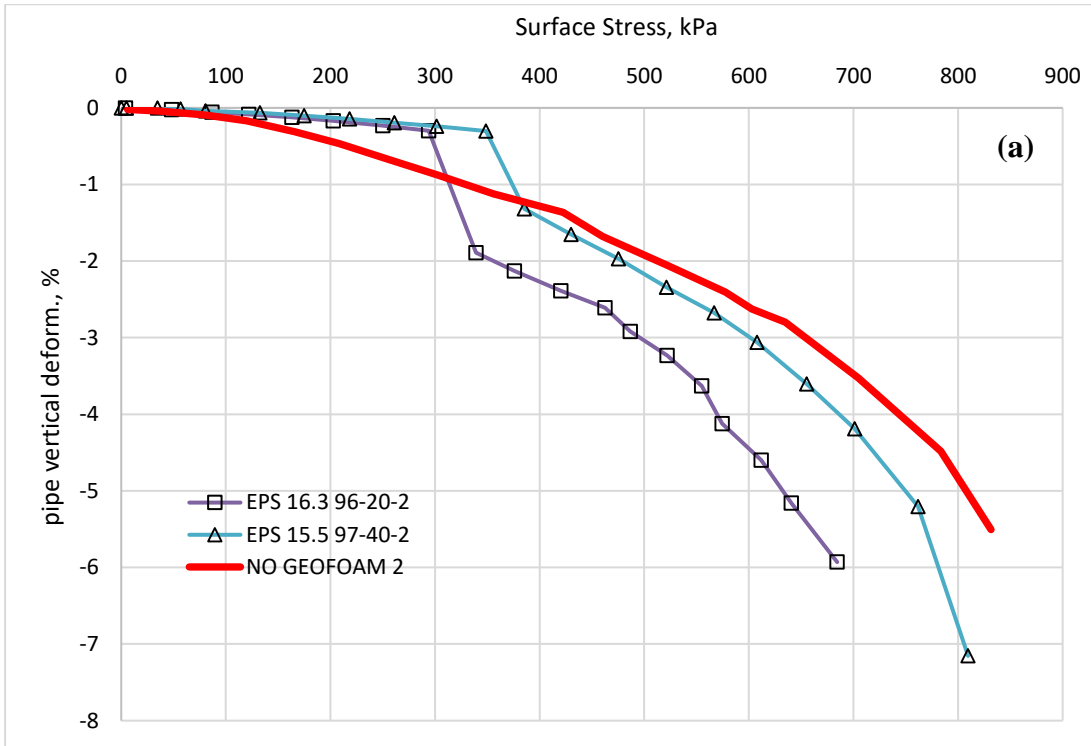


Figure 5.5. EPS15 thickness 2 cm, width comparison up to (a) 6.0% & (b) 1.6% pipe vertical deformation

5.4. Effect of density

Their densities characterize geofoms. A denser geofom will have higher strength and modulus, will be more resistant to deformation. Even though it is well known, some experiments were done in materials lab to see the effect of geofom density in compression behavior of geofom. The results can be seen in chapter 3. Four tests are conducted to investigate the effect of geofom density (Figure 5.6), test numbers 8, 9, 2 and 4 as seen in Table 5.1.



Figure 5.6. Four tests conducted to investigate the effect of geofom density

According to the results of the experiments with different geofom densities, lower density geofom shows a better improvement initially. Due to its lower modulus value, it will experience higher vertical compression deformation comparing with high-density geofom. In other words, lower density geofom creates a more compressible zone and creates the arching effect with a smaller load. Therefore, load transfer happens in low-density geofom case earlier, reducing the pipe deformation. On the contrary, failure of geofom is also earlier, and for the higher load cases, denser geofom shows better performance.

It is also clearly seen that it requires more than 1.5 times load to fail the denser EPS comparing with lower density EPS (i.e., about 260 kPa and 430 kPa surface stress in Figure 5.7. (b), for EPS 14.3 and EPS 28.2, respectively). Up to surface stress of 260 kPa, using EPS 14.3 is beneficial than using EPS 28.2. After 260 kPa surface stress, the denser EPS should be preferred, since it performs better for protecting the pipe, up to about 430 kPa surface stress. For surface stresses that are larger than 430 kPa, use

of lower and higher density geofoams do not provide any benefits in reducing the pipe deformations, since geofoams fail and pipe deformation is more, as compared to the no-geofoam case. Therefore, it can be concluded that the benefit of using geofoam depends on the magnitude of the applied vertical stresses, in relation to the geofoam compression failure stress (which takes place at about 2 to 4% compression strain in geofoam).

Similar results are obtained when two same geometry geofoam (thickness 2 cm and width 20 cm) with different densities (EPS 16.3 and EPS 28) are compared. Up to 300 kPa surface loading, EPS with lower density showed better performance, however as the load increased, lower density geofoam failed. On the other hand, denser geofoam showed improvement up to 550 kPa surface load (Figure 5.8 (a) & (b)).

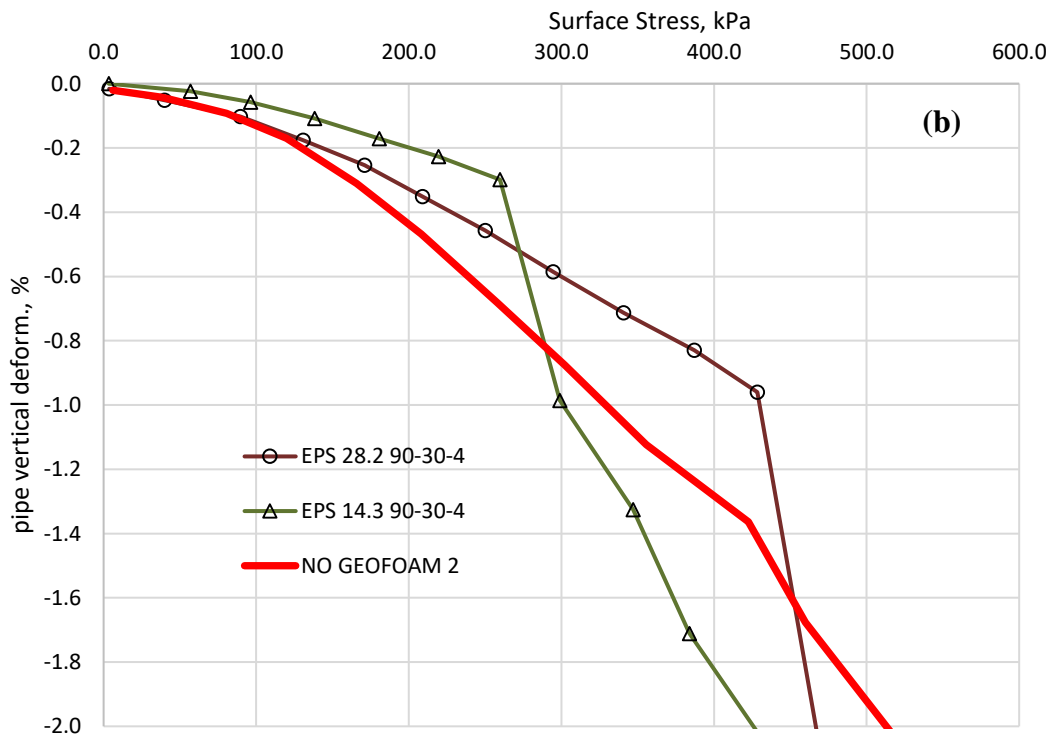
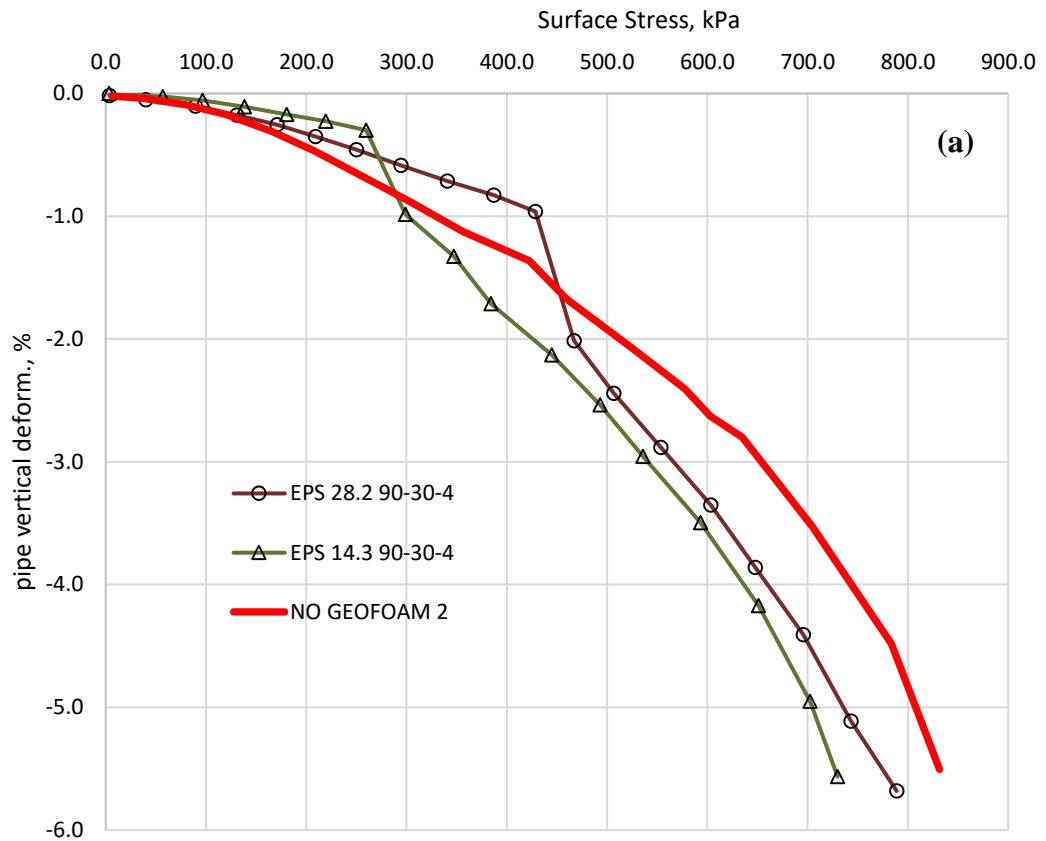


Figure 5.7. Width 30 cm & thickness 4 cm, EPS density comparison up to (a) 5.0% & (b) 2.0% of the pipe vertical deformation

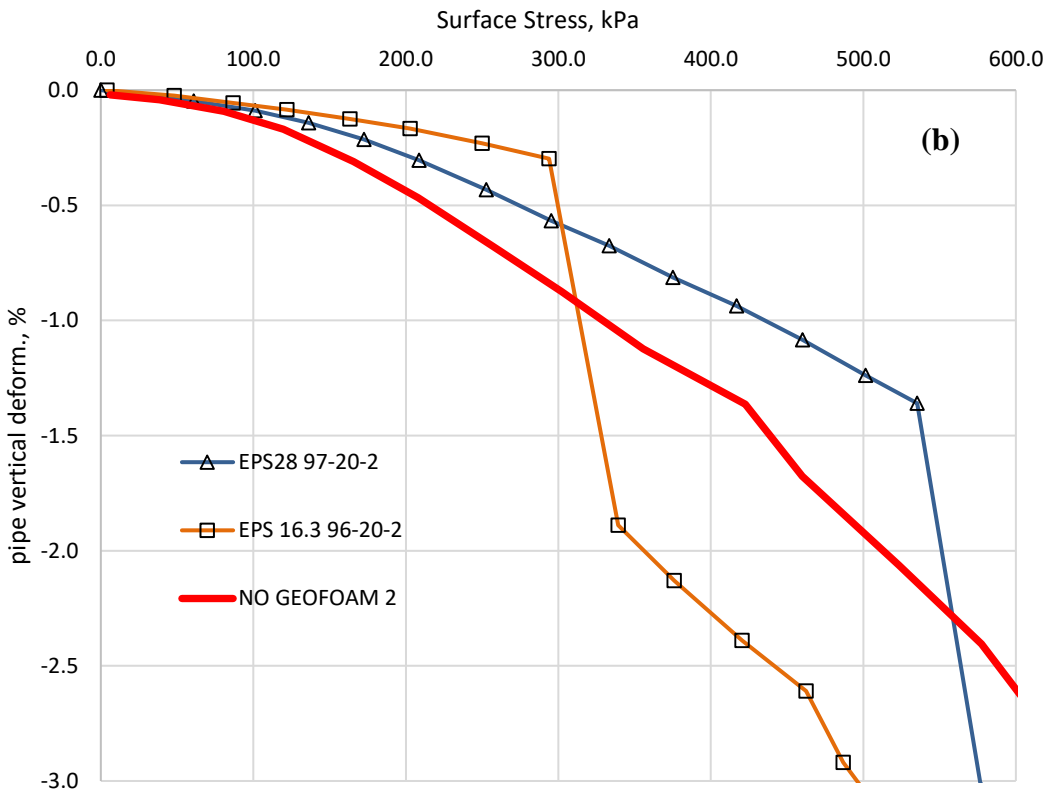
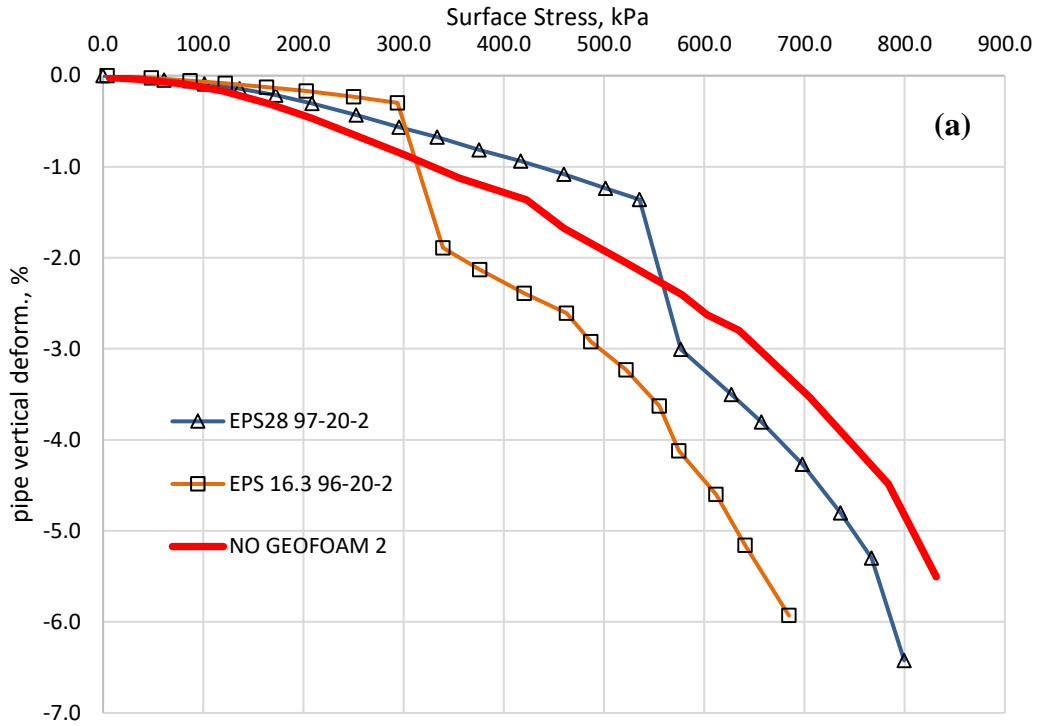


Figure 5.8. Width 20 cm & thickness 2 cm, EPS density comparison up to (a) 5.0% & (b) 3.0% pipe vertical deformation

5.5. Effect of thickness

To evaluate the effect of the thickness of geofoam, three different thicknesses are used in experiments, all placed at 5 cm above the crown of the pipe (Figure 5.9). The test results about thickness showed a similar behavior compared to width criterion, as the thicker geofoam used, the better performance is obtained for pipe protection. It is seen from the Figure 5.10 that geofoams improve the pipe deformation up to nearly 330 kPa. Theoretically, two identical geofoams regarding density and dimensions but thickness, under the same load, the one with the higher thickness will create a larger compressible zone above the pipe. With this larger compressible zone, a larger amount of load will be transferred to stationary zone and it will benefit the pipe by causing less vertical deformation. Also, a thicker geofoam layer means a smaller overburden load on the pipe, as compared to a thinner geofoam.

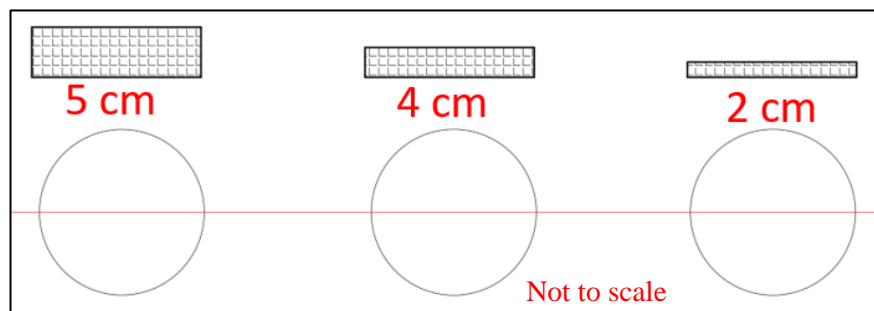


Figure 5.9. Three different geofoam thicknesses used in experiments

Figure 5.10 shows the comparison of varying geofoam thickness values as 2 cm, 4 cm and 5 cm. Unfortunately, densities of the geofoams are not the same in thickness criterion experiments. However, it was observed that a denser geofoam yields at higher compression stress. Pipe deformation behavior becomes very similar to no-geofoam case deformation behavior. Based on this fact, same geometry geofoam with higher density would yield at higher stress and pipe deformation behavior would shift downward (Figure 5.4). Therefore after the arrangement was made for figure 5.6, it would be clearly seen that thicker geofoam would improve the pipe deformation better. Another comparison of tests results seen in Figure 5.11. 40 cm wide geofoams with 2 and 4 cm thicknesses are used in the experiments. Density values are not identical but

close to each other. Test results can be seen in the graph below (Figure 5.11 (a) and (b)). If the density of specimen with thickness 4 were higher, the graph would shift to upward and it would create a better improvement in the initial part of the graph.

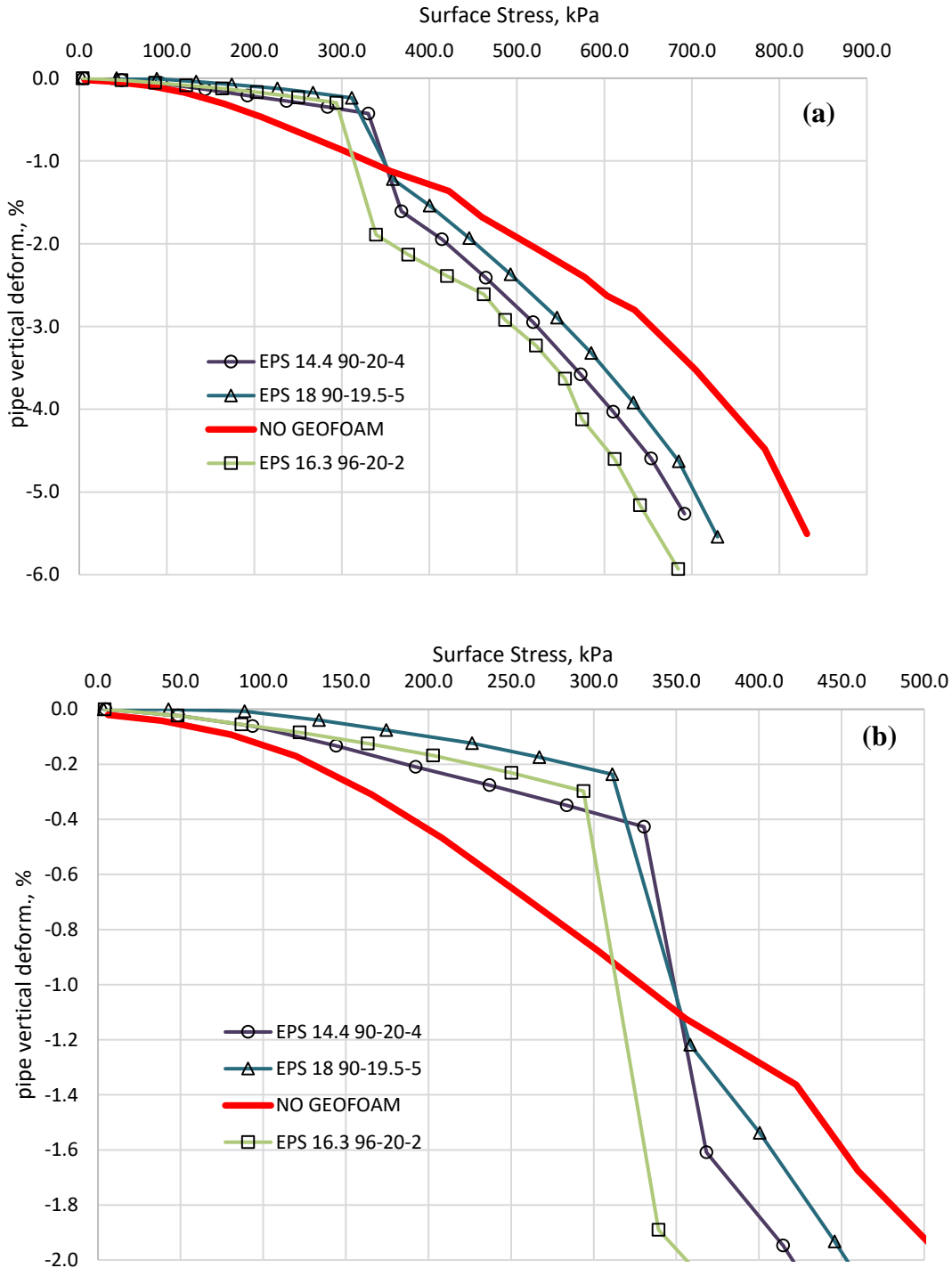


Figure 5.10. Width 20 cm, thickness comparison up to (a) 6.0% & (b) 2.0% pipe vertical deformation

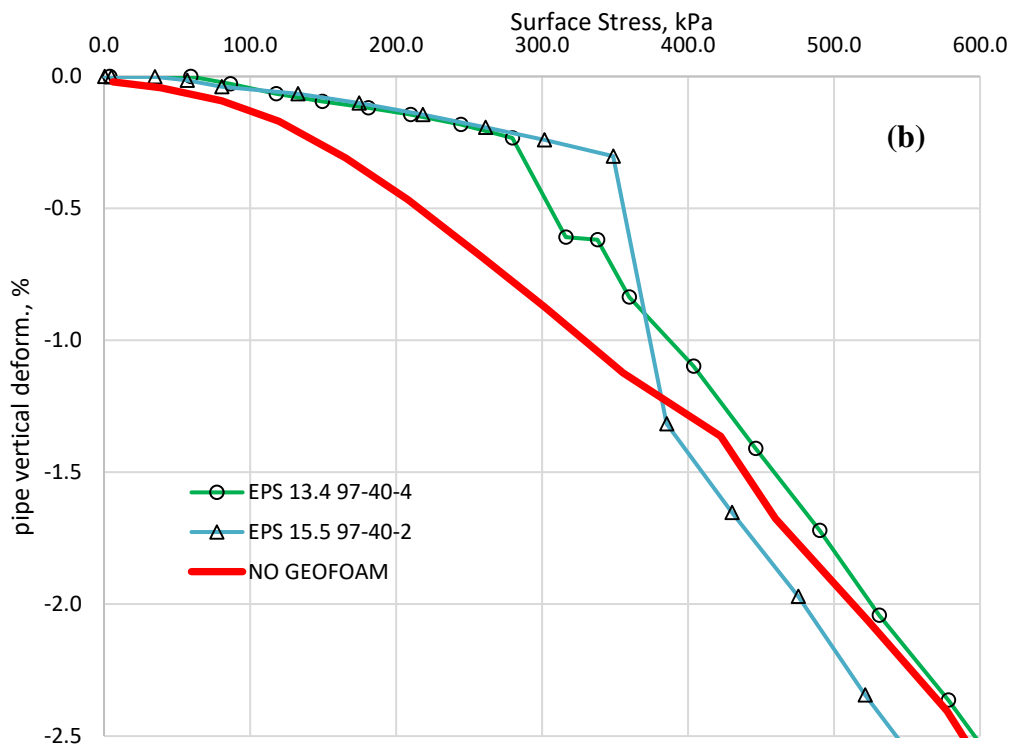
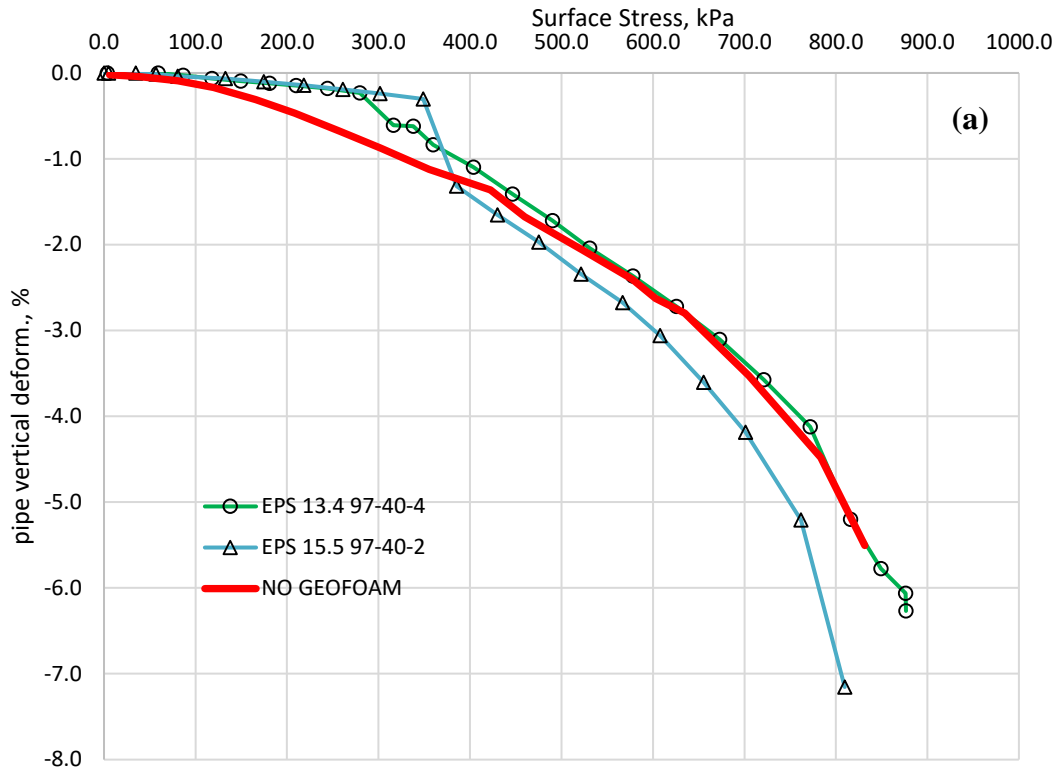


Figure 5.11. Width 40 cm, thickness comparison up to (a) 7.0% & (b) 2.5% pipe vertical deformation

5.6. Location criteria

In all the experiments in the preceding sections, the geofoam is laid at 5 cm above the pipe crown. However, the location of the geofoam can affect the behavior of the pipe due to changing the compressible inclusion above the pipe. To see the effects of this, three very similar geofoams were used in experiments, putting them just above the pipe, 5 cm and 10 cm above the pipe crown (Figure 5.12).

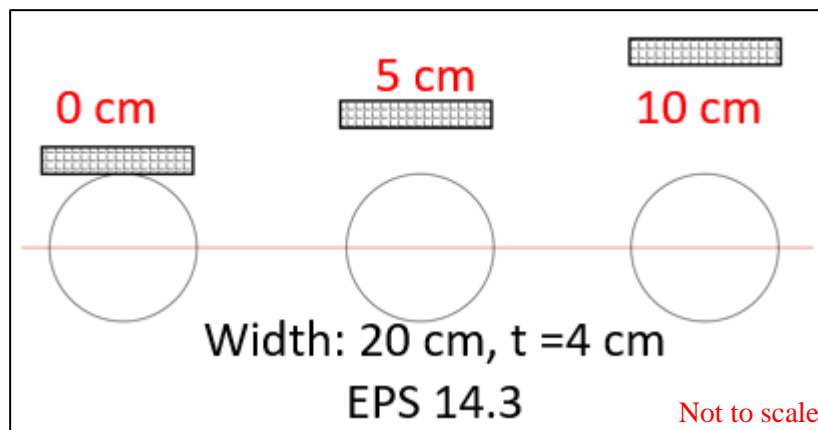


Figure 5.12. Experiments with varying vertical distance between geofoam and pipe crown

It is seen that as geofoams are placed closer to the pipe crown, higher loads are required to fail them. This can be expected because the effect of the applied surface load will be less as going deeper in the soil layer. Therefore, it can be stated that for higher loads, placing geofoam closer to the pipe crown is more effective.

Geofoam location over the pipe significantly affects the sudden deformation of pipe, at geofoam failure too. As seen in Figure 5.13, when geofoam is located just above the pipe, sudden vertical deformation of the pipe is more than six times comparing it with the case when geofoam is located 10 cm above the pipe. It is also important to notice that, pipe behavior in the tests with 5 cm and 10 cm crown distance, after failure their effect to the system is nearly the same. However, the case in which geofoam is put in contact with the pipe shows different behavior than these two cases.

Shortly, ensuring that geofoam failure load is not exceeded, putting the geofoam on the top of the pipe allows higher surface loads to be applied, as compared to having some distance between the pipe and geofoam.

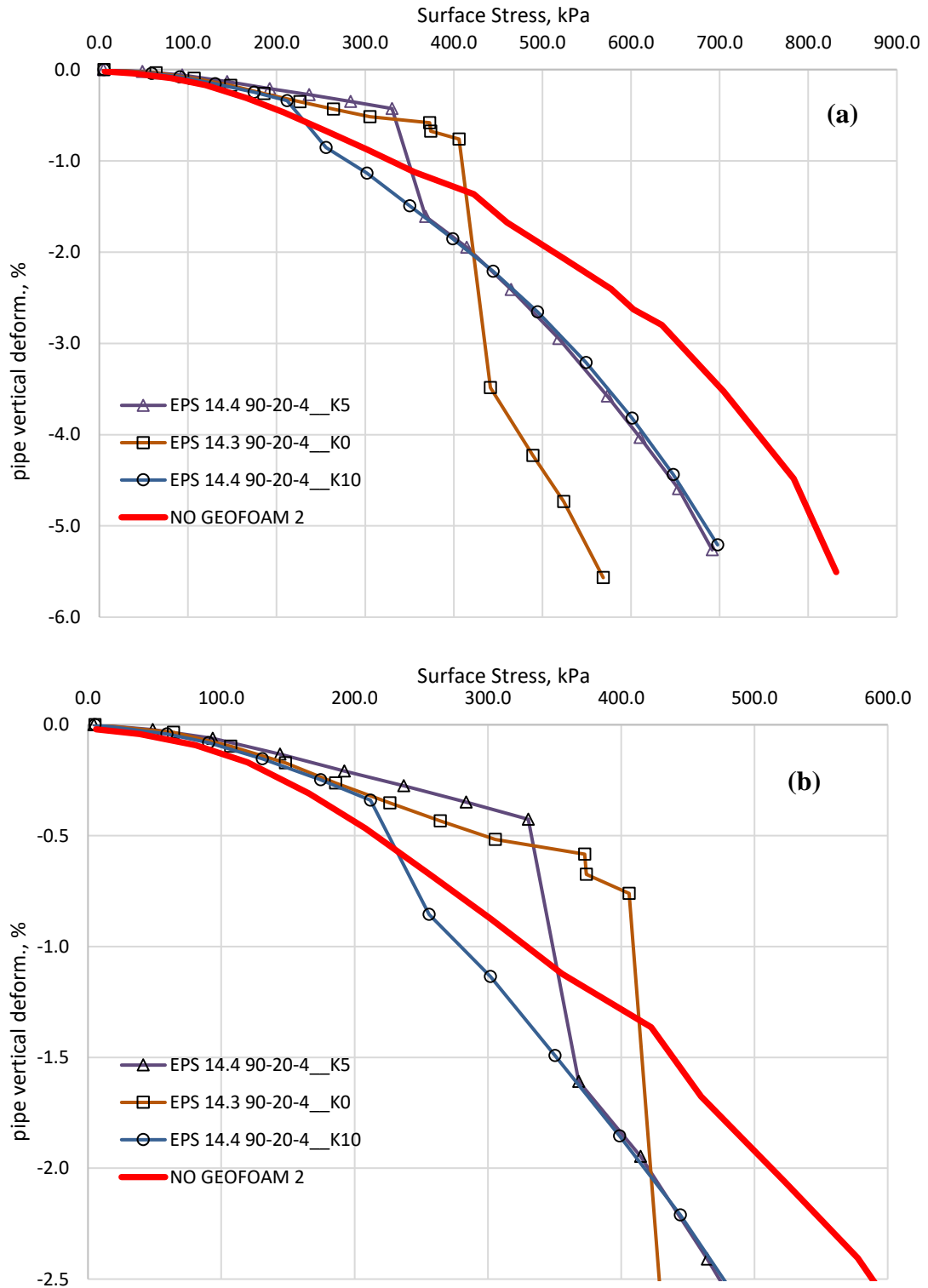


Figure 5.13. Comparison according to geofoam distance related to the pipe crown up to (a) 6.0% & (b) 2.5% pipe vertical deformation

5.7. Effect of spacing between multiple geofoams

The aim of using a different width, thickness, density or different location of geofoams have a purpose of improving the compressible zone above the pipe and hence reduce the vertical compression of the pipe and improve the behavior of the pipe under loading. For that, instead of putting a 4 cm thick geofoam, with the same width and density, two geofoam panels were used. Lower geofoam was placed at 5 cm above the pipe crown like in other experiments; the second geofoam was put 5 cm or 10 cm above the lower geofoam in two experiments (Figure 5.14). Results are compared with one layer 4 cm geofoam application case and shown below (Figure 5.15 (a) and (b)).

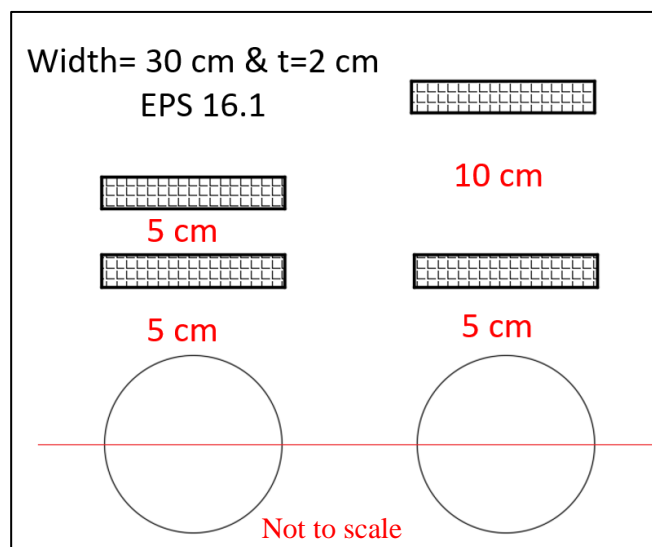


Figure 5.14. Location of two geofoams in the experiments

Results in Figure 5.15 show that a 4-cm-thick geofoam panel shows better performance than two-2-cm-thick geofoam. Two geofoam panels show failure at about 170 kPa surface stress values, whereas 4-cm-thick geofoam failed nearly at 260 kPa. 4 cm geofoam has a density as 14.3 kg/m^3 whereas 2 cm geofoams have 16.1 kg/m^3 . If the density of 4 cm geofoam were higher, its line on the graph would shift up and failure stress would be higher than 260 kPa. Under the lights of these observations, it seems more efficient to use one thick layer of geofoam than two thinner layers of geofoam. It is also seen that spacing of the panels does not affect the pipe improvement for these spacings. More experiments can be done to see the effect of other spacings.

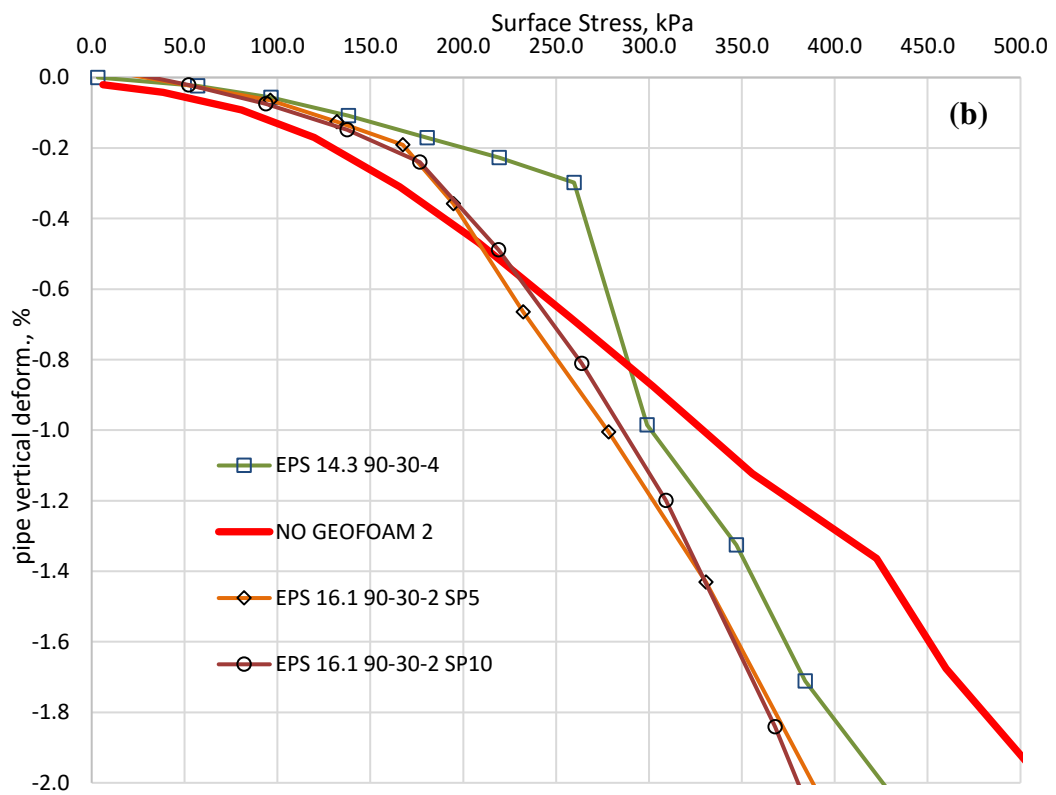
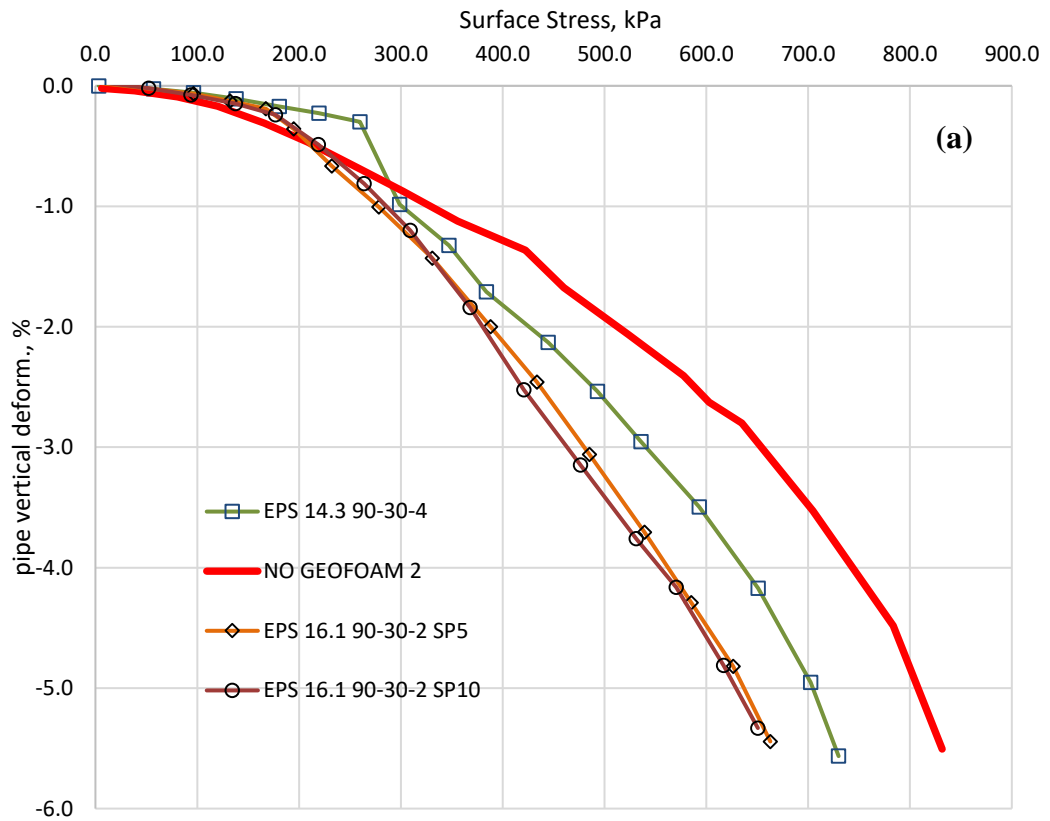


Figure 5.15. Spacing of double layer comparison up to (a) 6.0% & (b) 2.0% pipe vertical deformation

5.8. Effects on surface settlement and subgrade reaction modulus

Nearly in each experiment with geof foam(s) application, subgrade reaction modulus of the soil-geof foam composite structure decreased (Figure 5.16 and Figure 5.18). This is an expected result because the placement of geof foam creates a more compressible region compared to no geof foam case. Lower density geof foams decreased the subgrade modulus the most, whereas denser geof foams showed the same surface settlement behavior up to 500 kPa surface stress compared to the no-geof foam case.

Double geof foam applications decrease the subgrade modulus more, nearly 50% and 70% for 10 cm and 5 cm vertical spacings, respectively. Other geof foam applications reduced the subgrade modulus in the range of 15% to 35%, depending on their density and geometry.

Once the geof foam yields, a sudden and significant amount of settlement observed on the surface. As illustrated in Figure 4.17, geof foams collapse totally with a nearly 90% final vertical compression strain (Table 5.2). Such large deformation causes abrupt surface settlements, also sudden considerable vertical deformation on pipe geometry. Therefore, it is vital to be aware of potential design load on the geof foam.

Regarding pipe deformation, nearly all geof foams showed improvement up to yield stresses (Figure 5.17 and Figure 5.19). Geof foam % strain at the yield stress was calculated by making interpolation according to the geof foam compressive stress test results done in the Materials of Construction Lab of Civil Engineering Department of the university. It is seen that geof foams yielded in a wide % vertical compression strain range, such as 3% to 18% (Table 5.2), however mostly 2% to 4% strain. In practice, depending on the projects, the compressive strength of geof foam at 1%, 5% or 10% strain values are taken as design stress as explained in Chapter 2. However, attention should be paid to the yield strain range.

Table 5.2 shows the required surface load to deform the pipe vertically for some amounts. According to these comparisons, for smaller pipe deformation (up to 1.3 mm) nearly all of the geof foam applications show improvement. However, for larger deformations, geof foam would yield already and pipe deformation would be worse

compared to the no-geofoam case. In design, according to allowable pipe deformation and surface load, choice of geofoam geometry and density has paramount importance.

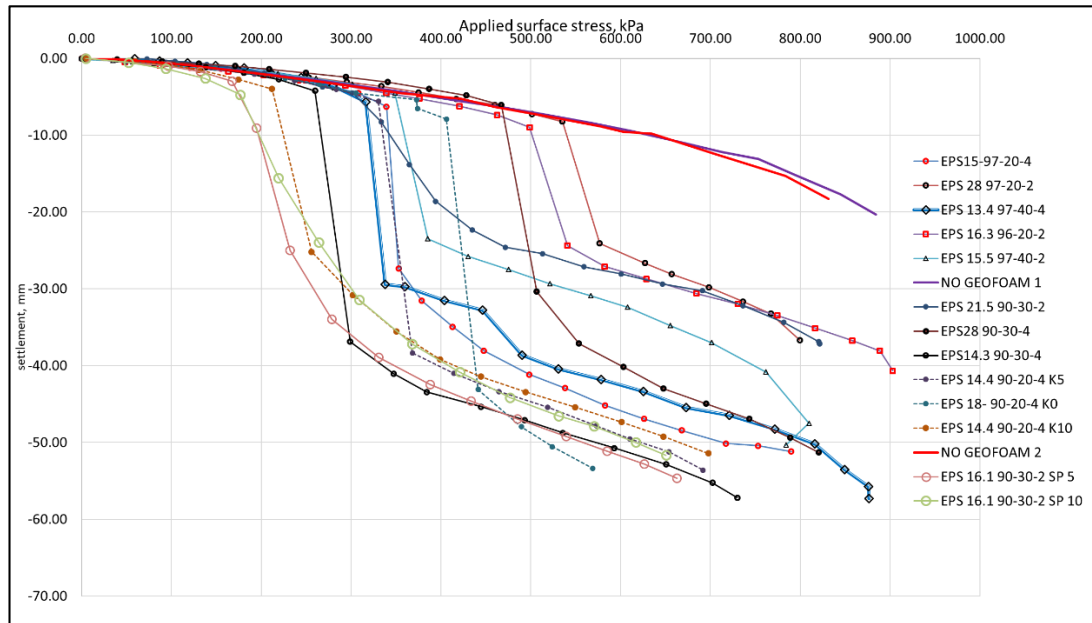


Figure 5.16. Surface settlements observed till the end of the experiments

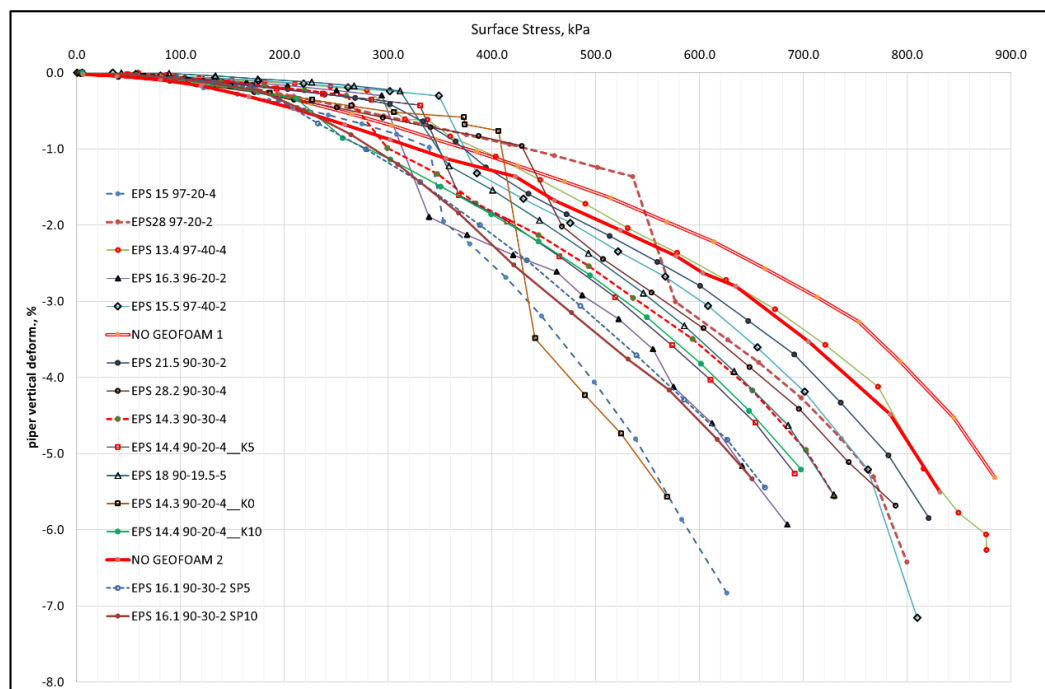


Figure 5.17. 5% vertical pipe deformations observed in the experiments

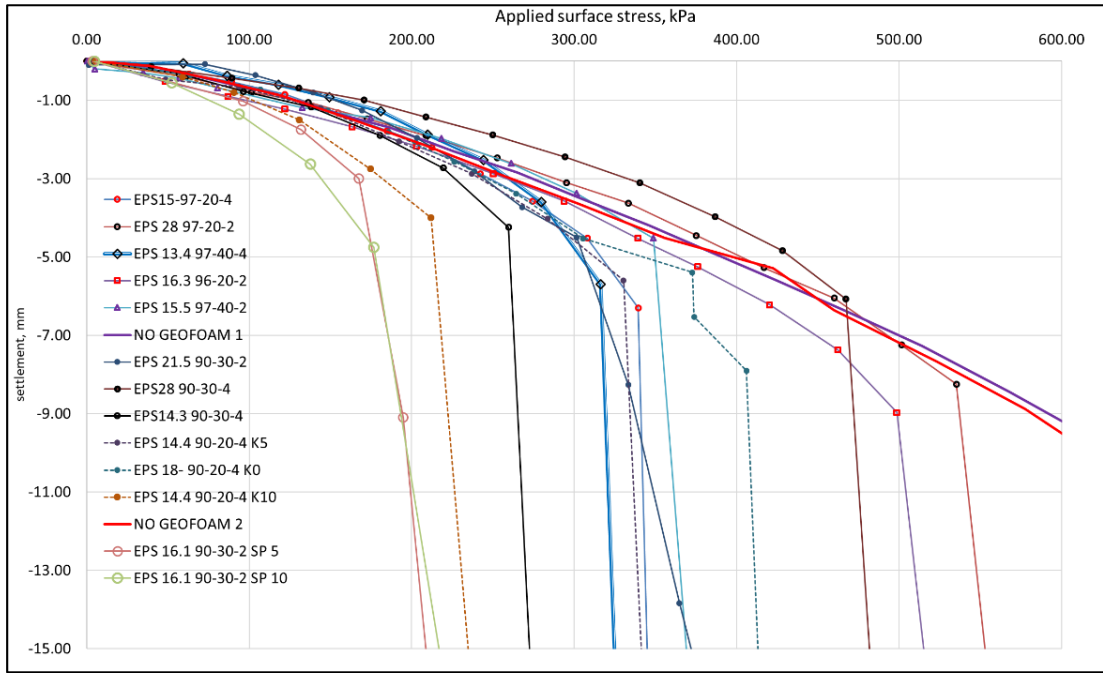


Figure 5.18. Surface settlements observed till 15 mm

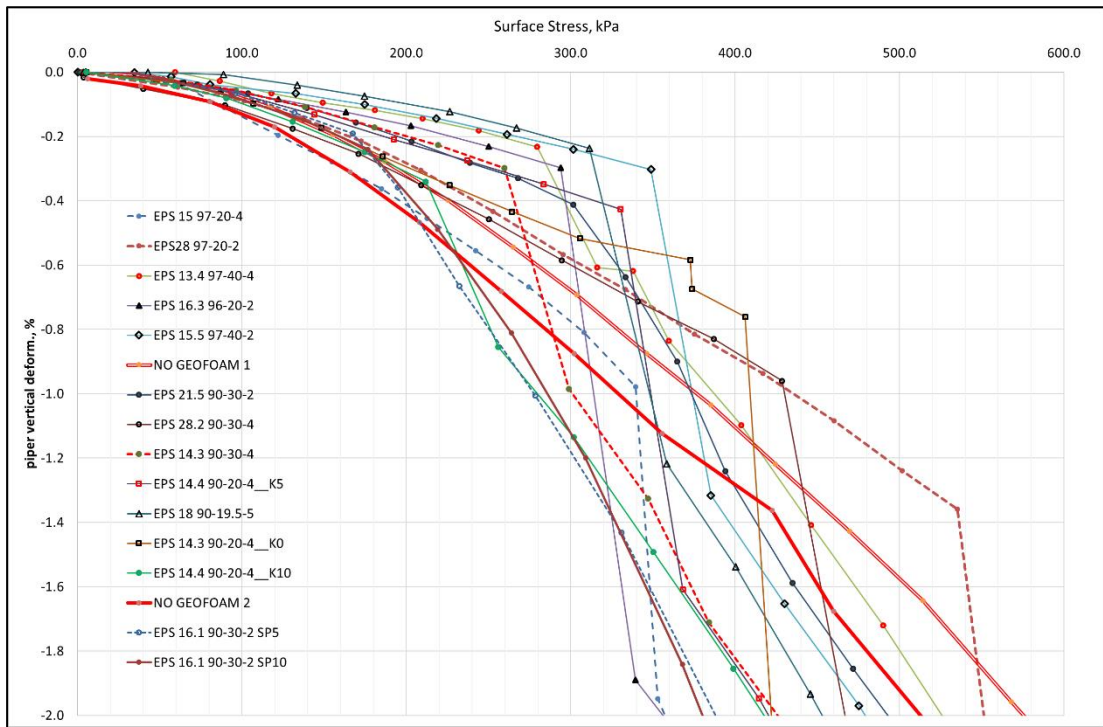


Figure 5.19. 2% vertical pipe deformations observed in the experiments

Table 5.2. Summary of the results of the experiments (Subgrade modulus, geofoam stress and strain, surface settlements)

experiment number	Location above pipe & configuration	EPS				Corresponding values @ geofoam break			Subgrade Modulus		Ultimate geofoam change			Surface load at ... mm vertical pipe deformation,					
		Density, kg/m ³	Length, cm	Width, cm	Thickness, cm	Surface settlement, mm	Surface stress, kPa	Stress on geofoam level, kPa	Approx. geofoam strain, %	k _{linear} , kPa/m	Subgrade modulus reduce %	geofoam final thickness, mm	geofoam final strain, %	10 mm	5 mm	2.6 mm	2 mm	1.3 mm	1 mm
1	Crown-5cm	15.4	97	20	4	-6.30	339.4	88.21	13	5387.4	31.60	3.0	92.6	3914.1	2901.3	2162.6	1905.9	1825.9	1803.6
2	Crown-5cm	28	97	20	2	-8.25	535.3	139.12	12	6488.4	17.62	2.59	87.10	3973.7	2993.7	2754.0	2311.1	1722.5	1455.0
3	Crown-5cm	13.4	97	40	4	-5.70	316.2	82.19	18	5548.1	29.56	2.57	93.60	4188.2	3165.9	2290.6	2056.6	1810.6	1623.0
4	Crown-5cm	16.3	96.5	20	2	-4.58	293.8	76.37	7	6422.4	18.46	1.23	93.90	4101.3	3358.0	2444.9	1878.0	1711.7	1077.9
5	Crown-5cm	15.5	97	40	2	-4.53	348.7	90.63	14	7706.1	2.2	1.25	93.75	3979.8	2881.3	2042.7	1985.2	1918.2	1889.5
6	no geofoam					-5.59	424.5			7594.6	3.6			4612.0	3467.7	2347.8	1999.6	1553.1	1342.8
7	Crown-5cm	21.5	90	30	2	-4.50	301.6	78.37	3	6701.1	14.9	1.50	92.50	4142.7	2981.8	2129.5	1982.6	1778.3	1667.1
8	Crown-5cm	28.2	90	30	4	-6.08	467.3	121.45	6	7692.2	2.3	5.88	85.30	4149.6	2974.0	2548.5	2488.9	1933.9	1046.3
9	Crown-5cm	14.3	90	30	4	-4.24	259.0	67.31	9	6108.5	22.4	2.85	92.90	3740.5	2594.3	1823.5	1597.9	1485.4	1440.0
10	Crown-5cm	14.4	90	20	4	-5.60	330.4	85.87	14	5900.0	25.1	2.62	93.50	3573.7	2481.6	1891.8	1840.8	1781.3	1755.8
11	Crown-5cm	18	90	19.5	5	-6.26	311.3	80.91	5	4972.8	36.9	4.69	90.60	3733.0	2687.4	1959.9	1847.4	1758.3	1720.1
12	Crown-0cm	14.3	90	20	4	-7.91	406.0	87.52	18	5136.0	34.8	3.60	91.00	2857.7	2275.4	2193.0	2172.4	1983.4	1577.4
13	Crown-10cm	14.4	90	20	4	-4.00	211.9	67.70	10	5297.5	32.7	2.80	93.00	3632.5	2532.1	1721.8	1485.4	1265.8	1197.5
14	no geofoam 2					-4.51	355.6			7876.0	0.0			4289.1	3123.9	2149.1	1746.9	1330.7	1145.2
15	Crown-5 & space 5	16.2	90	30	2	-9.10	194.8	62.22	3	2140.1	72.8	1.51	92.45	3381.7	2320.5	1670.4	1474.0	1223.3	1126.0
16	Crown-5 & space 10	16.2	90	30	2	-4.75	176.7	71.05	5	3719.4	52.78	1.80	91.00	3340.2	2224.7	1689.9	1517.9	1282.4	1171.5

CHAPTER 6

CONCLUSION AND FUTURE STUDIES

6.1. Conclusion

In this thesis study, a total of 16 lab scale model tests were conducted to see the effect of geofoam usage for the protection of a buried flexible pipe. The pipe is made of PVC, with an outer diameter of 20 cm and 3.9 mm thickness.

In each experiment, depth of the pipe and relative density of the backfill were constants; the pipe is laid 10 cm above a bedding (compacted soil at the bottom) and relative density of the sand was approximately 90% or more in all experiments.

The factors that may influence the geofoam improvement would be the width of geofoam, thickness, the density of the geofoam panels and configurational properties such as the location of the geofoam above the pipe crown and distance between geofoam panels if two geofoams were used.

Geofoam width has a significant effect on the pipe compression behavior. Test results showed that as the width increased, vertical deformation of the pipe is reduced under the same loading. However, these results are deduced from these specific experiment conditions; more experiments should be conducted considering different conditions.

Effect of geofoam thickness was also studied in the experiments. A thicker geofoam would benefit the system regarding less overburden load on the pipe. It also creates a bigger compressible zone over the pipe, which will result in a bigger arching effect on the system. Experiment results reveal that the thicker the geofoam, better improvement is achieved on the vertical pipe deformation.

Geofoam density is the identity of the material. A denser material will have higher modulus, will be subjected to less deformation under the same load. Experiment results showed that denser materials show improvement over a wider stress range comparing with lighter EPS panels. However, for the smaller loads, EPS with low density shows better performance compared with the heavier one. Reason beneath this outcome is the mobilization of arching. Arching will be initiated earlier in low-density EPS application comparing with high-density EPS. On the other hand, lower EPS will fail earlier and with this, not only improvement is vanishing but also deformation amount of pipe increases compared to the no-geofoam case. Higher density EPS failed under higher loads, so it is clear to say higher density EPS shows better performance for wider stress range.

Effect of the compressible layer location was studied by changing the geofoam panel's location referencing to pipe crown. Results show that placing the geofoam just above the pipe crown is more effective than geofoam placement at 5 cm or 10 cm above the pipe crown. It was also seen that putting geofoam higher is not a good idea for expected higher loads since geofoam will be subjected to greater stress under the same surface load compared to lower position geofoam. However, once failure occurs, 5 cm or 10 cm location is not important, they show the same effect on the pipe deformation. On the other hand, geofoam on the pipe crown failure becomes catastrophic for the system since pipe will be subjected to more than 1.5 times deformation comparing with other cases. This result is believed to occur due to lack of soil layer between pipe and geofoam.

Lastly, the effect of geofoam layer distance is also studied. Instead of putting a 4cm thick geofoam, two 2 cm thick geofoams are placed in the system. The distance between geofoam layers was 5 cm and 10 cm respectively. Results showed that no significant difference is obtained over the pipe deformation. Moreover, when these cases are compared with the 4 cm thick geofoam case, it is seen that one thick geofoam layer shows far better performance over the pipe deflection comparing than two thinner geofoams. Still, more experiments should be done to observe the effects of other distances and to confirm the current deduction.



Figure 6.1. Geofoms are cut to measure final strain %

After experiments, final strain % of the geofoms is measured by cutting them through the mid-span (Table 5.2 and Figure 6.1). Introducing the geofoms into the projects is good if attention is paid for the strain value of the geofoms. Because consistently, nearly in all experiments geofom showed improvement against vertical pipe deflection as long as it did not fail. However, once failure is seen, all the systems showed worse performance compared with no geofom case. The main reason for this outcome is, geofom failure results in highly compressed and very thin geofom and the plate that is acting on a higher position before the failure of the geofom is suddenly starts to act on a closer altitude to the pipe. Therefore, the same load on the surface now results in higher stress values over the pipe, which causes more deformation

(Figure 4.17). Geof foam, a good, helpful friend can be an undesirable enemy if one pushes the strain limits of geof foam.

6.2. Future Studies

Geof foam lab experiments can be very fruitful for the applications in real life. If one understands the behavior of the geof foam in a detailed way, better designs can be done considering safety and economy of the projects. Therefore, for future studies, the mentioned topics can be studied

- Geof foam applications for different relative density of the backfill soil and varying backfill materials
- Geof foam applications for repetitive/dynamic loadings
- Varying geometry and density of geof foams for higher and lower layer of the soil if two or more panels will be introduced to the system.
- Numerical modeling of the experiments should be done to confirm the results and to assign a correlation (if any) for the parameters.

REFERENCES

ACPA (1994). *ACPA Concrete Pipe Technology Handbook*. Second Printing, American Concrete Pipe Association, Vienna, VA

Akınay, E., Kılıç, H., and Rouzegari, B. (2016). Reduction of Soil Stress Acting ON Buried Flexible Pipe by Using EPS Geofoam (in turkish). *Zemin Mekaniği ve Geoteknik Mühendisliği 16. Ulusal Kongresi, Erzurum*

Anil Ö., Erdem R.T. and Kantar E. (2015) “Improving the impact behavior of pipes using geofoam layer for protection”, *Int. J. Press. Vessels Pip.* 132 (133) 52–64 (Elsevier Science).

Anil Ö, Akbas, S.O., Gezer O, Yılmaz M.C. (2017), Investigation of the impact behavior of steel and composite pipes with a protective layer. *Structural Concrete*. 18:421–432. [https:// doi.org/10.1002/suco.201600128](https://doi.org/10.1002/suco.201600128)

American Association of State Highway and Transportation Officials (1998), *AASHTO LRFD Bridge Design Specifications (Second edition)*. Washington, D.C

Bartlett, S.F., Lingwall, B. N., Trandafir, A. C. and Lawton E. C, (2011) “Protection of Steel Pipelines from Permanent Ground Deformation Using EPS Geofoam,” in *Increasing the Seismic Resilience of Natural Gas Systems - Select Topics of Interest*, ASCE Technical Council and Lifelines and Earthquake Engineering, 33 p. In press, 08/2011

Bartlett, S. F., Lingwall, B. A., and Vaslestad, J. (2015) “Methods of Protecting Buried Pipeline and Culverts Using EPS Geofoam in Transportation Infrastructure”, *Geotextiles and Geomembranes*, Volume 42, Issue 5, October 2015, pp. 450-461. Published, 10/2015.

Bjerrum, L., Frimann, Clausen, C.J. and Duncan J.M., 1972,” Earth Pressures on Flexible Structures – A State-of-the-Art Report”, 5th European Conf. on Soil Mechanics and Foundation Engineering, Madrid Proceedings Vol.2, pp. 169-196.

Choo Y.W., Abdoun, T.K., O'Rourke, M.J., and Ha, D. (2007). “Remediation for buried pipeline systems under permanent ground deformations.” *Soil Dynamics and Earthquake Engineering*, 27 (2007), 1043-1055

Edgar, T. V., Puckett, J. A. & D'Spain, R. B. (1989). Effects of geotextiles on lateral pressure and deformation in highway embankments. *Geotextiles and Geomembranes*, 8(4), 275-292.

General Technical Specification for HDPE Pipelines by State Hydraulic Works (in Turkish)

Hastey, A. R., Geotechnical Properties of Sawdust Used in Induced Trenches, Department of Civil Engineering, Senior Report, University of New Brunswick, Fredericton, New Brunswick, Canada, March 2000.

Horvath, J. S. (1997) “The compressible inclusion function of EPS Geofoam,” *Geotextiles and Geomembranes*, 15: 77-120

Jean, P. A. and Long, N. T., “Creation of Arching (Pneusol and other techniques),” *Geotechnical Instrumentation in Practice*, Proceedings of Institution of Civil Engineers, Nottingham, 1990, pp. 663–670.

Kang, J. (2007). SOIL-STRUCTURE INTERACTION AND IMPERFECT TRENCH INSTALLATIONS AS APPLIED TO DEEPLY BURIED CONDUITS. Auburn University.

Kawa, I., Zhang, Z. and Hudson, W.R. (1998). “Evaluation Of The Aashto 18-Kip Load Equivalency Concept”. Research Project 0-1713 The University of Texas, Austin

Kim, K., and Yoo, C.H. (2005). Design loading on deeply buried box culverts. *Journal of Geotechnical and Geoenvironmental Engineering*, 131(1): 20–27

Kim, H., Choi, B., and Kim, J. (2010), "Reduction of Earth Pressure on Buried Pipes by EPS Geofoam Inclusions," *Geotechnical Testing Journal* 33(4):1-10 · July 2010

Larson, N. G., (1962). "A Practical Method for Constructing Rigid Conduits under High Fills," *Highw. Res. Board, Proc. Annu. Meet.*, Vol. 41, pp. 273–280

Lingwall, B. (2009). "Protection of Buried Pipelines from Permanent Ground Displacement Using EPS Geofoam," Dissertation, Department of Civil and Environmental Engineering, University of Utah.

Lingwall, B. N. and Bartlett, S. F., (2014) "Full-scale Testing of an EPS Geofoam Cover System to Protect Pipelines at Locations of Lateral Soil Displacement, 2014, ASCE Pipelines Conference, Portland Oregon, August 3rd – 6th, 2014. Published, 08/03/2014

McAffee, R. P. and Valsangkar, A. J., (2004). "Geotechnical Properties of Compressible Materials Used for Induced Trench Construction," *J. Test. Eval.*, Vol. 32, pp. 143–152.

McAffee, R.P. 2005. Soil-structure interaction in rigid culverts installed in induced trenches. Ph.D. dissertation, Department of Civil Engineering, University of New Brunswick, Fredericton, N.B.

McGuigan, B.L., and Valsangkar, A.J. (2010). Centrifuge testing and numerical analysis of box culverts installed in induced trenches. *Canadian Geotechnical Journal*, 47(2): 147–163. doi:10.1139/T09-085.

McGuigan, B.L., Valsangkar, A.J., (2011). Earth pressures on twin positive projecting and induced trench box culverts under high embankments. *Canadian Geotechnical Journal*, 2011, 48(2): 173-185, <https://doi.org/10.1139/T10-058>

McQueen, C., Geotechnical Characteristics of Wood Chips and Hay Used in an Induced Trench, Department of Civil Engineering, Senior Report, University of New Brunswick, Fredericton, New Brunswick, Canada, November 2000

Marston, M. G., and A. O. Anderson (1913), "The Theory of Loads on Pipes in Ditches and Tests of Cement and Clay Drain Tile and Sewer Pipe," Iowa State University Engineering Experiment Station, Bulletin 31, Ames, Iowa

Marston, A. (1922). "Second Progress Report to the Joint Concrete Culvert Pipe Committee." Iowa Engineering Experimental Station, Ames, IA.

Marston, M. G. (1930), "The Theory of External Loads on Closed Conduits in the Light of the Latest Experiments," Iowa State University Engineering Experiment Station, Bulletin 96, Ames, Iowa

Moser, A. P. (1990). Buried Pipe Design. McGraw - Hill

Okabayashi, K., Ohtani, W., Akiyama, K., and Kawamura, M. (1994). Centrifugal model test for reducing the earth pressure on the culvert by using the flexible material. In Proceedings of the 4th International Offshore and Polar Engineering Conference, Osaka, Japan, 10–15 April 1994. International Society of Offshore and Polar Engineers, Cupertino, Calif. pp. 620–624.

Oshati, O.S., Valsangkar, A.J., and Schriver, A.B. (2012). Earth pressures exerted on an induced trench cast-in-place double-cell rectangular box culvert. Canadian Geotechnical Journal, 49(11): 1267–1284. doi:10.1139/t2012-09

Rahman, S. (2010). "Rigid and Flexible Pipes: An Objective Understanding of Pipe-Soil -Interaction, Design and Installation," Trenchless Technology-November 2010

Rogers, C. D. F., Fleming, P. R., Loeppky, M. W. J., Faragher, E., (1995). Structural performance of profile-wall drainage pipe-stiffness requirements contrasted with the results of laboratory and field tests. Transp. Res. Rec. 1514. Transportation Research Board, Washington, DC, pp. 83–92.

Spangler, M. G. (1941), "The Structural Design of Flexible Pipe Culverts," Iowa State University Engineering Experiment Station, Bulletin 153, Ames, Iowa

Spangler, M. G., (1958), "A Practical Application of the Imperfect Ditch Method of Construction," Highw. Res. Board, Proc. Annu. Meet., Vol. 37, pp. 271–277

Suleiman, Muhannad Taher, "The structural performance of flexible pipes " (2002). Retrospective Theses and Dissertations. Paper 1033.

Sun, L., Hopins T., and Beckham, T. (2005). Stress Reduction by Ultra-Lightweight Geofoam for Highfill Culvert: Numerical Analysis. Geotechnical Applications for Transportation Infrastructure.

Terzaghi, K., 1943, "Theoretical Soil Mechanics," John Wiley and Sons, Inc.

Vaslestad, J., Johansen, T. H., and Holm, W. (1993). "Load reduction on rigid culverts beneath high fills: Long-term behavior." Transp. Res. Rec., 1415, Transportation Research Board, Washington, D.C., 58–68.

Vaslestad, J., Sayd, M. Johansen, T. and Wiman, L. (2011). Load reduction and arching on buried rigid culverts using EPS Geofoam. Design method and instrumented field tests

Witthoeft, A. F. and Kim, H. (2016). Numerical investigation of earth pressure reduction on buried pipes using EPS geofoam compressible inclusions. Geosynthetics International, 23, No. 4, 287–300. [<http://dx.doi.org/10.1680/jgein.15.00054>]

Yap, P. (1989) "TRUCK TIRE TYPES AND ROAD CONTACT PRESSURES." Second International Symposium on Heavy Vehicle Weights and Dimensions. Kelowna, British Columbia

Yoo, C. H. & Kang J. (2007) "Soil-Structure Interaction for Deeply Buried Corrugated PVC and Steel Pipes." Highway Research Center, Auburn University.

Yoshizaka, K., and Sakanoue, T. (2003). "Experimental Study on Soil-Pipeline Interaction Using EPS Backfill," ASCE, Pipelines 2003, Baltimore USA, July 2003, 1126-1134.